
NEW INHIBITORS OF PATHOLOGICAL ANGIOGENESIS

Salvatore Ponticelli

Dottorato in Scienze Biotecnologiche – XX ciclo

Indirizzo Biotecnologie Industriali

Università di Napoli Federico II



Dottorato in Scienze Biotecnologiche – XX ciclo

Indirizzo Biotecnologie Industriali

Università di Napoli Federico II



NEW INHIBITORS OF PATHOLOGICAL ANGIOGENESIS

Salvatore Ponticelli

Dottorando: Salvatore Ponticelli

Relatore: Dott. Sandro De Falco

Coordinatore: Prof. Giovanni Sannia

*To Daniela for reminding me
what is important in life*

Index

I. Summary	3
1.1 Summary	4
1.2 Sommario	5
II. Introduction	10
2.1 Vasculogenesis and angiogenesis	11
2.2 Pathological angiogenesis	12
2.3 The concept of angiogenic switch	14
2.4 Molecular bases of angiogenesis	15
2.5 VEGF family	15
a. VEGF-A	16
b. PlGF	17
c. VEGF-B	17
d. VEGF-C	18
e. VEGF-D	18
f. VEGF-E	18
g. VEGF-F	19
h. VEGFR-1 (Flt-1)	19
i. VEGFR-2 (KDR/Flk-1)	20
j. VEGFR-3 (Flt-4)	20
k. Neuropilin-1 and -2	20
2.6 Molecules developed for angiogenic therapy: an overview	21
2.7 PlGF/Flt-1 pathway: a new therapeutic target?	22
2.8 Aims of the study	23
2.9 Biotechnological application	23
III. Results	25
3.1 Synthesis and screening of tetrameric tripeptide library	26
3.2 Peptide activity is sequence and structure dependent	34
3.3 4-23-5 peptide binds specifically to Flt-1 receptor	35
3.4 Evaluation of 4-23-5 activity on cell-based assays	38
3.5 <i>In vivo</i> activity of 4-23-5 tetrameric peptide	41
IV. Discussion	44
V. Material and Methods	48
5.1 Synthesis of combinatorial tetrameric tripeptide library and analogues of 4-23-5 peptide	49
5.2 Iterative deconvolution of tetrameric tripeptide library	50
5.3 ELISA-based assays for the screening of library and competition	50

itexperiments	
5.4 Inhibitory activity of 4-23-5 sequence-and structure- related analogues	50
5.5 ELISA assays for determination of binding of 4-23-5 peptide to Flt-1 receptors	51
5.6 Stability assay	51
5.7 Inhibition of Flt-1 phosphorylation assay	51
5.8 Capillary-like tube formation assay	52
5.9 Chicken embryo chorioallantoic membrane (CAM) assay	52
5.10 Cornea neo-vascularization	52
VI. References	53
VII. Abstracts and courses	59
VIII. Publications and Patents	73

I. Summary

1.1 Summary

Angiogenesis is a very complex biological process that drives the formation of new blood vessels starting from pre-existing one. In adulthood, it occurs both in physiological and pathological processes. Pathological angiogenesis is involved in several diseases, characterized from an excessive process (cancer), or an insufficient vessels support (ischemia) and it was proposed as the ideal target of several disorders. The best studied and characterized family of factors involved in angiogenesis is the VEGF (Vascular Endothelial Growth Factor) family. It comprises seven glycosylated dimeric secreted proteins that bind three tyrosine kinase receptors. In angiogenesis system, VEGF-A and placental growth factor (PlGF) have a crucial role. VEGF-A, binds VEGFR-1 (Flt-1) and VEGFR-2 (KDR/Flk-1) receptors while PlGF binds exclusively Flt-1 with high affinity than VEGF-A. *In vivo* studies have demonstrated that while VEGF-A is involved both in physiological and pathological angiogenesis, the role of PlGF and Flt-1 is restricted to pathological processes. Recent data demonstrated that PlGF and Flt-1 are not only involved in pathological angiogenesis but also in inflammation disorders and metastasis formation.

The aim of this study has been the identification of new small molecule able to prevent the binding of Flt-1 to its ligands, using the biotechnological approach of the screening of combinatorial peptide libraries. In general small molecules are more attracting for industrial production, with regard to recombinant protein and monoclonal antibodies, due to low cost and more easy process of production. The screening of a tetrameric tripeptide library made of 29 non natural aminoacids plus L-Glycine, has allowed the identification of the Gly-Lys(Lys₂)-[4-23-5]₄ peptide, named 4-23-5. Selected peptide is able to bind specifically Flt-1 receptor inhibiting the interaction with its ligands PlGF and VEGF showing an activity on micromolar range (IC₅₀ of about 10 μM). The activity of selected peptide depends both on aminoacidic sequence and on tetrameric structure as demonstrated respectively by assays performed with Ala-scanning peptides and structural analogues of tetrameric 4-23-5. Selected peptide has an elevated resistance to proteases since it is stable until 24 hours as expected using non natural aminoacids. On cell 4-23-5 peptide is able to prevent PlGF-induced Flt-1 phosphorylation indicating that it is able to prevent the first molecular event that activates angiogenesis in response to Flt-1. Moreover, 4-23-5 blocking peptide is able to inhibit both the formation of a capillary-like network induced by both PlGF and VEGF-A and the VEGF-induced angiogenesis on chicken embryo chorioallantoic membrane, showing that the inhibition of phosphorylation of Flt-1 alone is sufficient to inhibit angiogenesis both *in vitro* and *in vivo*. In addition, selected peptide is able to induce the vascularization of cornea *in vivo* confirming its ability to bind selectively Flt-1 without preventing VEGF-A/Flk-1 interaction that lead corneal vascularization.

On the base of these results, selected peptide represents a new specific anti-Flt-1 peptide that it can be used for molecular therapy approach of those pathologies in which angiogenesis represents crucial events, for the treatment of inflammation disorders and to prevent cancer metastases. This peptide represents a new molecular scaffold which can be further modified to generate new peptide variants with increased affinity for its specific target.

1.2 Sommario

Il sistema vascolare è il primo apparato formato durante lo sviluppo embrionale, esso infatti provvede a rifornire i tessuti di sostanze nutrienti e di ossigeno e allo stesso tempo allontana da questi i metaboliti di scarto. Il sistema vascolare viene formato attraverso due processi distinti: la vasculogenesi e l'angiogenesi. La vasculogenesi è il processo di formazione di nuovi vasi sanguinei a partire dagli emangioblasti, precursori di origine staminale comuni sia alle cellule endoteliali che a quelle ematopoietiche. Il plesso vascolare primitivo formatosi in seguito alla vasculogenesi è ancora fragile e pronò a rotture e necessita del processo angiogenico per ricevere stabilizzazione. L'angiogenesi è il processo di formazione di nuovi vasi sanguinei a partire dai vasi pre-esistenti. Tale processo avviene sia durante lo sviluppo embrionale, dove provvede a riorganizzare e stabilizzare la rete vasale primitiva, sia nell'adulto dove viene distinta in angiogenesi fisiologica e patologica. In particolare l'angiogenesi patologica interviene in numerose patologie caratterizzate sia da un'eccessiva angiogenesi, come nel cancro e nella retinopatia diabetica, che da un'insufficiente processo angiogenico come nelle ischemie. La terapia angiogenica nasce con l'intento di curare quelle patologie caratterizzate da un'eccessiva angiogenesi come il cancro, ma nel tempo è stata estesa a tutte quelle patologie causate o caratterizzate da un'angiogenesi alterata.

I meccanismi molecolari che governano l'angiogenesi sono molteplici e negli anni sono state individuate diverse famiglie di fattori molecolari coinvolti sia nell'induzione che nella regolazione di tale processo. Tra queste, la famiglia di fattori di crescita più studiata e meglio caratterizzata è la famiglia dei fattori vascolari-endoteliali chiamata VEGF (Vascular Endothelial Growth Factor). Tale famiglia comprende sette proteine secrete denominate come: VEGF-A, -B e PlGF coinvolte nell'angiogenesi, VEGF-C e -D che prendono parte nella linfoangiogenesi, VEGF-E isolata di recente nel Pox virus e la cui funzione non è ancora stata chiarita, e infine VEGF-F recentemente isolato nel veleno della vipera. Tutti i membri di tale famiglia sono attivi come dimeri glicosilati che, a livello strutturale sono caratterizzati da un motivo ricco in residui di cisteina altamente conservato, noto come *Cysteine knot*. Essi legano i recettori di tipo tirosina-chinasi chiamati VEGFR-1 (conosciuto come Flt-1 (fms-like tyrosine kinase)), VEGFR-2 (chiamato KDR (kinase domain receptor) nell'uomo e Flk-1 (Fetal liver kinase) nel topo) e VEGFR-3 (anche conosciuto come Flt-4), in particolare il recettore Flt-1 esiste anche in forma solubile generata attraverso un processo di *splicing* alternativo. Inoltre VEGF-A e PlGF legano anche i co-recettori Neuropilina-1 e -2, ma il ruolo di tali interazioni è ancora oggi oggetto di studi atti a chiarirne il significato biologico. Per quanto riguarda i fattori coinvolti nell'angiogenesi, è stato dimostrato che mentre VEGF-A lega entrambi i recettori Flt-1 e KDR/Flk-1 mostrando maggiore affinità per il primo, VEGF-B e PlGF legano esclusivamente Flt-1, e in particolare PlGF mostra affinità maggiore rispetto a VEGF-A e -B. Il legame dei fattori solubili ai recettori causa la dimerizzazione e la fosforilazione dei recettori, eventi molecolari che danno inizio alla cascata di trasduzione del segnale.

Studi genetici hanno dimostrato che VEGF-B è coinvolto nell'angiogenesi specifica del muscolo cardiaco, mentre VEGF-A ha un ruolo cruciale nell'induzione dell'angiogenesi in tutti i tessuti. In particolare, VEGF-A interviene sia nell'angiogenesi patologica che fisiologica, nonché nello sviluppo embrionale. Infatti la delezione di un singolo allele del gene *vegfa* provoca letalità embrionale, indicando che per il corretto sviluppo embrionale è importante non solo la sua presenza ma anche la sua concentrazione. Al contrario, il ruolo di PlGF e del recettore Flt-1 è ristretto alla sola angiogenesi patologica. I topi *Plgf*^{-/-} pur essendo vitali e fertili, presentano un'angiogenesi patologica alterata, infatti essi sviluppano tumori di dimensioni minori e meno vascolarizzati e hanno una minore capacità di recupero in seguito ad un evento ischemico. Un fenotipo simile è stato osservato nei

topo *Flt-TK*^{-/-}, nei quali è stato eliminato il dominio tirosina-chinasi del recettore, mentre la delezione del gene *Flt-1*, così come la delezione del gene *Flk-1*, provoca letalità embrionale in seguito a difetti nella migrazione e stabilizzazione del plesso vasale primitivo. Ulteriori dati ottenuti inibendo PIGF o Flt-1 con anticorpi monoclonali, dimostrano che tali fattori sono coinvolti non solo nell'induzione dell'angiogenesi patologica, ma anche nel richiamo di cellule muscolari lisce che hanno il ruolo di stabilizzare i neo-vasi, e nel richiamo dei monociti/macrofagi che intervengono nelle patologie infiammatorie. Inoltre, per il recettore Flt-1 è stato descritto un ruolo singolare nel processo di formazioni delle metastasi: *in vivo*, in sistemi modello di crescita tumorale Flt-1 è espresso dai precursori ematopoietici di origine staminale che promuovono la formazione di aggregati cellulari che colonizzano i siti dove si avrà la formazione delle metastasi, tali aggregati prendono il nome di 'nicchie pre-metastatiche'. L'utilizzo di un anticorpo anti-Flt-1 è capace di prevenire la formazione delle nicchie pre-metastatiche inibendo la formazione di metastasi.

Inizialmente la terapia angiogenica si è concentrata su VEGF-A e sul recettore KDR/Flk-1, in quanto la loro funzione è cruciale per l'attivazione delle cellule endoteliali per la formazione di nuovi vasi. Attualmente è in uso in terapia un anticorpo monoclonale anti VEGF-A (Avastin) per la cura del cancro. I risultati ottenuti con tale anticorpo mostrano chiaramente la validità del principio della terapia angiogenica, infatti inibendo l'angiogenesi è possibile osservare un rallentamento della patologia, tuttavia i pazienti trattati hanno manifestato una serie di effetti collaterali quali trombosi e ipertensione, dovuti al fatto che VEGF-A è un fattore che induce la permeabilizzazione dei vasi e che riveste un ruolo importante anche nei processi fisiologici.

In tale contesto si inserisce il seguente progetto di ricerca, volto ad identificare nuove piccole molecole capaci di inibire in maniera specifica l'angiogenesi patologica, che risulta essere più specificamente attivata dal recettore Flt-1 e dai suoi ligandi. A questo scopo è stato utilizzato come approccio la selezione di molecole bio-attive da collezioni peptidiche combinatoriali. Nell'ultimo decennio l'utilizzo in terapia di proteine ricombinanti e anticorpi monoclonali ha trovato largo impiego, tuttavia questo ha ancora degli svantaggi legati sia agli elevati costi di produzione che alle limitate modalità di somministrazione. In risposta a tali problemi, negli ultimi anni le biotecnologie si sono focalizzate anche sulle molecole a basso peso molecolare in quanto queste mostrano numerosi vantaggi primo fra tutti i bassi costi di produzione. In particolare è stata ampiamente studiata la realizzazione di collezioni di tali molecole, in modo da ottenere un numero elevato di molecole da analizzare, e sulle tecniche sperimentali per la loro analisi che permettano di selezionare molecole bio-attive. Nel seguente lavoro è stata eseguita la sintesi e l'analisi di una collezione di tri-peptidi tetrameric. La collezione è stata sintetizzata a partire da 29 aminoacidi non naturali più la L-Glicina in modo da ottenere peptidi stabili alle proteasi, mentre la struttura tetramerica è stata realizzata grazie ad un *core* di tre residui di lisina. Tale struttura è stata adottata per aumentare l'attività dei peptidi in quanto questa contiene la stessa sequenza tri-peptidica ripetuta 4 volte. Il processo di selezione è stato eseguito mediante un saggio di competizione basato sulla metodica ELISA (Enzyme-linked immuno sorbent assay). Tale saggio consente di selezionare molecole capaci di inibire l'attività di Flt-1 di legare i suoi ligandi: una forma ricombinante del recettore Flt-1 viene fatta adsorbire su un supporto solido, quindi si aggiunge una forma ricombinante della proteina PIGF, in presenza di un eccesso molare noto di molecole da analizzare. L'interazione tra PIGF e il recettore viene rilevata utilizzando un anticorpo anti-PIGF biotinilato. Il saggio è eseguito con la proteina PIGF in quanto questa presenta maggiore affinità per Flt-1 rispetto a VEGF-A e quindi aumenta la sensibilità del saggio. Allo scopo di verificare la specificità dei peptidi ottenuti, è stata valutata anche la capacità di questi di inibire l'interazione di Flt-1 con VEGF-A.

Inoltre tutte le molecole selezionate con il sistema murino sono state testate anche sul sistema umano per confermare la loro applicabilità in terapia.

La deconvoluzione di una collezione peptidica è un processo basato su un saggio funzionale, che consente di stabilire per ogni posizione aminoacidica del peptide, il residuo che presenta maggiore attività. Il processo di deconvoluzione della collezione tetramerica ha identificato un peptide con sequenza Gly-Lys(Lys₂)-[4-23-5]₄ (in seguito indicato solo con 4-23-5), tale peptide è capace di inibire l'interazione tra il recettore Flt-1 e i suoi ligandi PIGF e VEGF-A mostrando attività su scala micro molare (IC₅₀ 10 μM).

Allo scopo di stabilire le basi molecolari che guidano l'attività del peptide selezionato, sono stati eseguiti dei saggi ELISA con il peptide immobilizzato per determinare con quale fattore questo fosse in grado di interagire. Tali saggi hanno dimostrato che il peptide selezionato è capace di interagire esclusivamente con il recettore Flt-1 mentre non interagisce con i fattori solubili PIGF e VEGF-A e con il recettore KDR/Fik-1.

Per stabilire la relazione tra sequenza aminoacidica individuata ed attività inibitoria è stata eseguita una procedura nota come *Alanine-scanning*. Tale procedura consiste nel sintetizzare per ogni posizione aminoacidica, un peptide che presenta tale posizione sostituita con l'aminoacido L-Alanina. L'analisi di tali varianti peptidiche eseguita mediante saggio ELISA rivela l'eventuale presenza di residui cruciali per l'attività del peptide. Gli esperimenti di *Alanine-scanning* hanno dimostrato che l'attività inibitoria osservata dipende strettamente dalla sequenza aminoacidica, infatti tutti i residui aminoacidici sono essenziali per l'attività.

Altro parametro che determina l'attività di un peptide è la sua struttura. Allo scopo di stabilire il contributo della struttura tetramerica all'attività inibitoria mostrata dal peptide 4-23-5, sono stati sintetizzati e analizzati mediante saggio ELISA gli analoghi strutturali del 4-23-5, cioè il monomero, il dimerico e il trimero con sequenza 4-23-5. Il saggio funzionale ha dimostrato che la struttura tetramerica è essenziale per l'attività inibitoria del peptide, infatti solo il tetramero è capace di dare inibizione, il trimero che manca di una sola sequenza tri-peptidica mostra una considerevole perdita di attività, mentre il dimerico ed il monomero non presentano attività.

Prima di usare il peptide in saggi su colture cellulari, è stata verificata la sua stabilità alle proteasi. Una quantità nota di peptide è stata incubata con siero fetale bovino al 10%, quindi è stata misurata la concentrazione peptidica nel tempo mediante cromatografia HPLC. Il peptide 4-23-5 mostra stabilità fino a 24 ore di incubazione (24 è il tempo massimo analizzato) come atteso avendo usato aminoacidi non naturali.

Il peptide selezionato è stato usato per valutare la capacità di inibire la fosforilazione del recettore Flt-1. La stimolazione con PIGF (10 ng/ml) per 10 minuti di cellule 293 over-esprimenti il recettore Flt-1, è capace di indurre un'elevata fosforilazione di tale recettore, dovuta alla maggiore affinità che tale proteina presenta per Flt-1 rispetto a VEGF-A. Il peptide selezionato è stato usato a due diverse concentrazioni 4.0 e 20 μM insieme a PIGF. Dopo la stimolazione le cellule sono state lisate e il recettore Flt-1 è stato immunoprecipitato dal lisato proteico totale, quindi mediante *western blotting* è stata valutata la percentuale di recettore fosforilato rispetto alla quantità totale di recettore. Il peptide 4-23-5 è in grado di inibire la fosforilazione di Flt-1 indotta da PIGF in maniera dose-dipendente, inibendo quindi il primo evento molecolare che attiva la trasduzione del segnale attraverso il recettore Flt-1 e che attiva la risposta angiogenica.

Il peptide individuato è stato successivamente usato nel saggio di *capillary-like tube formation* (CTF) per valutare la capacità di inibire l'angiogenesi *in vitro* su cellule, e sia nel saggio di angiogenesi della membrana corioallantoidea dell'embrione di pollo (CAM) che nel saggio di neo-vascularizzazione della cornea (CNV). per valutare la sua attività *in vivo*. Il saggio CTF è ampiamente utilizzato per testare la capacità angiogenica o anti-angiogenica di sostanze: cellule endoteliali primarie cresciute su un supporto costituito da

estratti di matrice extracellulare (Matrigel) in presenza di specifici fattori di crescita, sono in grado di formare una rete di capillari primitivi. Esperimenti preliminari hanno dimostrato che i fattori PIGF e VEGF-A usati su cellule endoteliali umane del cordone ombelicale (HUVEC), ad una concentrazione di 100 ng/ml, sono capaci di indurre la formazione di una rete di capillari. Il peptide 4-23-5 è capace di inibire la formazione di tale organizzazione indotta sia da PIGF che da VEGF-A, mostrando un'attività dose-dipendente.

Nel saggio CAM, sfere pre-adsorbite con VEGF-A sono state poste sulla membrana corioallantoidea dell'embrione di pollo all'undicesimo giorno di sviluppo, l'attività angiogenica di VEGF-A viene valutata dopo 72 ore dall'impianto contando il numero di vasi che convergono verso l'impianto stesso. In tale saggio è stata utilizzata solo la proteina VEGF-A capace di indurre angiogenesi agendo su entrambi i recettori Flt-1 e Flk-1. Il peptide 4-23-5 è stato usato insieme a VEGF-A per valutare la capace di inibire l'attività pro-angiogenica di questa. I risultati ottenuti mostrano che il peptide selezionato è in grado di inibire l'attività di VEGF-A in maniera dose-dipendente, dando una completa inibizione con 0.25 nmol mentre 0.025 nmol sono in grado di dare un'inibizione del 30%. L'attività osservata è specifica in quanto un peptide tetramerico di controllo non è capace di dare inibizione.

Recentemente è stato dimostrato il ruolo della forma solubile di Flt-1 nel prevenire la vascolarizzazione della cornea. L'assenza di vascolarizzazione della cornea è fondamentale per l'ottimale trasparenza ottica e per una visibilità chiara, quindi in tale tessuto esiste un preciso meccanismo molecolare che in condizioni fisiologiche previene l'angiogenesi. Nella cornea è presente una grande quantità di forma solubile di Flt-1 mentre è assente la forma di membrana, è inoltre presente VEGF-A ma è assente il recettore Flk-1. In condizioni fisiologiche Flt-1 solubile è capace di titolare VEGF-A impedendogli di stimolare le cellule endoteliali della sclera (che esprimono Flk-1), inducendo angiogenesi nel tessuto. Tale meccanismo è stato dimostrato mediante l'utilizzo dell'anticorpo anti-Flt-1, infatti l'iniezione di questo nella cornea induce angiogenesi. Sulla base di tale modello, la cornea risulta essere la piattaforma ideale per analizzare molecole anti-Flt-1, infatti una molecola capace di legare tale recettore, iniettata nella cornea, è capace di sequestrare Flt-1 solubile inducendo angiogenesi. Paradossalmente una molecola capace di legare Flt-1, quindi con attività anti-angiogenica, nella cornea risulta essere pro-angiogenica. Allo scopo di valutare la specificità del tetramero selezionato per Flt-1, sono state iniettate nella cornea di topi Balb/c 0.4, 4.0 e 20 nmol di peptide bloccante e 20 nmol di peptide tetramerico di controllo. Dopo 7 giorni dalle iniezioni, è stata osservata la formazione di nuovi vasi, i topi sono stati sacrificati e da questi è stata isolata la cornea. I vasi formati in seguito ad angiogenesi sono stati individuati mediante l'analisi di immunofluorescenza usando quale marcatore CD31, specifico per le cellule endoteliali, mentre i vasi linfatici sono stati evidenziati usando come marcatore Lyve-1, che marca solo le cellule linfatiche. L'analisi ha dimostrato che il peptide 4-23-5 è capace di indurre vascolarizzazione della cornea in maniera dose-dipendente e l'attività osservata è specifica in quanto il peptide tetramerico di controllo anche se usato alla più alta quantità (20 nmol) non mostra nessuna induzione. Tale risultato conferma la specificità del peptide nel legare solo il recettore Flt-1 e non Flk-1, precedentemente osservata *in vitro* nei saggi ELISA eseguiti con il peptide immobilizzato. Inoltre la presenza nella cornea dei nuovi vasi ancora dopo 7 giorni dall'iniezione, conferma l'elevata stabilità del peptide già osservata *in vitro*. Infine, nei topi trattati con 20 nmol di peptide bloccante è stata riscontrata una notevole formazione di nuovi vasi linfatici, tale osservazione è in accordo con recenti risultati che dimostrano la capacità di VEGF-A di indurre linfoangiogenesi.

I risultati ottenuti mostrano chiaramente che il peptide selezionato attraverso la deconvoluzione di una collezione tri-peptidica tetramerica formata inizialmente da 27000 molecole, è capace di legare il recettore Flt-1 impedendo il legame dei suoi ligandi, PlGF e VEGF-A con il recettore Flt-1. La molecola selezionata è stabile nei confronti delle proteasi e inoltre non precipita in siero, proprietà che gli consentono di essere utilizzato *in vivo*. Inoltre è capace di inibire la fosforilazione di Flt-1 indotta da PlGF bloccando la cascata di trasduzione del segnale che porta alla risposta angiogenica mediata dal recettore Flt-1.

I risultati ottenuti nel saggio di CTF e nel saggio CAM dimostrano che l'inibizione della sola fosforilazione di Flt-1 è sufficiente a bloccare l'attività pro-angiogenica di VEGF-A *in vivo* e *in vitro*. Infine i risultati del saggio di CNV dimostrano la specificità del peptide per il recettore Flt-1.

Tali risultati dimostrano che il peptide 4-23-5 è un antagonista di Flt-1 e può essere utilizzato nella cura di quelle patologie caratterizzate da un'alterata angiogenesi.

Sulla base del ruolo di Flt-1 sia nelle patologie infiammatorie quali arteriosclerosi e artrite, che nel processo di metastatizzazione, tale molecola potrebbe essere usata anche nella cura di tali patologie.

Inoltre il peptide selezionato rappresenta un modello molecolare per la progettazione di nuovi peptidi ad attività maggiore nei confronti del recettore Flt-1.

Tale lavoro dimostra anche che l'approccio biotecnologico, mediante l'introduzione sia delle tecniche sintetiche che permettono di realizzare collezioni sempre più numerose e con elevata diversità chimica, che dello sviluppo di metodiche sperimentali che rendono l'analisi delle collezioni accurata e veloce, ha rivoluzionato la ricerca di nuove molecole di interesse farmacologico. Infatti, rispetto all'approccio classico che prevede l'analisi di molecole derivanti da svariati sistemi viventi quali piante, microorganismi e animali, l'approccio biotecnologico consente di razionalizzare il processo di selezione e allo stesso tempo aumentare il numero di molecole analizzate.

II. Introduction

2.1 Vasculogenesis and angiogenesis

The vascular system is one of the most important apparatus of an organism. It provides oxygen and nutrients to all tissues removing the metabolic discards. The vascular system is generated by two different processes: *vasculogenesis* and *angiogenesis*. The term vasculogenesis indicates the formation of new blood vessels from endothelial precursor cells (EPCs). During development hemangioblasts, a mesodermal common precursor of endothelial and hematopoietic stem cells (HSCs), aggregate to form the blood islands. These structures proliferate and migrate to form a network of tubular structures characterized by two layers: the internal layer becomes the endothelial coating of the nascent vessels, while the external layer differentiate to smooth muscular cells (SMCs) or pericytes. Between them there is the basal lamina rich in collagen. The fusion of blood islands forms the primitive vascular plexus, in which the venous and arterial systems are already distinct tanks to molecular signaling of Eprin family members [1]. This distinction is revealed by expression on arterial cells of a transmembrane ligand, ephrinB2, whereas its receptor EphB4 is expressed on venous cells [2]. Moreover, recent data demonstrate that ephB2/EphB4 signaling plays an important role in vascular development, especially in the determination and boundary formation between arteries and veins [3]. The vascular plexus is immature and fragile and it needs of the angiogenic process to be stabilized. Angiogenesis is the formation of new blood vessels from pre-existing vessels. It is a complex process divided in two phases. The process starts with the activation of ECs by several stimuli such as hypoxia and ischemia. Hypoxia is an important stimulus for expansion of vascular bed. Initially, cells are oxygenated by simple diffusion of oxygen, but when tissues grow beyond the limit of oxygen diffusion, hypoxia triggers vessel growth by signaling through hypoxia-inducible transcription factors (HIF). HIFs up-regulates many angiogenic genes, such as VEGFs, angiopoietins, fibroblast growth factors and their various receptors, but the induction of VEGF is perhaps the most remarkable-up to 30-fold within minutes. Moreover genes involved in matrix metabolism, including matrix metalloproteinases, plasminogen activator receptors and inhibitors, and collagen prolyl hydroxylase are also regulated [4]. Vessels are destabilized and increase their permeability. This process requires the breakdown by proteinases, including plasminogen activator, metalloproteinases, heparinases, chymases, tryptates and cathepsyns. The ECs can migrate to the sites where angiogenesis is required, where they proliferate and differentiate.

In the second phase there are the blocking of migration and proliferation processes and ECs form a new network of vessels. The new vascular network is stabilized from the addiction of several layers of SMCs that cover vessels. Finally the blood flow can start [5] (Fig. 1).

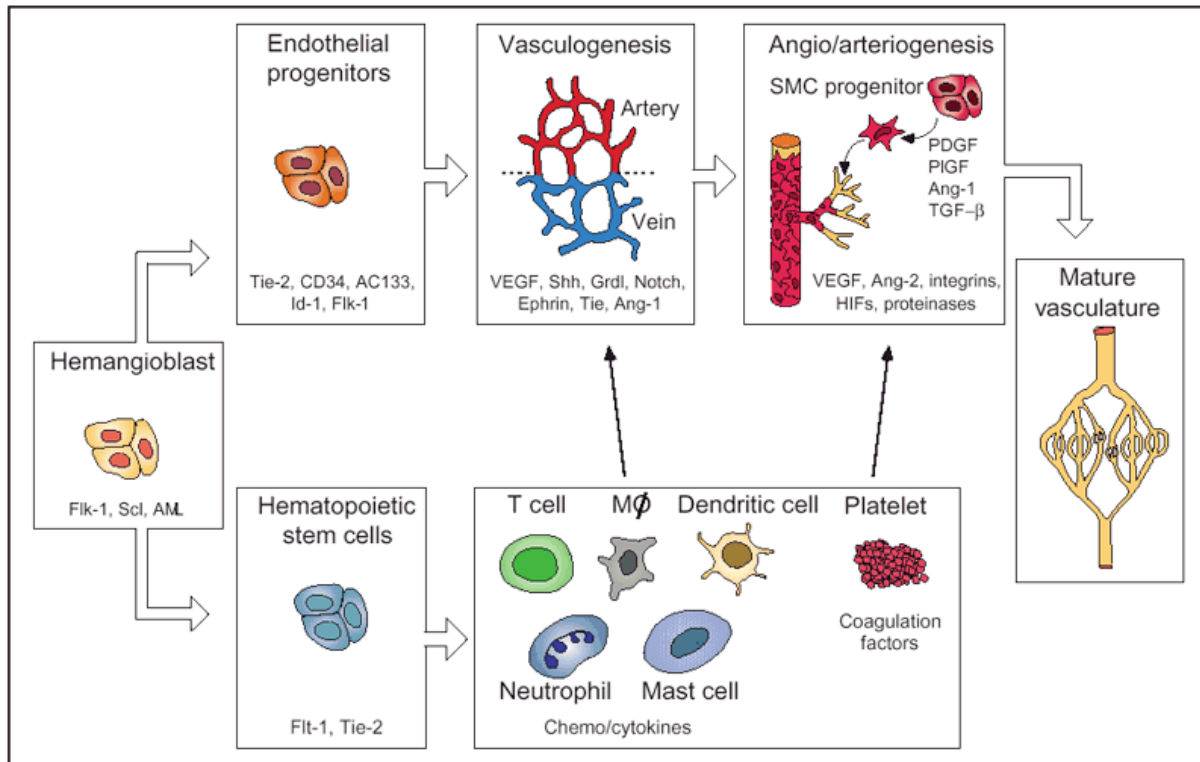


Fig.1: formation of a vascular network. A partial list of molecules is indicated [5]

2.2 Pathological angiogenesis

Pathological angiogenesis is characterized from an excessive or an insufficient vessels formation and is involved in a long list of disorders. The best known diseases characterized by abnormal angiogenesis are cancer, psoriasis, arthritis and blindness, but many additional common disorders such as obesity, asthma, atherosclerosis and infections disease are included and the list is still growing (Table 1). In addition, abnormal vessel obstruction or regression not only cause heart and brain ischemia, but can also lead neurodegeneration, hypertension, pre-eclampsia, respiratory distress, osteoporosis and other disorders (Table 2).

Table 1: Diseases characterized or caused by abnormal or excessive angiogenesis

Organ	Diseases in mice or humans
Numerous organs	Cancer(activation of oncogenes, loss of tumor suppressor); infectious diseases(pathogens express angiogenic genes, induce angiogenic programs or transform ECs); autoimmune disorders(activation of mast cells and leukocytes)
Blood vessels	Vascular malformation(Tie-2 mutation); DiGeorge syndrome(low VEGF and neuropilin-1 expression); HTT(mutation of endoglin or Alk-1); cavernous hemangioma(loss of Cx37 and Cx40); atherosclerosis; transplant arteriopathy
Adipose tissue	Obesity (angiogenesis induced by fatty diet; weight loss by angiogenesis inhibitors)
Skin	Psoriasis, warts, allergic dermatitis, scar keloids, pyogenic granulomas, blistering disease, Kaposi sarcoma in AIDS patient
Eye	Persistent hyperplastic vitreous syndrome(loss of Ang-2 or VEGF164); diabetic retinopathy; retinopathy of prematurity; choroidal neovascularization(TIMP-3 mutation)
Lung	Primary pulmonary hypertension(germline BMPR-2 mutation; somatic EC mutations); asthma; nasal polyps
Intestines	Inflammatory bowel and periodontal disease, ascites, peritoneal adhesions
Reproductive system	Endometriosis, uterine bleeding, ovarian cysts, ovarian hyperstimulation
Bone, joints	Arthritis, synovitis, osteomyelitis, osteophyte formation

Table 2: Diseases characterized or caused by insufficient angiogenesis or vessel regression

Organ	Disease in mice or humans
Nervous system	Alzheimer disease Amyotrophic lateral sclerosis; diabetic neuropathy Stroke
Blood vessels	Atherosclerosis Hypertension Diabetes Restenosis
Gastrointestinal	Gastric or oral ulcerations Crohn disease
Skin	Hair loss Skin purpura, telangiectasia and venous lake formation
Reproductive system	Pre-eclampsia Menorrhagia(uterine bleeding)
Lung	Neonatal respiratory distress Pulmonary fibrosis, emphysema
Kidney	Nephropathy
Bone	Osteoporosis, impaired bone fracture healing

On the base of these evidences, angiogenesis represents an ideal therapeutic target of described diseases, indeed in the last decade the concept of angiogenic therapy has been developed with the aim to individuate new modulators able to inhibit excessive vessel growth or to stimulate angiogenesis [5].

2.3 The concept of angiogenic switch

During development and after birth, blood vessels provide the growing organs with necessary oxygen and nutrients to develop. During adulthood, most blood vessels remain quiescent and angiogenesis occurs only in the cyclic ovary and in placenta during pregnancy. Moreover, ECs maintain their ability of dividing rapidly in response to stimulus, such as hypoxia for blood vessels and inflammation for lymph vessels. Angiogenesis is regulated from several pro- and anti-angiogenic factors, the balance between them prevents angiogenic process. In many disorders pro-angiogenic stimulus becomes excessive destroying the balance and inducing angiogenesis (angiogenic switch). Tumor is one of the best known condition in which angiogenesis is switch on. Several studies demonstrate that tumor cells induce angiogenesis through the secretion of pro-angiogenic factors. Moreover, the inhibition of these factors causes a decrease of tumor vascularization and consequent reduction of tumor growth [6]. Neoplastic cell population can only form a clinically observable tumor if the host produces a vascular network

sufficient to sustain their growth. Furthermore, new blood vessels provide them a gateway through which enter the circulation and metastasize distant sites.

2.4 Molecular bases of angiogenesis

Angiogenesis is a complex process, involving multiple gene products expressed by different cell types, all contributing to an integrated sequence of events. Since the complexity of angiogenesis, the molecular mechanisms involved in induction and regulation of angiogenic process are in part characterized and the list is still growing. Nevertheless, a large number of molecular factors that play a crucial role has been identified on the base of studies performed *in vivo*, on model organisms, and *in vitro*, on ECs systems. One of the most important and more characterized growing factors family is the Vascular Endothelial Growth Factor (VEGF) family.

2.5 VEGF family

The VEGF family plays an integral role in angiogenesis, lymphangiogenesis, and vasculogenesis. The family comprises seven proteins that are designated VEGF-A, VEGF-B and PlGF (Placental Growth Factor) involved in angiogenesis, VEGF-C, VEGF-D that take place in lymphangiogenesis and VEGF-E and VEGF-F recently isolated which biological function are not well known. All factors are biologically active as secreted dimeric and glycosylated proteins, characterized by a conserved structural motif known as cysteine knot. The VEGFs exert their biologic effect through interaction with specific tyrosine kinases receptors. The binding of ligands to their extracellular domain induces the dimerization and autophosphorylation of the intracellular receptor tyrosine kinases. The receptors identified so far are designed VEGFR-1 (also known Flt-, fms-like tyrosine kinase), VEGFR-2 (named KDR (kinase domain receptor) in human and Flk-1 (Fetal liver kinase-1) in mouse), VEGFR-3 (also known Flt-4). In angiogenesis system, VEGF-A binds to both receptors Flt-1 and KDR/Flk-1 inducing vasculogenesis and angiogenesis. In contrast, PlGF and VEGF-B bind exclusively to Flt-1. PlGF shows more affinity for receptor than VEGF-A. VEGF-C and VEGF-D bind to KDR/Flk-1 and Flt-4 inducing lymphangiogenesis. Moreover, VEGF-A and PlGF also bind the co-receptors Neuropilins (NP-1 and NP-2) but the molecular pathways activated has not been fully characterized (Fig.2) [7].

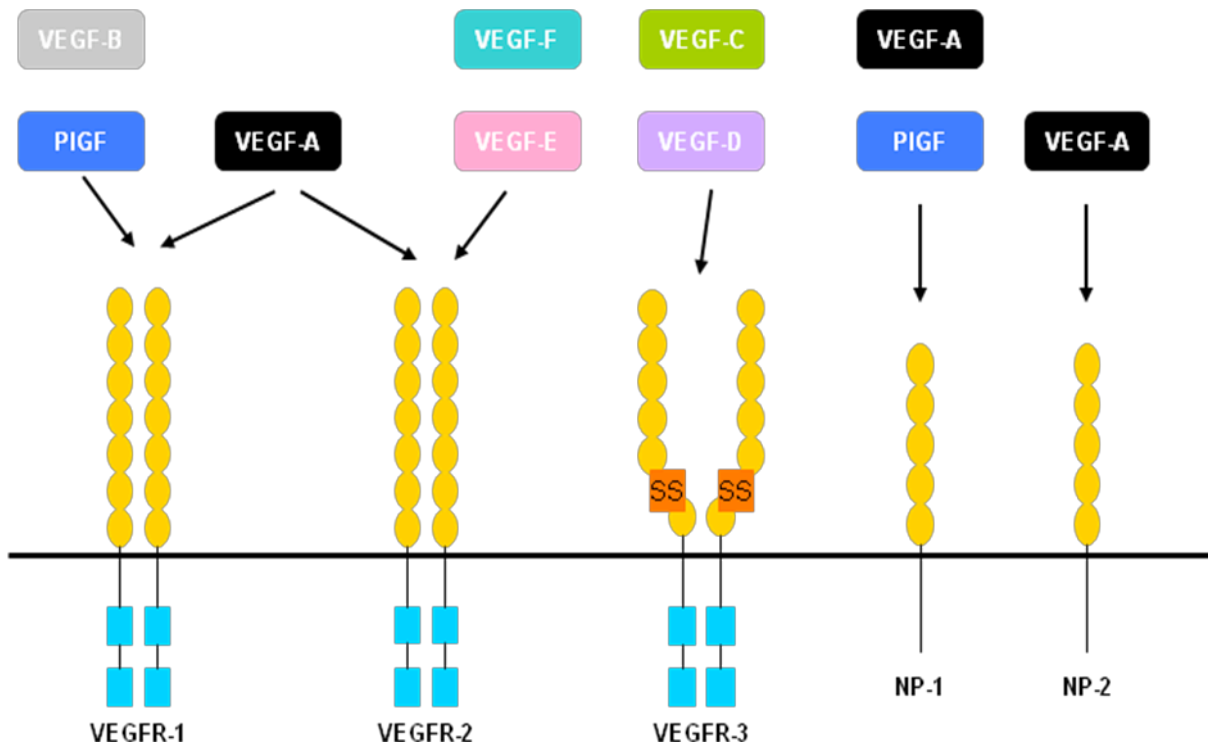


Fig.2: Interaction of VEGF family members with the VEGFR-1, -2 and -3, and Neuropilins-1 and -2.

a) VEGF-A

VEGF-A is the best characterized and the most studied VEGF family member. The VEGF gene which is composed of eight exons and is differentially spliced generates four mature isoforms (VEGF121, VEGF165, VEGF189 and VEGF206) [8]. The numeric designation of the isoforms denotes the number of amino acids composing the molecule. In addition, some less commonly expressed isoforms were identified (VEGF145 and VEGF183) [9]. VEGF165 is the predominant isoform. VEGF-A exerts its biologic effect through interaction with cell-surface receptors Flt-1 and KDR/Flk-1, selectively expressed on vascular endothelial cells, and the Neuropilin co-receptors (NP-1 and NP-2), expressed on vascular endothelium and neurons [10] (Fig. 2). In vivo, VEGF-A expression has been shown to be associated with significant steps in angiogenesis and vasculogenesis [11]. Deletion of a single allele of VEGF-A gene causes embryonic lethality due to vascular defects and cardiovascular abnormalities [12]. Transgenic mice, over-expressing VEGF-A in the skin, have abundant cutaneous angiogenesis and a psoriasis-like skin condition [13] and develop experimental tumor that growth more rapidly than in wild type mice [14]. In contrast, mice with a mutated VEGF-A exhibit delayed wound healing [15]. Moreover, VEGF-A is expressed in practically all solid tumors studied as well as in some hematological malignancies [16], indeed correlations have been found between the level of VEGF-A expression, disease progression and survival of several cancers [14]. VEGFR-2 appears to be the main receptor responsible for mediating the pro-angiogenic effects of VEGF-A [16]. VEGF-A is the most potent pro-angiogenic protein described to date. It induces proliferation, sprouting and tube formation of endothelial cells (ECs) [16]. It is also a potent survival factor for ECs and has been shown to induce the expression of anti-apoptotic proteins in these cells [17]. In hypoxic condition VEGF-A transcription is strongly up-regulated by HIF-1 [18], mRNA stability is increased by binding of proteins to specific sequence in the 3'UTR [19], and an internal ribosomal entry site allows preserved translation in the face of normal cellular hypoxic shutdown [20]. The biological activity of

secreted VEGF-A is further influenced by hypoxia-inducible expression of Flt-1 receptor [21] inducing an up-regulation of soluble Flt-1 [22] which inhibits VEGF activation, and post-transcriptional regulation of KDR/Flk-1 receptor [23].

VEGF-A also causes vasodilatation by inducing the endothelial nitric oxide synthase and so increasing nitric oxide production [24]. It induces HSC mobilization from the bone marrow, monocyte chemoattraction and osteoblast-mediated bone formation [16]. Many cytokines including platelet-derived growth factor, basic fibroblast growth factor, epidermal growth factor and transforming growth factors induce VEGF-A expression in cells [25].

b) PIGF

PIGF was originally discovered in placenta [26] but it is also expressed in heart and lungs [27]. PIGF gene transcripts two isoforms named PIGF-1 and -2 by alternative splicing process. They differ in size, PIGF-2 contains a sequence of 21 aminoacids that confers it the ability to bind heparan sulfate proteoglycans [28].

PIGF binds specifically to Flt-1 with strong affinity than VEGF-A and VEGF-B. Activation of Flt-1 by either PIGF or VEGF-A induce different gene expression profiles reflecting the different phosphorylation pattern in the tyrosine kinase domain of Flt-1 [29]. Moreover, if co-expressed from the same cells, PIGf and VEGF-A can form an heterodimers able to bind Flt-1 or to induce Flt-1-KDR/Flk-1 heterodimerization [30]. Autiero et al have demonstrated that both PIGF and PIGF/VEGF-A heterodimers can lead the transactivation of Flk-1 through Flt-1 activation enhancing the response to VEGF-A.

PIGF knockout mice do not have an evident phenotype. They born at a mendelian frequency and are healthy and fertile. However, these mice present an impaired pathological angiogenesis as demonstrated in different models of diseases like cancer, diabetic retinopathy and myocardial infarct. Moreover healing of skin incisions progressed more slowly in PIGF knockout mice versus wild-type, while collateral growth model reveals an enlarged and tortuous collateral growth in wild-type but not in PIGF deficient mice, and this phenotype is accompanied from a reduced macrophages infiltration. The absence of PIGF also causes a reduced plasma extravasation [31]. Overexpression of PIGF in the skin of transgenic mice results in a significant increase in the number and size of skin blood vessels as well as in enhanced vascular permeability [32]. Conversely, PIGF deficiency resulted in a diminished and abbreviated inflammatory response, together with a reduction of inflammatory angiogenesis and edema formation [33].

These data indicate that PIGF is involved only in pathological angiogenesis and not in physiological angiogenic process.

c) VEGF-B

The human VEGF-B gene contains eight exons and six introns. The promoter region of VEGF-B gene contains some important differences relative to those of VEGF-A, and these are likely to explain differences in regulation by physiological stimuli [34]. The VEGF-B promoter lacks HIF-1 sites found in the VEGF-A promoter. Accordingly, hypoxia, which can induce VEGF-A expression, does not appear to regulate levels of VEGF-B [35]. VEGF-B gene expresses two isoforms VEGF-B₁₆₇ and VEGF-B₁₈₆ generated as a result of alternative splicing process. These proteins contain an identical 116 aminoacid N-terminal region, that includes the receptor binding domain. The C-terminal region differs between them and affects their distribution in the body. VEGF-B₁₆₇ has a C-terminal heparin binding domain, thus it is associated with cell surface, in contrast, VEGF-B₁₈₆ does not bind heparin and is thus likely to circulate freely. VEGF-B binds to Flt-1 receptor, since the activation of Flt-1 induces a poor mitogenic signal for ECs, VEGF-B is an inefficient EC mitogen [36].

In vivo, VEGF-B is highly expressed in striated muscle, myocardium and brown fat [37]. Moreover, VEGF-B levels increase both throughout development and after birth, closely correlating with the progression of cardiac angiogenesis [38]. Mice deficient in VEGF-B present smaller heart size and impaired recovery after experimentally induced myocardial infarctions suggesting that the regeneration of coronary collaterals through arteriogenesis could at least in part dependent on VEGF-B [38]. VEGF-B might have a role also in inflammatory angiogenesis as demonstrated by knockout mice which displayed reduced angiogenic response in collagen-induced arthritis [39]. In pathology, high levels of VEGF-B expression were associated with metastasis to lymph node in colorectal cancer. Future studies should provide a more comprehensive understanding of the role of VEGF-B in cancers to validate it as a therapeutic target.

d) VEGF-C

VEGF-C is produced as a precursor protein, which is activated by intracellular secretory proprotein convertases furin, PC5 and PC7 [40].

During development VEGF-C is expressed along its receptor Flt-4 mainly in regions where lymphatic vessels develop [41]. The expression then decrease in most tissue, remaining high in lymphatic nodes. VEGF-C induce selectively lymphangiogenesis without accompanying angiogenesis as demonstrated by early experiments in transgenic mice. Mice lacking both VEGF-C alleles showed failure in lymphatic vessels development and they died of edema [41]. Likewise, loss of one VEGF-C allele results in lymphedema characterized by hypoplasia of the cutaneous lymphatic vessels indicating that the VEGF-C protein concentration is imperative for the development of the lymphatic vasculature [41]. VEGF-C mRNA transcription is induced in ECs in response to pro-inflammatory cytokines indicating that it could regulates lymphatic vessel function during inflammation [41]. This evidence reflects the role of the lymphatic vasculature in the control of immune function and leukocyte trafficking. VEGF-C is also chemotactic for macrophages and its receptor Flt-4 is expressed by a fraction of peripheral blood monocytes and activated tissue macrophages [42]. Moreover, several clinicopathological studies of cancer patients have demonstrated a correlation between VEGF-C expression and lymphatic invasion by metastatic cells [43, 44].

e) VEGF-D

VEGF-D is closely related to VEGF-C by virtue of the unique presence of N- and C-terminal extensions that other VEGF family members lack [45]. It binds to and activates KDR/Flk-1 and Flt-4 stimulating growth of vascular and lymphatic ECs *in vivo* [46]. VEGF-D is present in most human tissues, most abundantly in the lungs and skin during embryogenesis. In experimental tumors VEGF-D plays a pivotal role in stimulating lymphangiogenesis and lymphatic metastasis [47]. VEGF-D is expressed by many tumor types and has been proposed to have a role in tumor angiogenesis and lymphangiogenesis in melanoma, pancreatic cancer, esophageal squamous cell carcinoma, breast cancer and lung cancer.

f) VEGF-E

The VEGF-E members show only 20% to 25% amino acid identity with VEGF-A. The first isoform of VEGF-E is the VEGF-_{ENZ-7} which is encoded by the Pox viruses of the Orf family [48]. This ligand specifically binds at high affinity and activates KDR/Flk-1 resulting in receptor autophosphorylation and rise in free intracellular Ca²⁺ concentration [49]. VEGF-E can stimulate angiogenesis efficiently. Two other VEGF-E family members, VEGF-_{ENZ-2} and VEGF-_{E_{D1701}} were also isolated, both with essentially the same activity as that of VEGF-_{ENZ-7} [50, 51]. One significant characteristic of VEGF-_{ENZ-7} is its very strong affinity

to KDR/Flk-1 and ability to induce significant angiogenesis *in vivo* with few side effects. Thus, VEGF-E family members should be carefully studied as candidates for a potential angiogenic factor for clinical use in pro-angiogenic therapy .

g) VEGF-F

Recently a seventh member of the VEGF family with unique properties, VEGF-F, was identified from snake (viper) venom. VEGF-F consists of two VEGF-related proteins designated vamin (110 residues) and VR-1 (109 residues) that have a 50% structure homology with VEGF₁₆₅ and bind selectively to VEGFR-2. VEGF-F was found to exhibit potent biological activity both *in vitro* and *in vivo* when compared with VEGF₁₆₅ [52]. VEGF-F contains a short C-terminal heparin-binding region and the C-terminal peptide of VEGF-F exhibits a specific blockage of VEGF-A₁₆₅ activity both *in vitro* and *in vivo* [53].

h) VEGFR-1 (Flt-1)

Flt-1 (fms-like tyrosine kinase; Flt-1) is composed of seven extracellular immunoglobulin (Ig) like domains, a single transmembrane region and an intracellular tyrosine kinase domain [54]. VEGFR-1 is recognized by VEGF-A, VEGF-B and PlGF, showing the highest affinity for PlGF. During development, it is expressed less strongly than KDR/Flk-1, in angioblasts and in the endothelium. Its expression subsides during later embryonic stages [55, 56]. VEGFR-1 is expressed in ECs as well as in monocytes/macrophages [57], placental trophoblasts, osteoblasts renal mesangial cells [58], smooth muscle cells [59] and also in bone marrow stem/progenitors derived cells [60] and its expression is up-regulated by hypoxia via a HIF-1-dependent mechanism [21]. Flt-1 null mutant mice die at embryonic stage E 8.9-9.0 due to the over-growth and disorganization of blood vessels [56] suggesting Flt-1 involvement in reorganization and stabilization of primitive vascular plexus. In contrast mice lacking the tyrosine kinase domain of Flt-1 are vital and fertile but in these mice the tumor growth and tumor angiogenesis are inhibited, suggesting that the tyrosine kinase domain is required for pathological angiogenesis. The activation of Flt-1 by PlGF, is not only crucial for ECs stimulation during neo-angiogenesis process, but plays a fundamental role also in stabilization of neo-vessels through the recruitment of SMC and in the recruitment and differentiation of monocyte-macrophage cells [31], [61]. Recent studies have emphasized the effects of VEGFR-1 in hematopoiesis and recruitment of endothelial progenitors. Hattori et al. have shown that PlGF promotes recruitment of VEGFR-1(+) HSCs from a dormant to a proliferative bone marrow environment, favoring differentiation and reconstitution of hematopoiesis [60]. Moreover, recently Kaplan et. al. have demonstrated the pivotal role of Flt-1 in the regulation of metastasis, they have published that Flt-1 marks bone-marrow derived haematopoietic progenitor cells that migrate to tumor-specific pre-metastatic sites and form cellular cluster before the arrival of tumor cells [62]. In fact, preventing VEGFR1 function using antibodies or by the removal of VEGFR1⁺ cells from the bone marrow of wild-type mice abrogates the formation of these pre-metastatic clusters and prevents tumor metastasis. A naturally occurring, soluble form of VEGFR-1 (sFlt-1) exists and it could act as an efficient specific antagonist of VEGF-A, VEGF-B or PlGF. Soluble Flt-1 is expressed in several tumors, including astrocytic tumors and breast cancer, although its actual role in these tumors remains to be investigated [63]. Moreover, recently Ambati et. al. have demonstrated that sFlt-1 has a crucial role in the maintenance of corneal avascularity. In the cornea is absent the membrane bound form of Flt-1, while is present an high amount of sFlt-1 essential for preventing binding of VEGF-A to Flk-1 receptor expressed on conjunctiva creating an anti-angiogenic barrier. When an injury of cornea occurs, there is an increase of VEGF-A level, it titles sFlt-1 and binds to Flk-1 inducing angiogenesis [64].

i) VEGFR-2 (KDR/Flk-1)

VEGFR-2 is known as KDR (Kinase Domain Receptor) in human and Flk-1 (Fetal Liver Kinase-1) in mouse. Like Flt-1 it bears an extracellular region with seven Ig-like domains, a transmembrane domain and a tyrosine kinase domain with about 70-amino-acid insert. VEGFR-2 is recognized by VEGF-A, VEGF-C, VEGF-D and VEGF-E. It is expressed in ECs, neuronal cells, osteoblasts, megakaryocytes and hematopoietic stem cells [16], [65]. Flk-1 gene knock-out mice die at E8.0-8.5 due to a lack of vasculogenesis. This indicates that VEGFR-2 signaling is essential for the differentiation of VEGFR-2-positive endothelial precursor cells into vascular ECs and for their proliferation [66]. This process goes through the activation of the RAF-MEK-ERK pathway. Moreover, a role of VEGFR-2 in hematopoiesis has been described, indeed KDR has been identified on a subset of multipotent human HSCs [67]. Since KDR/Flk-1 is the main receptor for ECs proliferation and differentiation in response to VEGF-A, the first approach for anti-angiogenic therapy of tumor has been focalized to inhibit this pathway. At this regards, an humanized antibody against VEGF-A, bevacizumab (Avastin) is actually used in combination with chemotherapy [68].

j) VEGFR-3 (Flt-4)

Flt-4 has only six Ig-homology domains [69] and it is recognized by VEGF-C and VEGF-D. In humans, Flt-4 expression was correlated with transient lymphangiogenesis in wound healing and was upregulated in blood vessel endothelium in chronic inflammatory wounds [70]. Thus, VEGFR-3 is believed to play various roles in cardiovascular development and remodeling of primary vascular networks during embryogenesis and enhancing lymphangiogenesis in adulthood. More interesting is its role in pathology, indeed VEGFR-3 is distributed widely in vascular tumors and can be considered as a marker of endothelial cell differentiation of vascular neoplasms [71]. Moreover, Jennbacken et al. showed that increased expression of VEGF-C and VEGFR-3 plays a role in prostate cancer progression and lymph nodes metastasis [72] and its activation accompanied by upregulation of its ligands were also observed in melanoma and breast cancer [73]. Accordingly with these data, VEGFR-3 blockade significantly inhibited lymphangiogenesis and lymph node metastasis [72].

k) Neuropilin-1 and -2

Neuropilin NP-1 was identified initially as a cell-surface glycoprotein that served as a receptor for the semaphorin/collapsins, a large family of secreted and transmembrane proteins that serve as repulsive guidance signals in axonal and neuronal development [74], [75]. NP-1 binds VEGF-A and PlGF while NP-2 binds only VEGF-A (Fig. 2). During embryonic development, NP-1 is expressed in the nervous, cardiovascular, and skeletal systems [74], [76], whereas in adults it is also expressed in ECs, tumor cells, lung, heart, liver, kidney, pancreas, osteoblasts, and bone marrow stromal cells [77], [78]. NP-2 has a similar expression pattern. NP-1 acts as a co-receptor enhancing VEGF-A-VEGFR-2 interactions, forming complexes with VEGFR-1 and augmenting tumor angiogenesis *in vivo*, while NP-2 is expressed on lymphatic ECs, and mutated NP-2 induces abnormalities in the formation of small lymphatic vessels and lymphatic capillaries in mice [79]. The role of NP-1 in the development of the vascular system has been demonstrated by gene-targeting studies, documenting embryonic lethality in null mice [80]. Interestingly, recent studies have linked NP-2 to lymphatic vessel development [79].

2.6 Molecules developed for angiogenic therapy: an overview

In the last decade, the concept of angiogenic therapy has been developed as a strategy to treat cancer inducing the regression of vessels that provide sustenance of tumor mass. Recently, it has been re-defined and extended to all pathologies characterized from a reduced or excessive angiogenesis. Consequently, more attention has been devoted to molecular factors with anti- or pro-angiogenic properties. Different biotechnological approaches like production of recombinant proteins and monoclonal antibodies, and identification of small interfering molecules have been used to search for modulators of angiogenesis pathways. Due to the biological and functional properties above described, VEGF-A and KDR/Fik-1 receptor have been chosen initially as preferential target for angiogenic therapy [81]. In fact, the first anti-angiogenic drug is the humanized monoclonal anti-VEGF-A blocking antibody Bevacizumab (Avastin, Genetech, Inc.) [68]. Although it has showed encouraging results in patients with colorectal cancer, non-small cell lung carcinoma and breast cancer demonstrating that the angiogenic process could be a real target for cancer therapy, its activity is responsible for different undesired effects as thrombosis, pulmonary hemorrhage, hypertension and proteinuria [82], [83]. Moreover, Avastin alone did not show significant efficacy and it must be used in combination with traditional chemotherapy agents. Moreover, several classes of tyrosine kinase inhibitors have been developed [83]. These inhibitors are small molecules that bind to TP-binding site of the tyrosine kinase domain of VEGFRs, resulting in a blockade of intracellular signaling. In table 3 are reported the most important VEGFR small-molecule inhibitors, the specific molecular target, the activity in term of IC₅₀, and the current phase of clinical development

Table 3: VEGFR inhibitors, molecular targets, IC₅₀ and phase of clinical development

Agent	Molecular target	IC ₅₀ μM							Development
		Flt-1	KDR/Fik-1	Flt-4	PDGFR-β	c-Kit	Raf	Flt-3	
Vatalinib (PTK/ZK)	VEGFR-1, -2, -3, PDGFR-β, c-Kit	0,077	0,037	0,66	0,58	0,73	-	-	Phase III
Semaxanib (SU5416)	VEGFR-1 and -2	0,008	0,20	-	0,68	0,47	-	-	Stopped
Sutinib (SU11248)	VEGFR-1 and -2, PDGFR, c-Kit, Flt-3	0,002	0,009	0,017	0,002	0,0022	-	0,25	Phase III
Sorafenib (BAY 43-9006)	VEGFR-2 and -3, RAF, PDGFR, c-Kit, RET	-	0,09	0,02	0,057	0,068	0,006	-	Phase III
ZD6474	VEGFR-2, EGFR, FGFR-1, RET	1,6	0,04	0,11	1,1	>20	-	-	Phase II
SU6668	VEGFR-2, PDGFR-β, FGFR-1, c-Kit	-	2,1	-	0,008	0,1	-	-	Stopped
AG-013736	VEGFR-1, -2, and -3, PDGFR-β, c-Kit	0,0012	0,00025	0,00029	0,0025	0,0020	-	-	Phase I/II
AZD2171	VEGFR-1, -2, and -3, PDGFR-β, c-Kit	0,005	<0,001	<0,003	0,005	0,002	-	>1	Phase I
AEE788	VEGFR-1 and -2, EGFR	0,059	0,077	0,33	0,32	0,70	2,8	0,73	Phase I

The major part of these molecules present an IC₅₀ value in concentration range of nM, they are orally bio-available and all are in clinical trial of phase II or III. Unfortunately all these molecules present a lot of side effects such as hypertension, nausea, vomiting, fatigue, proteinuria and much more [83] due to their wide range of specificity, in fact they act on a large number of receptors, some of them involved in different biological processes.

2.7 PIGF/Flt-1 pathway: a new therapeutic target?

The first target for angiogenic therapy has been VEGF-A and its receptor KDR/Flk-1. In fact, VEGF-A was initially used to stimulate the angiogenesis after ischemic injury [84]. The trials have been conducted either by administering recombinant proteins or by gene transfer using viral vectors or naked plasmids [85]. One of the major limitations in using VEGF-A for stimulation of angiogenesis is its potent activity on vascular permeability. High levels of circulating VEGF-A, such as those obtained in mice over-expressing VEGF-A or those produced by adenoviral gene transfer, cause leaky vessels associated lethal edema [86]. In a study conducted in patients with lower extremity ischemia, 34% of patients developed edema when treated with naked plasmid DNA encoding VEGF-A. This side effect was confined to patients with critical limb ischemia, while it was absent from less severely ill patients with stress-related ischemia [84]. On the other hand, results obtained with Avastin show that inhibition of VEGF-A alone did not resolve cancer as expected but it induces only a weak effect reducing the growth of cancer, moreover it is accompanied from several collateral effects due to the involvement of VEGF-A in different physiological process. These data demonstrate that interfering on VEGF-A/KDR/Flk-1 pathway stimulating or inhibiting it, nevertheless it produces expected angiogenesis affect, it causes important undesired effects.

In contrast, data obtained on PIGF and Flt-1 demonstrate that their role is mainly confined to pathological angiogenesis. In *Plgf*^{-/-} mice, pathological angiogenesis is inhibited. Tumors induced by inoculation of *Plgf*^{-/-} embryonic stem (ES) cells are smaller and less vascularized than tumors induced by inoculating wild type ES and are comparable with VEGF-A deficient tumors induced by inoculation of *Vegf*^{-/-} ES cells. Thus, the loss of PIGF impairs the growth of VEGF-A-dependent tumors. At the same time, when conditions similar to the hypoxic ischemic retinopathy have been induced, the loss of PIGF significantly protects mice against intra-vitreous neo-vascularization, venous dilatation, and arterial tortuosity [31]. Thus, a physiological concentration of PIGF is still able to support this pathological events, since hypoxic conditions highly up-regulate VEGF-A, but not PIGF. At the same time, recombinant PIGF is able to stimulate neo angiogenesis in ischemic pathologies with an effect comparable to that observed with VEGF-A, without generate VEGF-A-induced side effect. This view is supported by the results obtained in mice lacking the tyrosine kinase domain of Flt-1, in which the tumor growth and tumor angiogenesis are inhibited, suggesting that the tyrosine kinase domain is strictly required for pathological changes. Flt-1 is also involved in the recruitment of both EPCs and SMCs and plays a pivotal role in the mobilization of bone marrow-derived myeloid progenitors into the peripheral blood, in the infiltration of Flt1-expressing leukocytes in inflamed tissues and in activation of myeloid cells [87]. These activities are crucial for a correct neo-angiogenesis process. Indeed, neutralizing monoclonal anti-Flt-1 antibody are able to strongly prevent tumor angiogenesis, as well as inflammatory disorders and tumor metastasis [62]. All together these data indicate that modulation of the PIGF/Flt-1 pathway could be an innovative and advantageous therapeutic target to treat pathological angiogenesis.

2.8 Aims of the study

In order to identify new modulators of pathway activated by interaction of VEGF family members with Flt-1 receptor, we planned to screen combinatorial peptide libraries.

The aim of this study is the identification of small molecules able to interfere in the VEGFs/Flt-1 interactions, in order to prevent the biological response of this pathway in the pathological angiogenesis.

Combinatorial chemistry has been widely employed for creating a number of different compounds simultaneously and screening rapidly for the identification of active compounds and is regarded as a powerful tool for the discovery of new drugs, catalysts and materials [88].

Among the wide libraries possibility, combinatorial peptide libraries have been the most developed and their synthesis is fully automated. The chemical properties and the elevated number of aminoacids (natural and modified) allow the realization of several different structures such as linear, branched, cyclic or multimeric scaffolds, increasing the number of molecules to assay. The most important event for the development of combinatorial chemistry was the solid phase synthesis method, developed by R. B. Merrifield [89]. Following on many research areas: solid supports, linkers and peptide coupling chemistry, automated synthesis, and screening methods have been developed [90]. Peptide libraries are largely utilized in drug discovery field for the easiness of preparation and purification and the robustness of the available chemistry. A peptide combinatorial library is a collection of several peptides that shared the same structure, the number of different obtained sequences depends both on the number of aminoacids used as building-blocks and on the peptide length, as reported in the following formula: $N=b^L$, in which N is the number of different peptides, b is the number of building-blocks and L is the peptide length. Deconvolution methods of a peptide library evaluates the contribution of each residue for each sequence position activity of peptide. In this study we have screened combinatorial libraries.

2.9 Biotechnological application

The use of recombinant proteins and monoclonal antibodies in therapy has been one of the main successes of biotechnology both on research and industrial production aspects. Nonetheless their use in therapy is limited due to the high costs of production.

Small molecules offer numerous advantages with respect to recombinant proteins. Low molecular weight often allows to escape recognition by the immunity system, small molecules can be more easily produced, and are generally free of contaminants of biological origin, they offer more opportunity for delivery allowing also oral administration and their costs of production are lower with respect to monoclonal antibodies or recombinant proteins.

In this regard, in the last two-decade a great efforts has been done to realize large collections of small molecules for screening purpose as well as small molecules design based on molecular modeling. In vitro analysis of these collections n has been possible thanks to recombinant protein production ability.

Among the opportunity to generate large collection of molecules, combinatorial chemistry has represented one of the main fields of application. Peptide combinatorial libraries represent one of the largely used approaches to search for modulators of protein-protein interaction.

Biotechnology approaches have been developed to fully automate both synthesis of libraries and High-Throughput Screenings (HTS) approaches, which have enormously increased the capacity in term of number of molecules and time reduction for the analysis.

The identification of biologically active small molecule open new perspective in term of industrial biotechnological application, both on new process for active molecule production and the use of selected molecule as chemical scaffold to further develop the molecule in term of target affinity and specificity.

III. Results

3.1 Synthesis and screening of tetrameric tripeptide library

In order to identify new peptides able to inhibit PIGF/Flt-1 interaction, it has been synthesized and screened a tetrameric tripeptide library which structure is shown in figure 3. The library has been prepared using 29 non-natural amino acids plus Glycine (Table 4). Non-natural amino acids have been chosen from the D-amino acids and modified L-amino acids to increase chemical diversity and protease resistance of peptides. The structure contains a lysine core to build the tetrameric scaffold. This structure has been adopted to increase the activity of the molecules that presented the same tripeptide sequence repeated four times (Fig. 3).

Table 4: List of building blocks amino acids used to generate tetrameric tripeptide library

3-letters code	building block
D-Ala	D-Alanine
D-Arg	D-Arginine
D-Arg(Tos)	D-Arginine(N γ -Tosyl)
D-Asn	D-Asparagine
D-Asp	D-Aspartic acid
D-Cys(Acm)	D-Cysteine(S-acetamidomethyl)
D-Gln	D-Glutamine
D-Glu	D-Glutamic acid
D-His	D-Histidine
D-Ile	D-Isoleucine
D-Leu	D-Leucine
D-Lys	D-Lysine
D-Met	D-Methionine
D-Phe	D-Phenylalanine
D-Pro	D-Proline
D-Ser	D-Serine
D-Thr	D-Threonine
D-Trp	D-Tryptophan
D-Tyr	D-Tyrosine
D-Val	D-Valine
Gly	Glycine
L-Cha	L-Cyclohexylalanine
L-Cys(Acm)	L-Cysteine(S-acetamidomethyl)
L-Cys(Bzl)	L-Cysteine(S-benzyl)
L-Cys(p-MeBzl)	L-Cysteine(S- <i>p</i> -methyl-benzyl)
L-Cys(tBu)	L-Cysteine(S- <i>tert</i> -butyl)
L-Glu(β -OAlI)	L-Glutamic acid-(β -allyl)
L-Met(O)	L-Methionine-sulphone
L-Met(O) ₂	L-Methionine-sulphoxide
β -Ala	β -Alanine

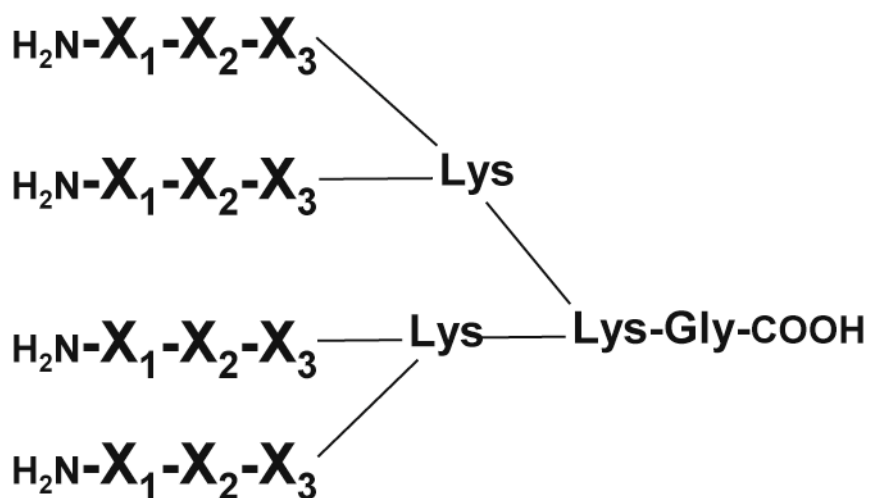


Figure 3: Structure of tetrameric tripeptide library. X letter denotes the unknown aminoacids to determine by deconvolution process.

The library was synthesized using the mix and split protocol [91] and after the first synthesis it was composed by 30 pools each of them contained 900 different peptides, realizing an initial complexity of 27,000 molecules. Pools differed only for the aminoacid in N-terminal position that varied among those chosen to synthesize the library, identifying the 30 pools, here indicated as pool 1 to pool 30. Peptide mixture were obtained in high yield (about 70%) as calculated assuming an average molecular weight of 2130 amu for each library component, and with an average purity of the crude products >85% (as determined for the single molecules assayed during the last screening round, table 4). The LC-MS analyses of some selected 30-components mixtures showed that the expected molecules were all equally represented and MWs were in very good agreement with those calculated.

Deconvolution of library was carried out by the iterative process [88] by an ELISA-based competition assay. In iterative approach a progressive selection is performed, choosing one aminoacid at a time for each position. Sequence of sub-libraries is dictated by the results of the previous one. ELISA-competition assay allows the identification of molecules able to inhibit the interaction of PIGF with the immobilized Flt-1 receptor. Screening was performed on PIGF/Flt-1 system because PIGF presents more affinity for Flt-1 than VEGF-A. At every steps of screening, peptides pools were assayed with a molar excess of 1.000-fold (calculated for each single peptide) over PIGF. In the first round of screening the pool with the aminoacid 4 in N-terminal position (pool 4-X-X, where X indicated all the possible aminoacids used for library synthesis), showed the best inhibition activity pwith a percentage of binding of 58% (Fig. 4). The active pool 4 was assayed in a dose-dependent competition assay using 500, 1.000, 1.500 and 2.000 fold excess and comparing it with pools 2 that showed about 20% of inhibition, and pool 14 that was inactive (Fig. 5).

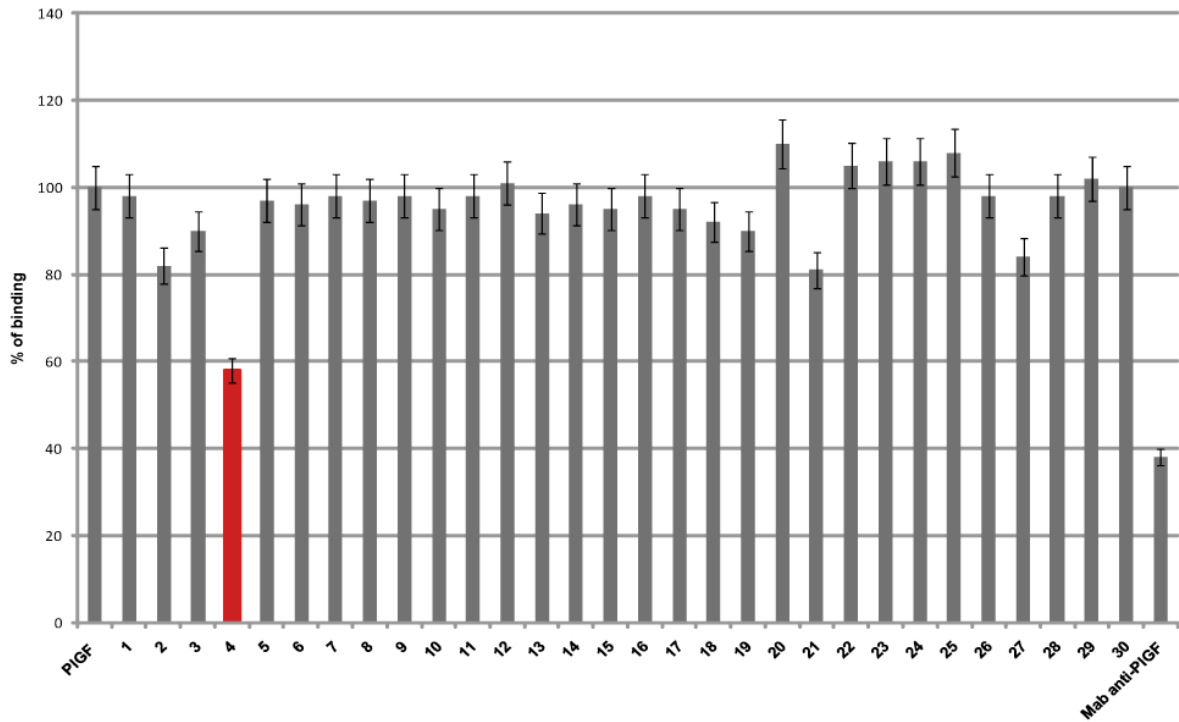


Figure 4: First screening of tetrameric tripeptide library performed by ELISA- based competition assay. Histogram reports the percentage of binding of each pool calculated assuming the binding of PIGF to Flt-1 as the 100% of binding. Monoclonal anti-PIGF antibody was used as inhibition control. In red was reported pool showing the best inhibition.

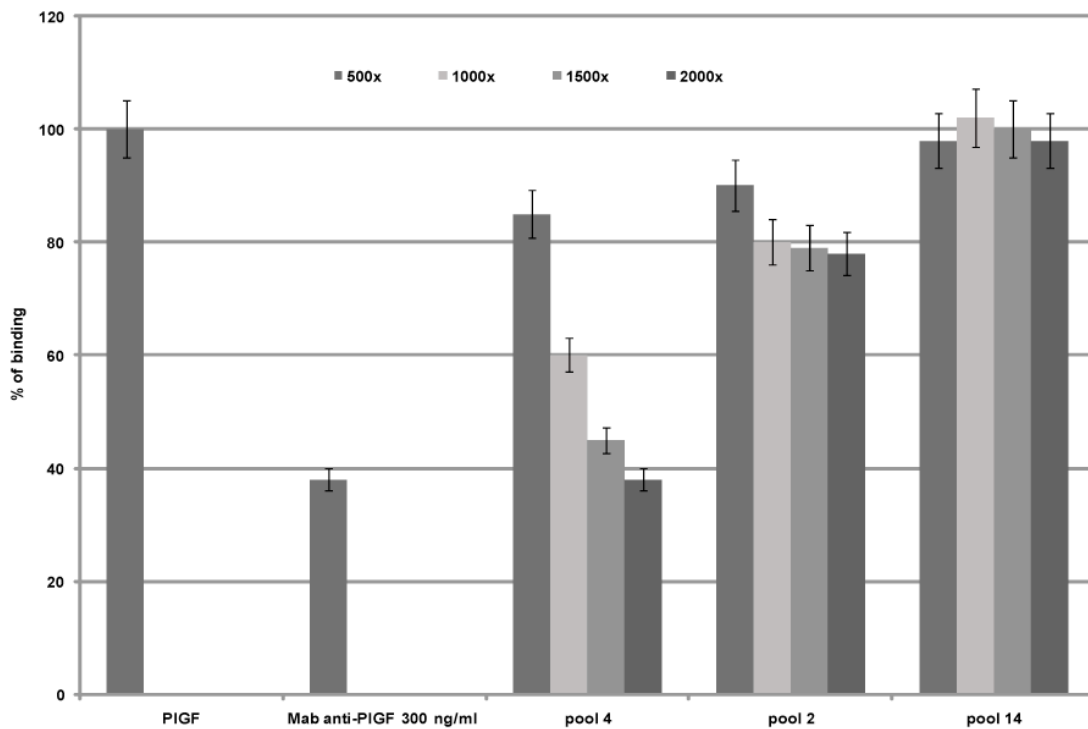


Figure 5: Dose-dependent ELISA-competition assay performed with positive pool 4 and pools 2 and 14 used as negative control.

Based on the results obtained in first screening the analysis of library was continued synthesizing sub-libraries of generic sequence 4-B-X. This sub-library was made of 30 pools, each of them containing 30 peptides, with the aminoacid 4 in N-terminal position, the second position (indicated as B), identify each pool with the 30 building-blocks used to synthesize the library, while the third position (indicated as X) was random. The pools were assayed by ELISA-competition assay using a molar excess of 1.000-fold (calculated for each single peptides) over PIGF (Fig. 6).

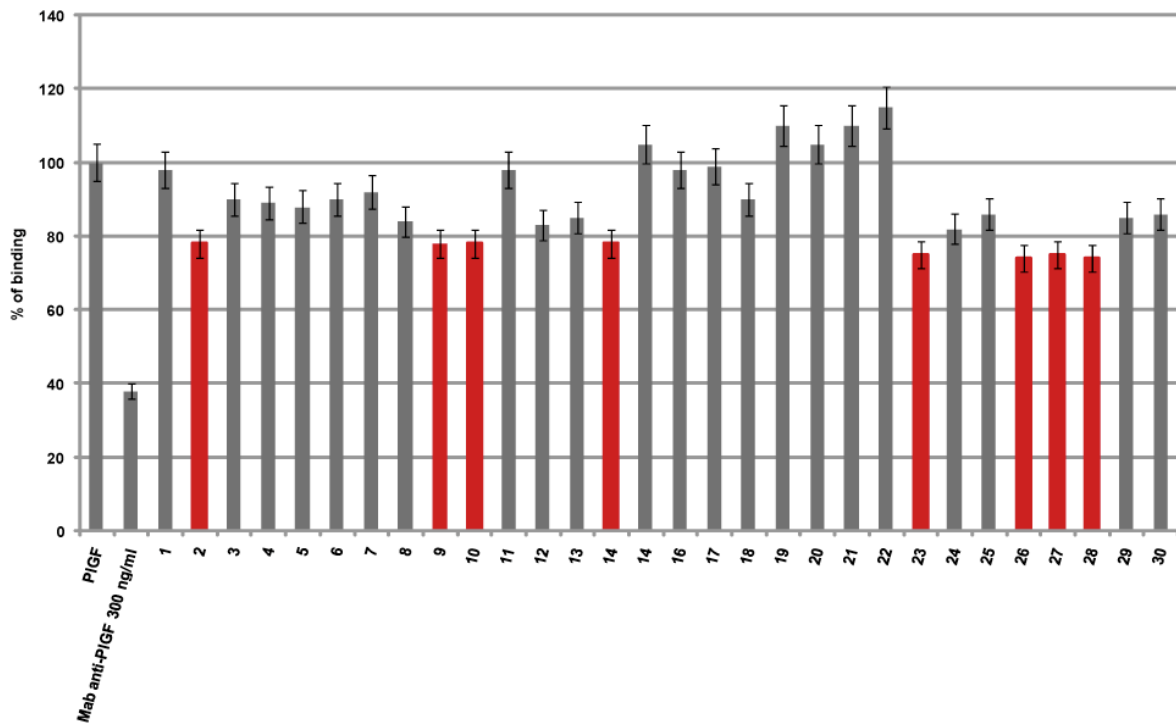


Figure 6: Screening of tetrameric sub-library 4-B-X performed by ELISA competition assay. Histogram reports the percentage of binding of each pool calculated assuming the binding of PIGF to Flt-1 as the 100% of binding. Monoclonal anti-PIGF antibody was used as inhibition control. In red were reported pools showing best inhibitory activity.

The pools labeled as 2, 9, 10, 14, 23, 26, 27 and 28, that presented the best inhibitory activity were assayed in a dose-dependent ELISA competition assay, using 1000 and 10.000 fold excess comparing them with pool 4 of original library and pool 4 reconstituted mixing equal amounts of sub-libraries 4-B-X, as positive control (Fig. 7).

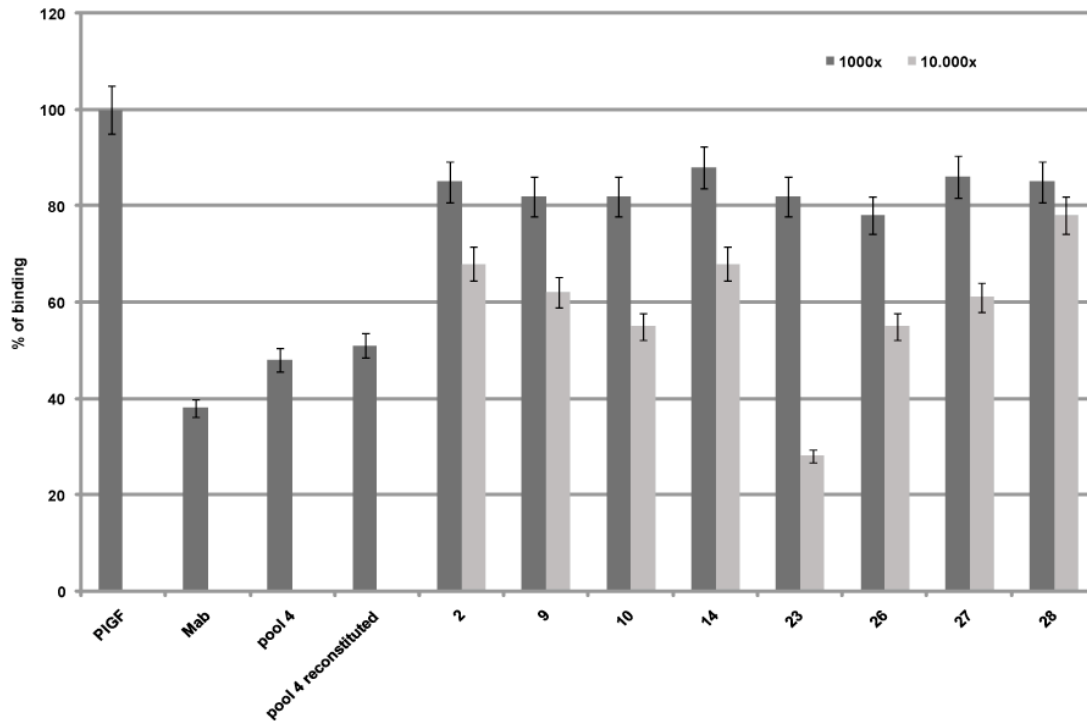


Figure 7: Dose-dependent ELISA assay performed with 4-B-X positive pools (2, 9, 10, 14, 23, 26, 27 and 28) and controls (monoclonal anti-PIGF antibody, original pool 4 of B-X-X library, reconstituted pool 4) used at 1000 and 10.000 molar excess

The second screening identified the aminoacid 23 as the most active residue in second position. Thus the pool 4-23-X showed the higher inhibition together with the best dose-dependent profile. Finally, 30 single peptides of 4-23-X pool were synthesized. These peptides differed only for the third position, identified with the 30 building-blocks. The LC-MS analyses of all 30 peptides showed that the expected molecular weights (MW) were in very good agreement with those calculated as reported in table 5.

Table 5: Characterization of the 30 single peptides assayed in the last screening. Theoretical MWs are calculated as average. MWs were obtained by LC-ESI-MS analysis of the crude products and were derived by the experimentally determined $[M+2H]^{2+}$ values (3rd column). Product purities were determined by integrating chromatogram peaks on the 215 nm trace and excluding peaks within the first 5 minutes of the run. Data of the 4-23-5 peptide are in bold.

Monomer n°	Theor. MW (amu)	Exp. $[M+2H]^{2+}$	Exper MW (amu)	Purity (% HPLC)
1	2033.46	1017.8	2033.6	87.5
2	2209.50	1105.6	2209.2	88.9
3	2145.66	1074.0	2146.0	95.3
4	2265.58	1133.9	2265.8	97.5
5	2362.02	1182.1	2362.2	90.5
6	2387.82	1169.8	2337.6	86.0
7	2153.54	1077.7	2153.4	88.7
8	2273.90	1137.9	2273.8	83.7
9	2446.02	1224.1	2446.2	84.5
10	2261.82	1132.0	2262.0	98.0
11	2401.82	1201.8	2401.6	90.4
12	2137.58	1069.6	2137.2	91.0
13	2201.78	1101.9	2201.8	83.9
14	2297.70	1150.0	2298.0	86.2
15	2261.66	1131.9	2261.8	89.0
16	2493.98	1248.0	2494.0	79.8
17	2373.90	1188.1	2374.2	85.9
18	2205.54	1103.8	2205.6	89.1
19	2201.78	1102.0	2202.0	95.2
20	2990.62	1496.2	2990.4	82.9
21	2097.46	1049.8	2097.6	88.6
22	2446.02	1224.0	2446.0	93.0
23	2522.22	1262.1	2522.2	96.1
24	2642.38	1322.2	2642.4	88.5
25	2386.22	1194.1	2386.2	86.3
26	2337.90	1169.8	2337.6	72.5
27	2401.90	1201.9	2401.8	70.4
28	2425.94	1213.9	2425.8	90.1
29	2033.46	1017.7	2033.4	89.2
30	1977.34	989.7	1977.4	96.5

Peptides were submitted to the screening (Fig. 8) and the most active peptide possess the residue 5 in this position.

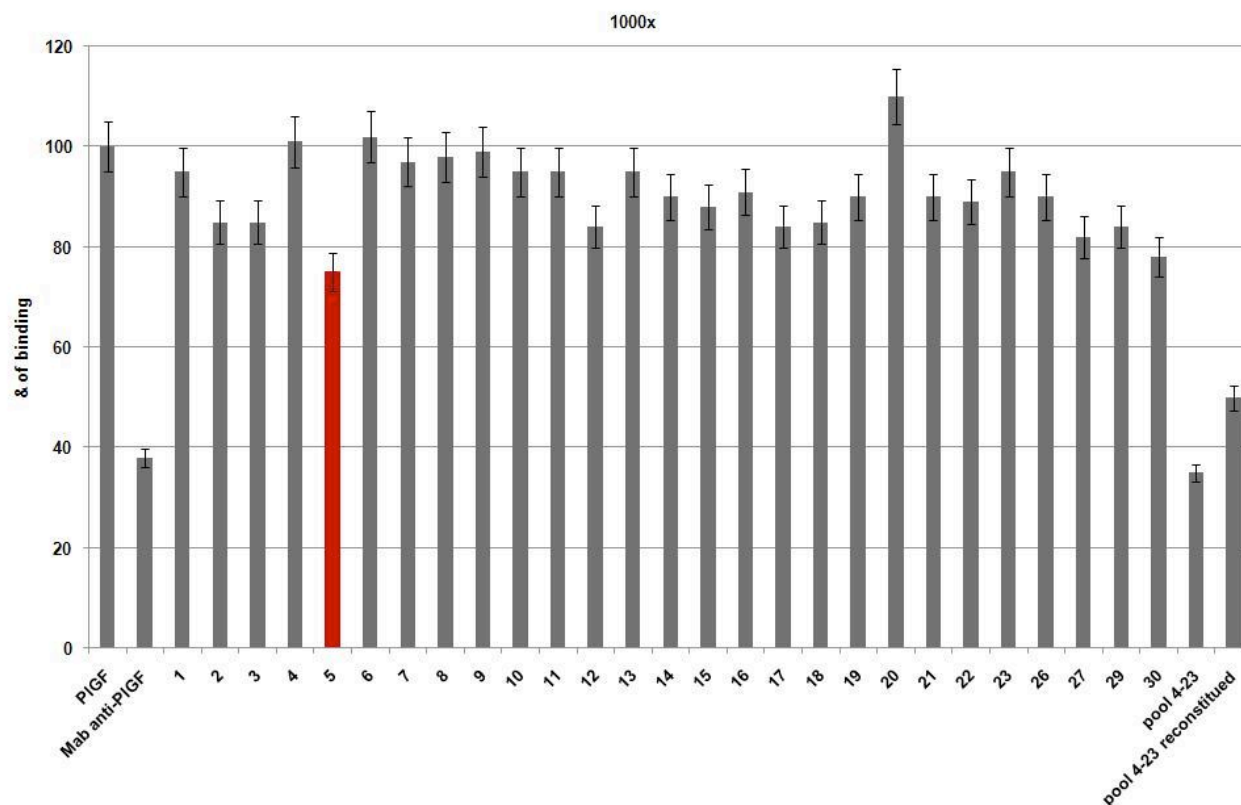


Figure 8: Third screening of 4-23-B peptides. Peptides were used at 1000x molar excess. Monoclonal anti-PIGF antibody, original pool 4-23-B and reconstituted 4-23-B pool from single peptides were used as positive controls of inhibition. In red are reported the most active aminoacids in third position

The screening of tetrameric tripeptide library allowed the identification of the tetrameric tripeptide Gly-Lys(Lys₂)-[4-23-5]₄, named 4-23-5. These numbers represent the selected aminoacids for each position and reflects the code used to catalogue building-blocks aminoacids. The inhibition activity of 4-23-5 peptide was evaluated in a dose-dependent ELISA assay comparing it with the tetrameric tripeptides 4-23-A (*Ala-scanning* related peptide, see above) and an unrelated tetrameric tripeptide, 21-1-5, as controls. The selected 4-23-5 peptide was able to inhibit PIGF/Flt-1 interaction with an IC₅₀ around 10 μM (Fig. 9). Since VEGF-A and PIGF interact in a very similar manner with Flt-1 receptor [92], the ability of 4-23-5 peptide to inhibit also VEGF-A/Flt-1 interaction was immediately investigated.

As shown in figure 10, the selected peptide inhibits VEGF-A/Flt-1 interaction with similar extent with an IC₅₀ around 10 μM.

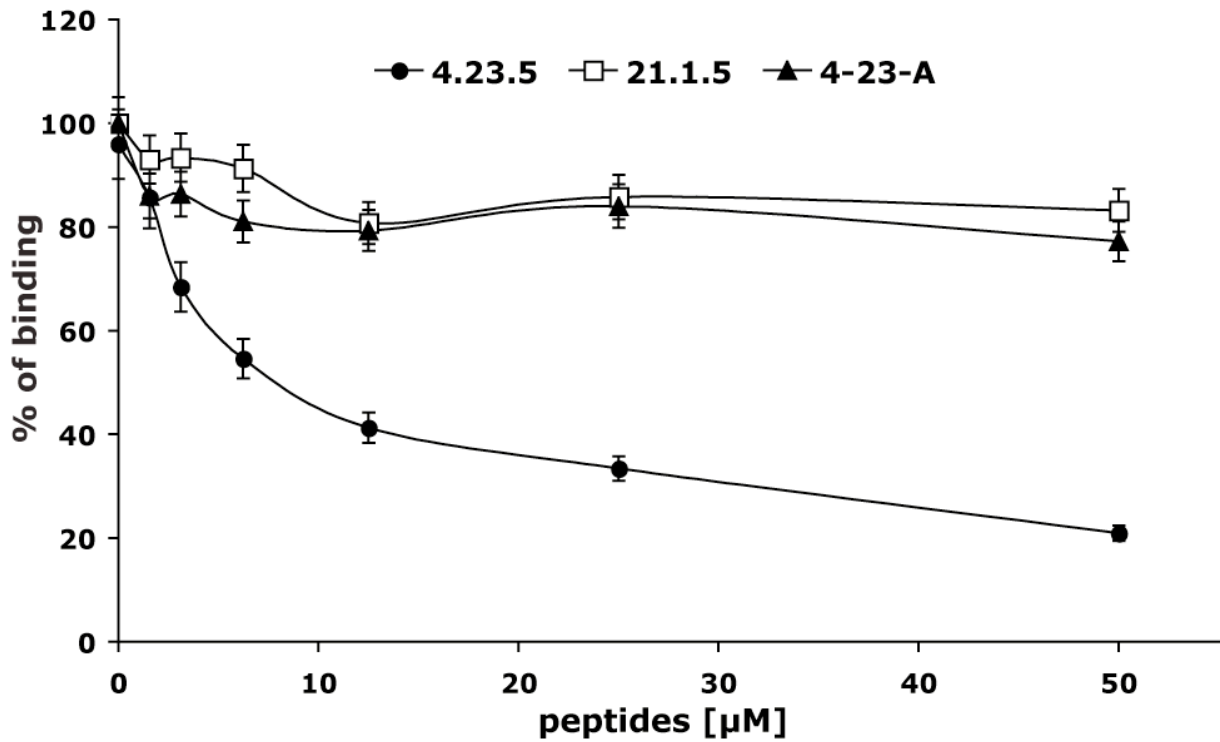


Figure 9: Dose-dependent inhibition of PlGF/Flt-1 interaction exerted by 4-23-5 peptide in competitive ELISA-based assay. Tetrameric 4-23-5, 4-23-A and 21-1-5 peptides were assayed at concentration ranging between 1.56 to 50 μM . Results present the average of three independent experiments.

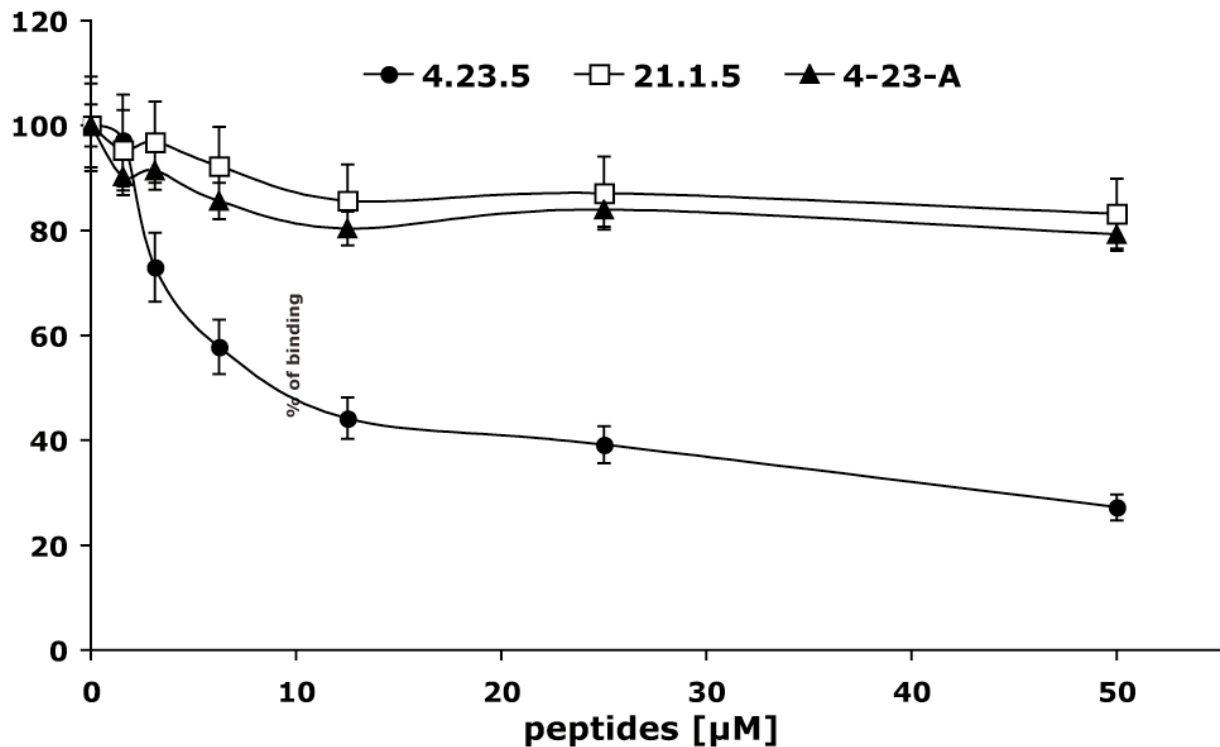


Figure 10: Dose-dependent inhibition of VEGF/Flt-1 interaction exerted by 4-23-5 peptide. All peptides were assayed at concentration ranging between 1.56 to 50 μM . Results present the average of three independent experiments.

3.2 Peptide activity is sequence and structure dependent

In order to evaluate the relation between peptide activity and its aminoacidic sequence, the Ala-scanning protocol has been used. Ala-scanning method allows to determine which residues play a critical role in biological activity of peptide. For each aminoacid position was synthesized a variant with the substitution of a single residue with L-Alanine, while the others residues were unchanged. To this end, the Ala-scanning related peptides 4-23-A, 4-A-23 and A-23-5 were assayed at a concentration of 50 μ M comparing them with 4-23-5 at a concentration of 12,5 μ M on both PIGF/Flt-1 and VEGF-A/Flt-1 systems (Fig. 11).

Results demonstrated how each residues substitution determined the lost of peptide activity indicating that the selected residues are all necessary for peptide inhibitory activity.

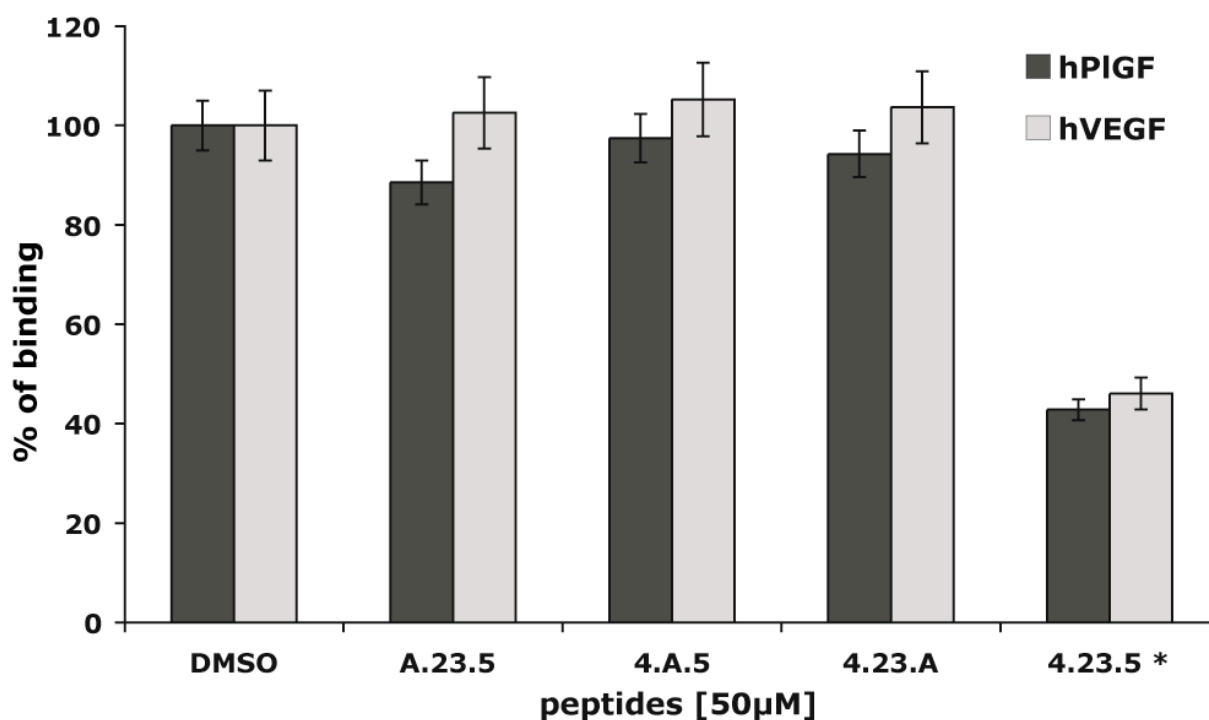


Figure 11: ELISA assay performed with Ala-scanning peptides on both PIGF/Flt-1 and VEGF-A/Flt-1 systems. DMSO refers to absence of competitor, while * refers to 4-23-5 peptide used at a concentration of 12,5 μ M.

Moreover, to evaluate the contribution of tetrameric structure on inhibitory activity of 4-23-5 peptide, the structural analogues monomer, dimer, cyclic dimer and trimer of tetrameric peptide were synthesized. The cyclic dimeric analogue was synthesized to stabilize the dimeric form through its cyclization. This structure has been realized thanks to the introduction of two Cysteine residues at N-terminal positions. The oxidation of their SH-groups occurs in aqueous solution and generates the desired cyclic structure. All analogues were assayed in ELISA competition assay at concentration of 50 μ M (Fig. 12), as well as performed with Ala-scanning peptides.

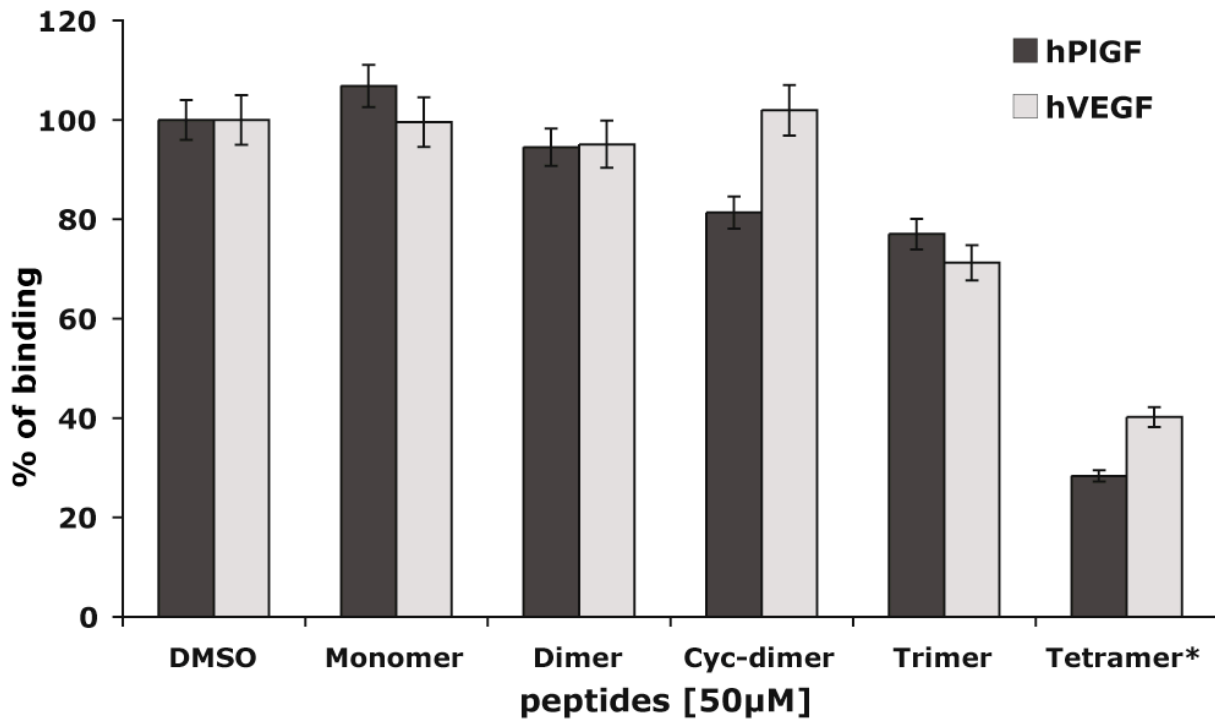


Figure 12: Structure analogues in ELISA competition assay. DMSO refers to absence of competitor, while * refers to 4-23-5 peptide used at a concentration of 12,5 μ M.

The results showed how the 4-23-5 activity is closely dependent also on tetrameric structure. The loss of even a single tripeptide strand as well as in trimer 4-23-5, caused a great loss of inhibitory activity of tetrameric 4-23-5.

3.3 4-23-5 peptide binds specifically to Flt-1 receptor

To evaluate the molecular mechanism that lead peptide activity, it has been realized an ELISA-binding assay performed with peptide 4-23-5 coated on microtiter plate. The plate were incubate with recombinant soluble growth factors or receptors both of human and mouse origins. While the soluble factors VEGF-A and PlGF were unable to recognize 4-23-5 or control peptides (data not shown), both human and mouse Flt-1 receptors were able to recognize the peptide in a dose-dependent manner (Fig. 13). The binding was specific since Flt-1 receptor did not recognize control peptides (Fig. 14). More important, KDR and Flk-1 receptors were unable to interact with control peptide (Fig 15), indicating that 4-23-5 is specific for VEGFR-1 and do not interfere with VEGFR-2 activity.

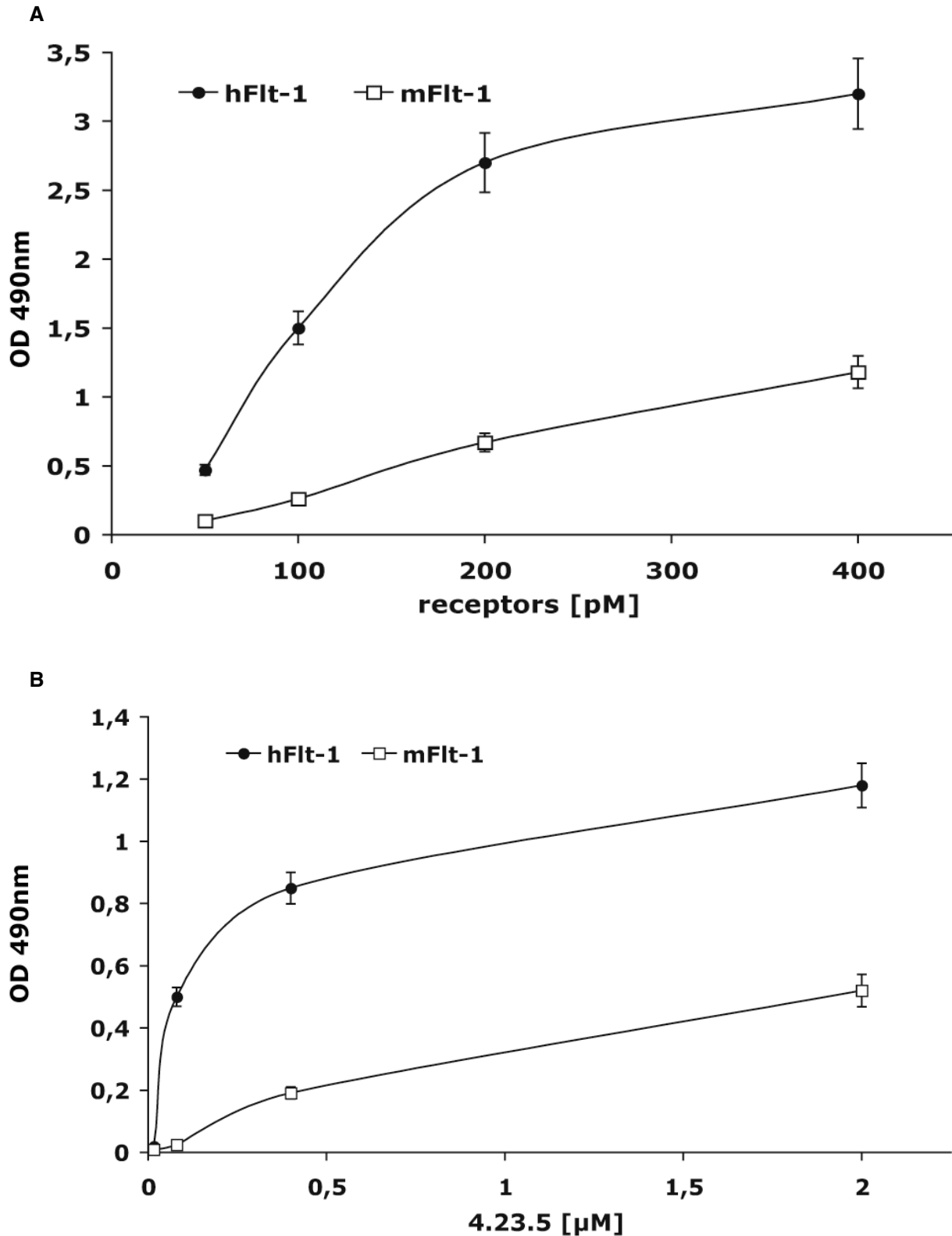


Figure 13: Binding profile of human and mouse Flt-1 receptor on coated 4-23-5 peptide. The binding was dose-dependent as demonstrated both using a fixed concentration of coated peptide (20 μM) and concentration ranging 50 to 400 pM of Flt-1 receptor (a) and using concentration ranging 0.1 to 2 μM of peptide in coating and a fixed concentration (125 pM) of Flt-1 in binding (b).

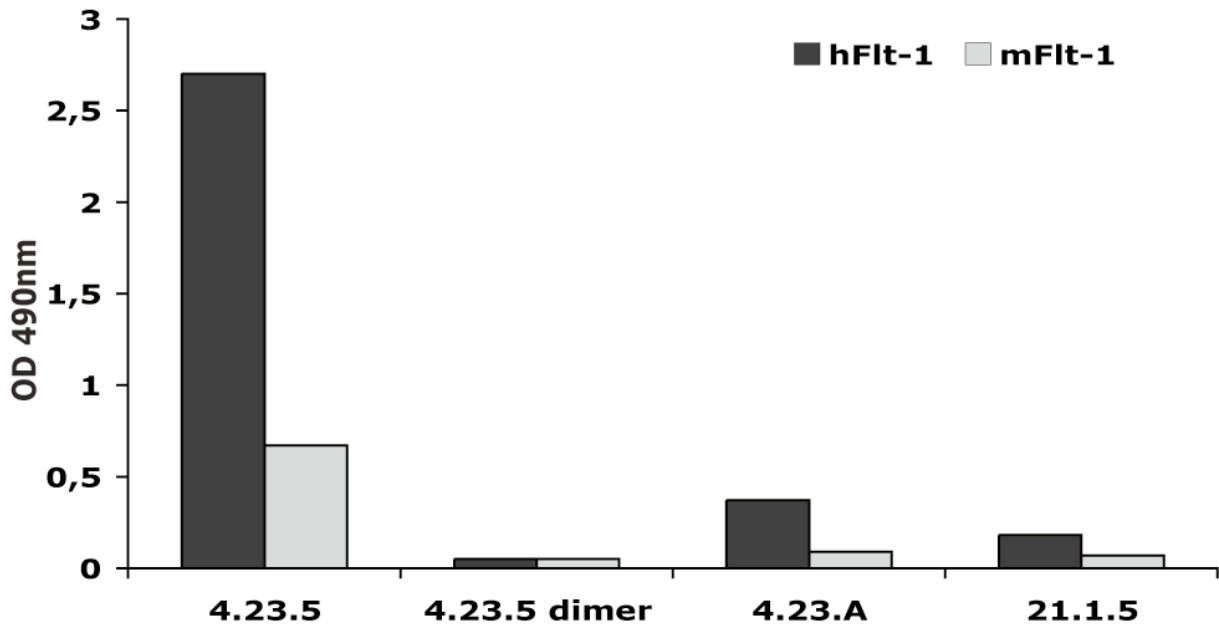


Figure 14: Binding of human and mouse Flt-1 receptors (250 pM) to coated 4-23-5 and control peptides at 20 μ M.

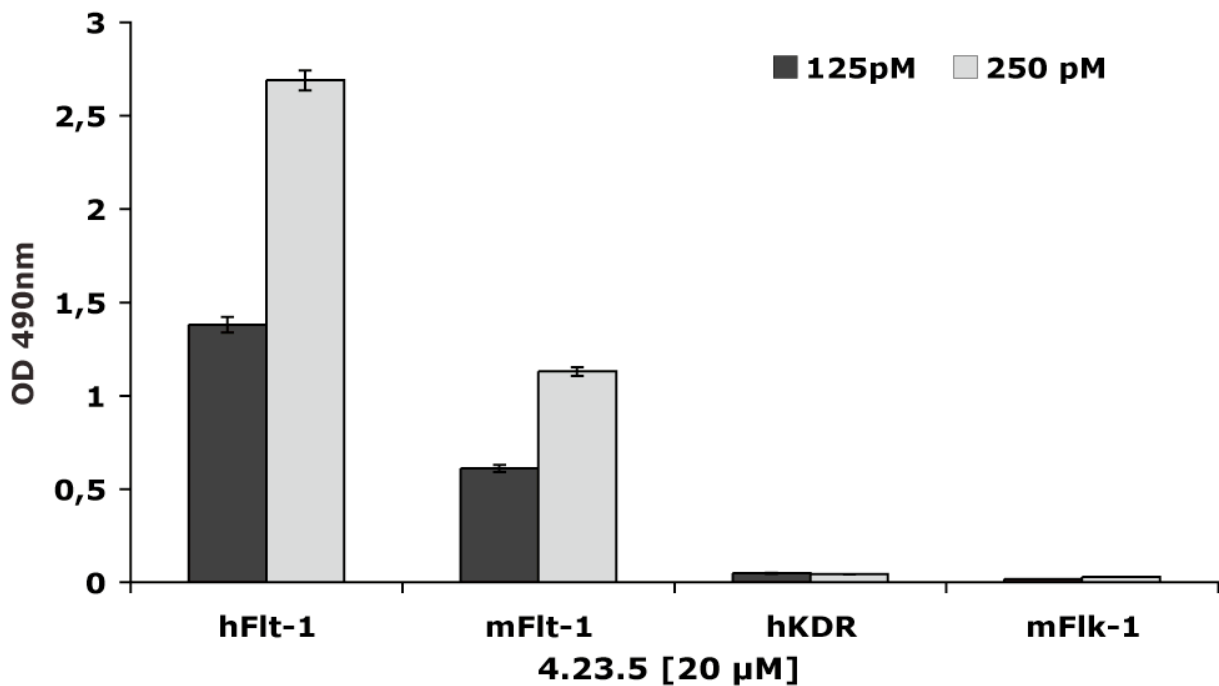


Figure 15: Binding assay of both human and mouse Flt-1 and KDR/FIk-1 receptors at 125 and 250 pM to coated 4-23-5 peptide at 20 μ M.

3.4 Evaluation of 4-23-5 activity on cell-based assays

Before assaying peptide in cell-based assay, it was evaluated its protease resistance over the time. Peptide was incubated in 10% fetal bovine serum for 24 hours, and peptide concentration was evaluated measuring the peak area corresponding to peptide on chromatographic profile at different times of incubation. As shown in figure 16 peptide was fully stable after 24 hours (Fig. 16). Moreover, this experiment also demonstrated that, under these conditions, the peptide did not bind to pelleted serum proteins.

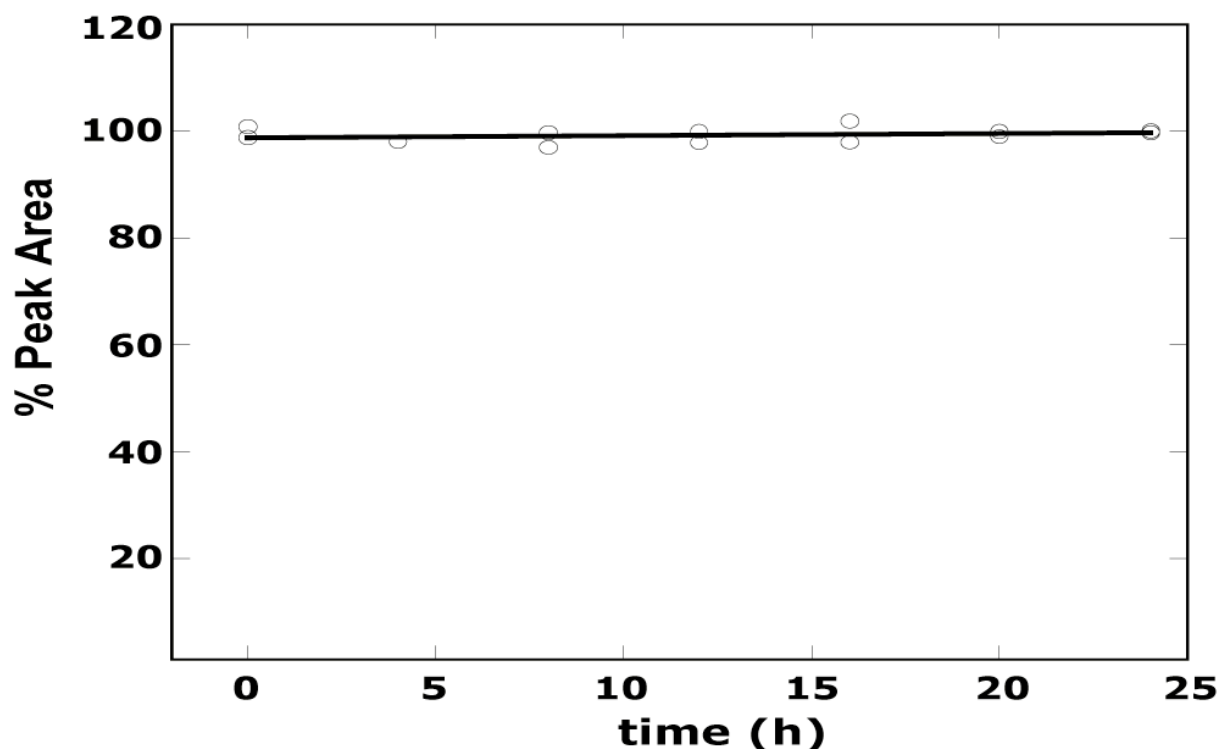


Figure 16: concentration profile of 4-23-5 peptide during 24 hours of incubation in 10% fetal bovine serum. At the indicated times, aliquots were removed, centrifuged to remove proteins and analyzed by HPLC (10 μ L, 1 μ g). Peak area, expressed as the percentage of the initial amount, versus time was plotted.

The neutralizing activity of 4-23-5 peptide was evaluated in the inhibition of Flt-1 receptor phosphorylation. PIGF added at 10 ng/ml was able to induce strong Flt-1 phosphorylation in stable 293 cell line over-expressing the receptor [93]. The addition of selected peptide with PIGF, was able to prevent PIGF-induced Flt-1 phosphorylation in a dose-dependent manner. The observed inhibition was total at a concentration of 20 μ M while control tetrameric peptide 4-23-A at same concentration did not show inhibition. At a concentration of 4 μ M peptide caused a partial inhibition comparable to that observed with a neutralizing anti-PIGF monoclonal antibody (16D3, Thrombogenics) used at 1,6 nM (Fig. 17).

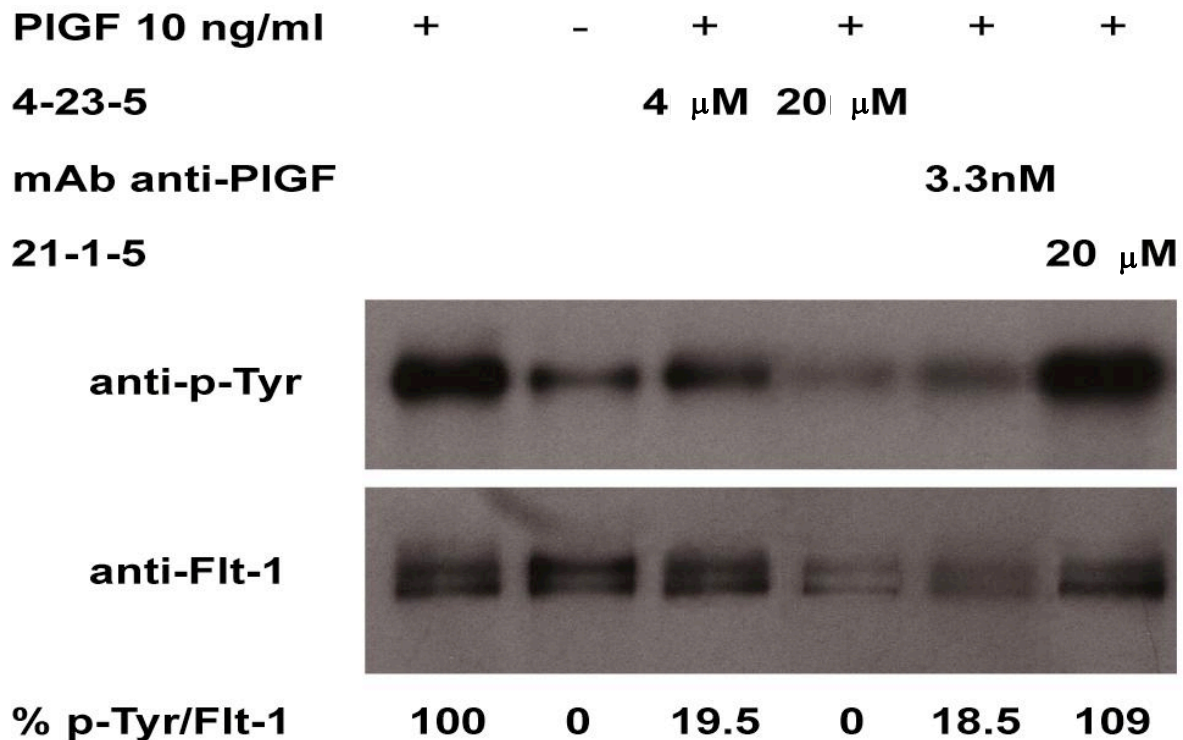


Figure 17: Inhibition of PIGF-induced Flt-1 phosphorylation on 293 cells over-expressing Flt-1 receptor. The values of densitometry analyses performed using ImageQuant 5.2 software are reported. Values of 0 and 100 have been assigned arbitrary, to non-induced and PIGF-induced samples.

In order to evaluate the anti-angiogenic activity of 4-23-5 peptide, it was assayed in capillary-like tube formation (CTF) assay. This assay is widely utilized to investigate the pro- or anti-angiogenic activity of molecules: primary endothelial cells plated on membrane extract (Matrigel) in presence of angiogenic stimuli, such as growth factors like VEGF-A, EGFR and FGF, are able to migrate and differentiate generating a network of capillary-like structures. PIGF and VEGF-A alone in endothelial basal medium were able to stimulate human umbilical vein endothelial cells (HUVECs) inducing a capillary-like network (Fig. 18.1 And 18.8). Peptides were added with PIGF or VEGF-A at concentration ranging from 0.16 to 20 μ M. Selected peptide 4-23-5 were able to suppress completely the PIGF or VEGF-A induced CTF at a concentration of 20 μ M (respectively Fig. 18.2 and 18.9), this activity is specific of selected peptides because control peptides 4-23-A (12.8 and 18.10) and 21-1-5 (18.4 and 18.11) at 50 μ M failed to block CTF. Observed inhibition was dose-dependent, indeed tetrameric 4-23-5 peptide still completely inhibited CTF stimulated by both PIGF and VEGF-A at 4.0 μ M (Fig. 18.5 and 18.12), whereas at 0,8 μ M (Fig. 18.6 and 18.13) and 0,16 μ M (Fig. 18.7 and 18.14), showed respectively strong and partial inhibition. These data confirm that selected peptide is able to prevent PIGF and VEGF-A activity on endothelial cells, inhibiting angiogenesis-related process such as the formation of a capillary-like network.

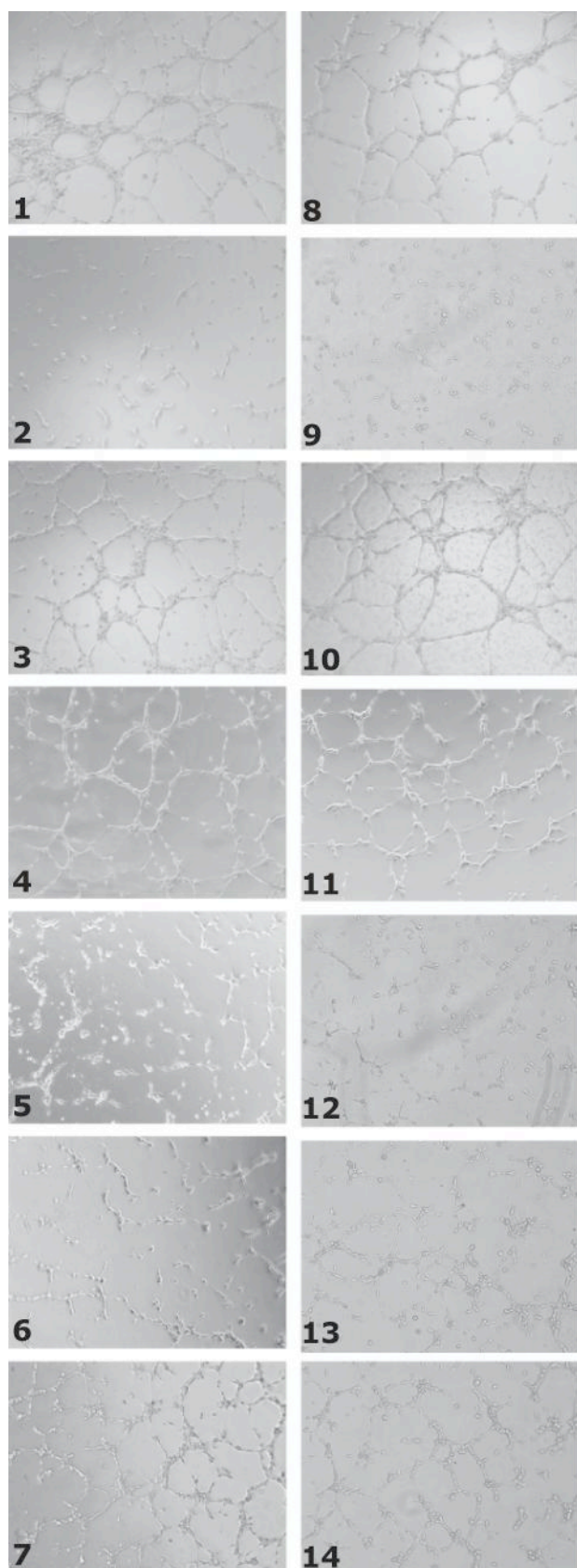


Figure 18: Inhibition of CTF assay induced by both PIGF (1-7) and VEGF-A at 100 ng/ml (8-14).

1, 8: PIGF and VEGF-A.

2, 9: 4-23-5 at 20 μ M.

3, 10: 4-23-A at 50 μ M.

4, 11: 21-1-5 peptide at 50 μ M.

5, 12: 4-23-5 peptide at 4.0 μ M.

6, 13: 4-23-5 at 0.8 μ M.

7, 14: 4-23-5 at 0.16 μ M.

3.5 *In vivo* activity of 4-23-5 tetrameric peptide

The anti-angiogenic activity of blocking 4-23-5 peptide was also evaluated *in vivo* using the model of chicken embryo chorioallantoic membrane (CAM) assay [94]. This assay is based on the implantation of a gelatin sponge or absorbing beads on the top of the CAM during embryonic development. The implanted support is treated with a stimulator of blood vessel formation in the absence or presence of an angiogenesis inhibitor. New blood vessels that are growing into sponge or converging towards the beads after 72 hours, are counted under stereomicroscope. VEGF-A alone exerted a strong angiogenic response (49 ± 4 vessels/embryo) when compared to beads absorbed with vehicle (7.0 ± 2.2) or peptides alone (4.5 ± 2.5 and 8.0 ± 5.5 vessels for 4-23-5 and 21-1-5 peptides, respectively). The blocking peptide 4-23-5 was able to inhibit the angiogenic response in all tested embryos. The number of new vessels was reduced to 33.6 ± 4.3 ($n=6$, $p < 0.005$ vs VEGF-A) and to 16.6 ± 4.9 ($n=8$, $p < 0.0001$ vs VEGF-A) with 0.025 and 0.25 nmol (Fig. 19) of peptide, respectively. In contrast, no inhibition was elicited by 0.025 nmol of control peptide ($n=8$, 45.0 ± 4.7 vessels) whereas a partial inhibition ($\geq 50\%$) was observed only in 2 out of the 6 embryos treated with 0.25 nmol of the control peptide (26.8 ± 14.3 vessels, $p < 0.005$ vs VEGF-A, Fig. 19 and 20).

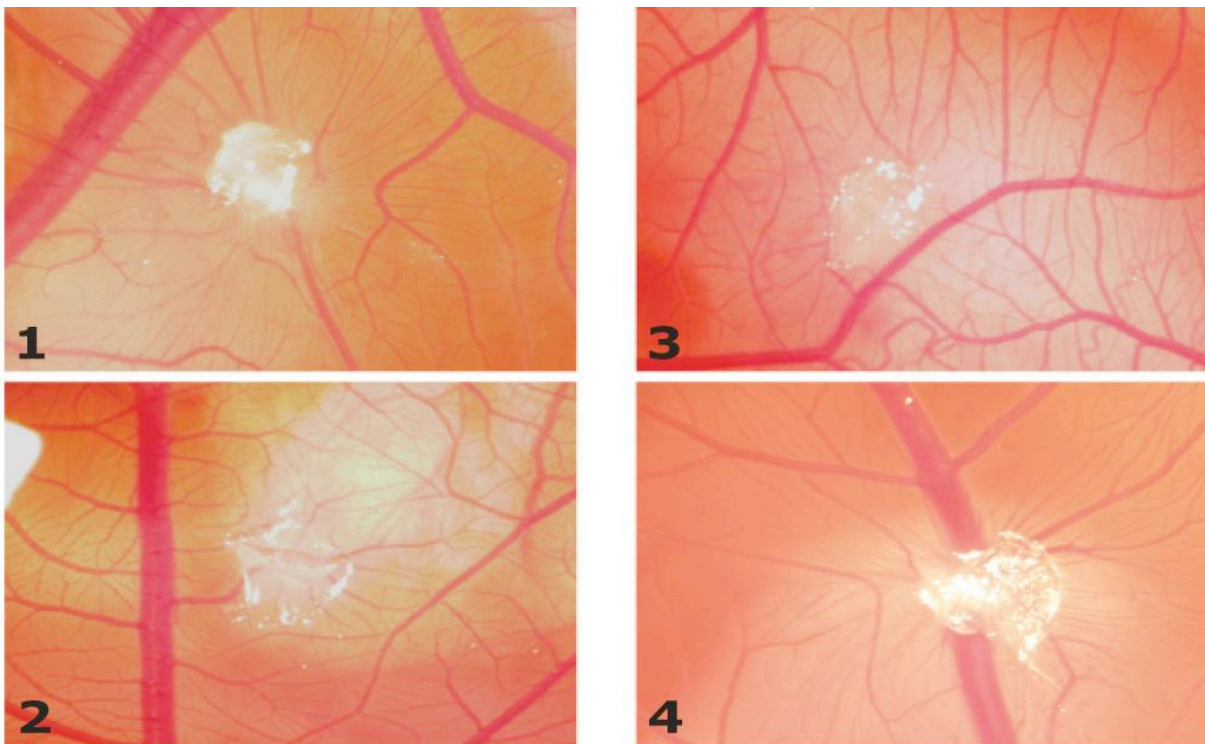


Figure 19: Anti-angiogenic activity of 4-23-5 peptide on CAM assay. Representative pictures of: 1. Beads containing VEGF-A alone, 2. PBS, 3. VEGF-A in presence of 0.25 nmol of 4-23-5 peptide, 4. VEGF-A in presence of 0.25 nmol of 21-1-5 peptide.

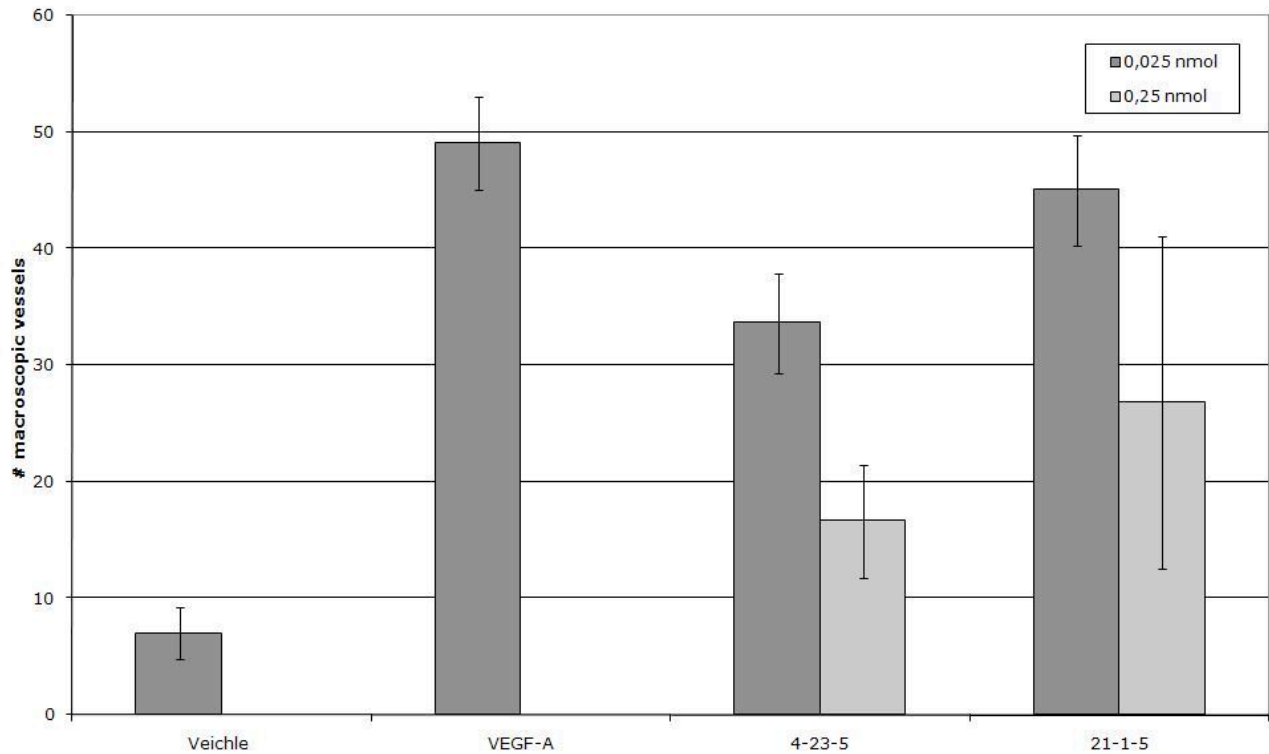


Figure 20: graphic representation of CAM assay results. Histogram reports the number of new blood vessels converging towards the beads counted under stereomicroscope. The high standard deviation presented from 0.25 nmol of control peptide 21-1-5 is due to the partial inhibition showed from 2 of the 6 embryos treated.

Recently, Ambati et al have demonstrated the involvement of sFlt-1 in the maintenance of cornea avascularity [64]. These data make the cornea the best platform to assay anti-Flt-1 molecules. Based on these data, 4-23-5 peptide was assayed in cornea neovascularization (CNV) assay. The injection of 20 nmol of 4-23-5 peptide induced a strong angiogenic response (Fig. 21) and the effect was dose-dependent. Indeed, injection of 4.0 nmol or 0.4 nmol still produced clearly visible effects, though to reduced extent. Conversely, the injection of 20 nmol of control peptide 21-1-5 was unable to induce CNV. Of utmost importance, a single injection of 4-23-5 produced a sustained effect detectable up to 7 days, confirming the high stability to degradation observed *in vitro*.

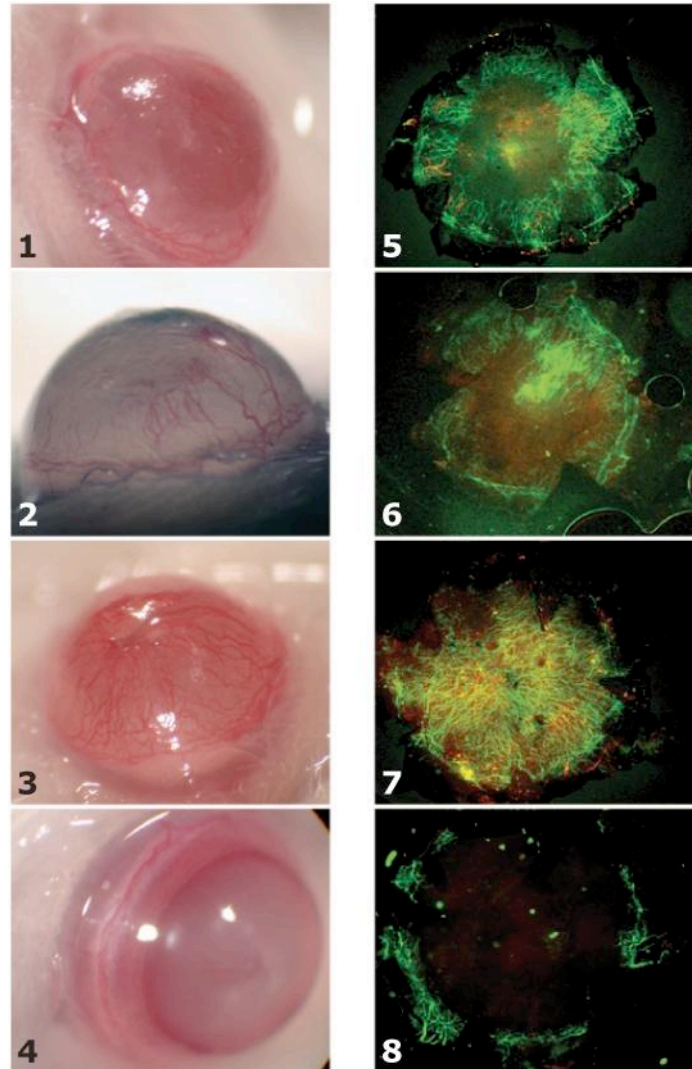


Figure 21: Corneal neo-vascularization induced by 4-23-5 peptide. A total of 0.4 (1 and 5), 4.0 (2 and 6) and 20 (3 and 7) nmol of 4-23-5 peptide and 20 nmol of 21-1-5 control peptide (4 and 8) in DMSO were injected in the corneas of Balb/c mice. After 7 days corneas were harvested and flat-mounted. New vessels were immunostained (4-8) using anti-mouse CD31 antibodies (green), and anti-mouse-LYVE-1 antibodies (red). Blood vessels were defined as CD31 positive and Lyve-1 negative.

IV. Discussion

In the last decade, the concept of angiogenic therapy has been developed as a strategy to treat cancer inducing the regression of vessels that provide sustenance to the tumor. Recently, it has been re-defined and extended to all pathologies characterized from a reduced or excessive angiogenesis.

Among the several molecular factors involved in the regulation of angiogenesis, VEGF family has assumed a central role [7].

At the beginning more attention has been conferred to VEGF-A and its specific receptor KDR/Flk-1, since this pathway is crucial for endothelial cells activation in angiogenesis process and their interaction has been proposed as ideal target for angiogenic therapy [81]. However, recent data demonstrate that PlGF and its receptor Flt-1 have a role more confined to pathological angiogenesis.

The deletion of Flt-1 gene in mice causes embryonic lethality due to overgrowth and disorganization of blood vessels, not due to a poor vascularization [56], suggesting that VEGFR-1 plays a role in the reorganization and stabilization of primitive vascular plexus. In contrast, deletion of tyrosine kinase domain of Flt-1 does not cause lethality but it generates mice that show a reduced pathological angiogenesis. The same phenotype has been described for PlGF knockout mice, indicating that both molecular factors are crucial in the induction of angiogenesis in pathological states. Recent data demonstrate that Flt-1 is not only expressed in ECs but also in monocytes/macrophages, smooth muscle cells and also in bone marrow stem/progenitors derived cells, indicating that Flt-1 has also a role in stabilization of new blood vessels through the recruitment of SMCs and in the recruitment and differentiation of monocyte-macrophage cells which express SMCs and ECs mitogens [61]. Moreover, in tumor the inhibition of Flt-1, using an anti-Flt-1 monoclonal antibody, is able to inhibit tumor growth through the decrease of its vascularization. Very recently, similar results have been obtained with an anti-PlGF monoclonal antibody [95]. All together these data demonstrate that Flt-1 and its ligand PlGF are a target of pathological angiogenesis and their inhibition consistently reduce the pathology progression.

The first anti-angiogenic molecule approved for clinical use has been a humanized anti-VEGF-A blocking antibody (Avastin, Genetech, Inc.). Moreover human patients treated with Avastin have showed undesired effects such as hypertension and thrombosis, due to physiological activity of VEGF-A in vessels permeabilization. In contrast, results obtained from Fischer et al show that the anti-PlGF monoclonal antibody is able to inhibit tumor growth without induce the side effects observed with both anti-VEGFR-2 antibody and VEGFR inhibitors, confirming the restricted role of PlGF and Flt-1 to pathological angiogenesis.

Despite the progresses made by biotechnological industry, the using of monoclonal antibodies and recombinant proteins is still much expensive mainly because of high costs of production. In this contest, small molecules offer numerous advantages: low molecular weight often allows to escape recognition immunity system, they can be more easily produced, and are generally free of contaminants of biological origin, they offer more opportunity for delivery allowing also oral administration and their costs of production are lower than that of monoclonal antibodies or recombinant proteins. In this regard, in the last two decade a great efforts has been focused both on the realization of combinatorial libraries, to increase significantly the number of available molecules, and on the development of methods to screen them efficiently and rapidly. Thanks to biotechnology progresses, several methods to synthesize and screen in automated way complex libraries are available and the only limit is the ability of the investigator to think and design new molecular scaffolds, as well as identify new molecular targets.

In this work it has been performed the screening of a tetrameric tripeptide library to identify new inhibitors of pathological angiogenesis.

The screening (deconvolution) of a tetrameric tripeptide library, performed with the iterative process, has allowed the identification of a peptide named 4-23-5 (Fig. 3).

The selected peptide is able to inhibit the interaction between Flt-1 receptor and its ligands PIGF and VEGF-A, showing an IC_{50} value of about 10 μ M estimated by ELISA-competition dose-dependent assay (Fig. 9 and 10). The ability to inhibit both interactions is due to binding activity of peptide, since it recognizes exclusively Flt-1, while fails to bind KDR/Flk-1 or soluble factors. The ability of peptide to bind selectively Flt-1 confers it a particular interest: it can inhibit the role of Flt-1 in the earliest steps of angiogenesis preventing the recruitment of endothelial precursors and monocyte-macrophage and, at the same time, it can prevent stabilization of blood vessels by SMCs inducing fragility of the nascent vascular network.

Structural investigation has showed that peptide activity is closely dependent both on the aminoacidic sequence, indeed the substitution of a single aminoacid with Alanine causes the loss of inhibitory activity (Fig. 11) and on tetrameric structure, indeed this structure presents the best inhibition compared with structural analogues (Fig. 12).

The presence of un-natural aminoacids confers to peptide an utmost resistance to protease degradation as compared to other recently reported anti-Flt-1 peptides [96, 97, 98]. The stability of peptide is crucial for its application in cell-based and *in vivo* assays.

The selected peptide is able to inhibit the PIGF-induced phosphorylation of Flt-1 receptor indicating that it is able to prevent the first molecular event of signal transduction of PIGF through Flt-1 that lead the activation of downstream target gene involved in Flt-1-induced response (Fig. 17).

The inhibition of CTF demonstrates that the inhibition of Flt-1 phosphorylation alone is sufficient to inhibit all biological processes that lead the formation of the capillary-like network, such as cell proliferation, migration and differentiation.

Moreover, the inhibition of VEGF-induced CTF together with a sustained inhibition of VEGF-induced angiogenesis in CAM assay show that, despite the presence of both VEGFRs, the inhibition of the high affinity receptor alone is able to prevent *in vivo* and *in vivo* angiogenic response to VEGF-A.

The induction of cornea vascularisation in CNV assay confirms that 4-23-5 peptide is able to bind Flt-1 receptor displacing VEGF-A from a pre-formed complex with the receptor. Moreover, it does not interfere with Flk-1 receptor because corneal vascularisation is a process driven by VEGF-A/Flk-1 interaction. This data demonstrates that also *in vivo* system, the selected 4-23-5 peptide has a high specificity for Flt-1 receptor and do not interfere with Flk-1 receptor. Furthermore, at the higher peptide concentration used, the formation of new lymphatic vessels is also evident (Fig. 21.3 and 21.7) as showed by anti-Lyve labelling. This results is consistent with recent data on the ability of VEGF-A to stimulate also lymphangiogenesis indicating that for this process the VEGF/Flk-1 interaction is crucial.

Although initially in *in vitro* assay, selected 4-23-5 peptide has showed activity in micromolar range (IC_{50} of 10 μ M), in all cell-based and *in vivo* assays it presents an inhibitory activity at lower concentration. These results show that selected peptide represent a new specific anti-Flt-1 peptide that can be used for molecular therapy approach of those pathologies in which angiogenesis represents a crucial event. Moreover, anti-Flt-1 antibody is able to reduce atherosclerotic plaques growth and suppresses autoimmune arthritic joint destruction through the inhibition of the recruitment of myeloid progenitors [61]. Recently, Kaplan et al have demonstrated that Flt-1 marks bone-marrow derived haematopoietic progenitor cells and is crucial for their migration to tumor-specific pre-metastatic sites, where these cells form a cellular cluster named 'pre-

metastatic niche' before the arrival of tumor cells [62]. Anti Flt-1 monoclonal antibody is able to completely prevent metastasis formation.

These results indicate that anti-Flt-1 molecules can be also used for the treatment of inflammation disorders and to prevent cancer metastasis, other than all pathologies in which angiogenesis have a fundamental role.

Finally, selected peptide represents a new molecular scaffold which can be further modified to generate new peptide variants with increased affinity for Flt-1 receptor.

V. Matherial and Methods

5.1 Synthesis of combinatorial tetrameric tripeptide library and analogues of 4-23-5 peptide

For the library synthesis, 30 different blocks were utilized (Table 4), and a theoretical number of 27,000 peptides was generated, split in 30 separate pools of 900 peptides each. The synthesis was manually carried out on a 300 μ moles scale following standard Fmoc methodologies and using PyBOP as coupling agent. A typical acylation/deprotection cycle consisted of a 15 minutes coupling step (0.25 M amino acid solutions *in situ* activated with PyBOP and DIEA) and a 10 minutes deprotection step with 30% piperidine in DMF. Peptide mixtures were then detached from the corresponding resins by treatment with a cleavage cocktail containing TFA-TIS-H₂O (95:2.5:2.5, v/v/v) for 2h at RT, then they were lyophilized twice, dissolved in DMSO at 5 mg/mL and stored at -80°C until use. Assuming an average molecular weight of 2128 amu for the tetrameric tripeptides, calculated by summing the average MW of the single building blocks (138.2 amu) multiplied by 12, to that of the polylysine scaffold (458 amu), a theoretical 2.6 μM concentration for each library component was achieved. No specific characterization were performed at this stage given the high complexity of the resulting sub-libraries (900 components). After the first screening round, the selected sub-library carrying the D-Glutamic acid (D-Glu, building block 4) on the N-terminus, was prepared following the same synthetic approach. A theoretical number of 900 molecules arranged in 30 pools of 30 peptides each was thus generated. Characterization at this step on selected sub-libraries was achieved by LC-MS using an LC-MS system equipped with a Surveyor HPLC, comprising a quaternary pump and a PDA detector, and the LCQ Deca Ion Trap mass spectrometer (ThermoFisher). For the analyses, C18 narrow bore 30x1 mm ID Biobasic column (ThermoFisher) equilibrated at 200 $\mu\text{L}/\text{min}$ with 5% CH₃CN, 0.05% TFA were used. Analyses were carried out applying a gradient of CH₃CN, 0.05% TFA from 5% to 70% over 90 minutes. The mass spectrometer mounted an ESI source maintained at 320 $^{\circ}\text{C}$ and 4.2 kV. Spectra in positive mode were continuously acquired between 200 and 2000 amu. Mixtures were detached from the resin as described previously and the products were stored in DMSO at 5 mg/mL concentration. The 30 peptides composing the sub-library identified in the second screening round and carrying the Cys(Bzl) (building block 23) on the known position, were prepared in parallel as single molecules. After cleavage from the resin and lyophilisation, the peptides were all characterized by LC-MS using a narrow bore 30x1 mm ID Biobasic column equilibrated at 200 $\mu\text{L}/\text{min}$ with 5% CH₃CN, 0.05% TFA. Analyses were carried out applying a gradient of CH₃CN, 0.05% TFA from 5% to 70% over 13 minutes. Peptides were firstly tested in the competition assay as crude products, then the active molecules and those assumed as negative controls were purified by semi-preparative RP-HPLC using a 30x1 cm C18 column (Phenomenex, Torrance, CA, USA), characterized by LC-MS and re-submitted to the competition assay. The active peptides were tested in the cellular assays as acetate salts in order to prevent the cytotoxic effects of the TFA present as counterion. To this aim, peptides were dissolved in 0.1 M CH₃COOH and repeatedly lyophilized. Reagents for solid phase synthesis were from Chem-Impex or Novabiochem; solvents were all from LabScan (Dublin, Ireland). Reagents for peptide cleavage were from Sigma-Aldrich (Milan, Italy). LC-MS systems and columns for LC-MS analysis were from ThermoFisher (Milan, Italy).

5.2 Iterative deconvolution of tetrameric tripeptide library.

At every step of the deconvolution process, peptide pools were tested with a molar excess of 1,000-fold (calculated for each single peptide) over PIGF (1.3×10^{-10} M). Once identified an active pool, a dose-dependent inhibition using 500 - 1,000 - 1,500 and 2,000 fold excess was performed to confirm the inhibitory property. The first active pool identified was the 4.X.X (X indicated random positions) where “4” identifies the amino acid D-Glutamic (D-Glu, see Table 7). This peptide pool was synthesized in 30 sub-pools, each composed of 30 peptides, and submitted to the second screening that allowed the identification of the sub-pool 23 (4.23.X), where the number “23” identifies the amino acid L-Cysteine(S-benzyl) (L-Cys(Bzl), see Table 7). Finally the 30 single peptides composing the 4.23.X pool were synthesized and submitted to the final screening. The peptide 4.23.5, where the number “5” identifies the amino acid L-Cyclohexylalanine (L-Cha, see Table 7), was the unique molecule showing inhibitory activity.

5.3 ELISA-based assays for the screening of library and competition experiments.

The ELISA based assay for the screening of peptide library and for all competition and dose-dependent experiments was performed coating on 96-well plate a recombinant form of Flt-1(VEGFR-1-Fc chimera R&D Systems) at 0.5 mg/mL, 100 μ l/well, 16 hrs at room temperature. Wells were washed five times with PBS containing 0.004 % Tween-20 (PBT) and the plate was then blocked for three hrs at RT with 1 % Bovine Serum Albumin (BSA) in PBS, 200 μ l/well. Wells were washed as above, and a recombinant form of PIGF (R&D Systems) at 5 ng/mL in PBS containing 0.1 % BSA, 5 mM EDTA, 0.004 % Tween 20 (PBET), 100 μ l/well, was added and incubated for 1 h at 37°C followed by 1 h at RT. Wells were washed again and biotinylated anti-human PIGF polyclonal antibody (R&D Systems), diluted in PBET at 300 ng/mL, 100 μ l/well, was added to the wells and incubated for 1 h at 37°C followed by 1 h at RT. Wells were washed and incubated with a solution containing a preformed avidin and biotinylated HRP macromolecular complex (Vectastain *elite* ABC kit) for 1 hr at RT. After the last wash, 100 μ l of HRP substrate composed of 1 mg/mL of ortho-phenylenediamine in 50 mM citrate phosphate buffer pH 5, 0.006 % of H₂O₂, was added and incubated for 40 min in the dark at RT. The reaction was blocked by adding 30 μ l/well of 4 N H₂SO₄ and the absorbance measured at 490 nm on a microplate reader (Biorad BenchMark).

Peptide pools or single peptides dissolved in DMSO (Sigma) were properly diluted and added to the wells pre-mixed with ligand. For dose dependent experiments performed with VEGF (R&D Systems), 10 ng/mL of recombinant protein and 300 ng/mL of polyclonal antibody anti human VEGF (R&D Systems) were used. For dose-dependent experiments, 4.-23-5 peptide and control peptides were used at concentration ranging between 1.56 and 50 mM.

5.4 Inhibitory activity of 4.23.5 sequence- and structure-related analogues.

The inhibitory properties of Alanine-scan peptides and structurally related analogues in both PIGF or VEGF interaction with Flt-1 receptor were investigated using the ELISA-based assay described above. Peptides were used in competition at 50 μ M concentration. As positive control of inhibition, 4-23-5 was used at 12.5 μ M whereas as negative control was added the same volume of DMSO used to dissolved peptides at the reported concentration.

5.5 ELISA assays for determination of binding of 4-23-5 peptide to Flt-1 receptors.

To evaluate the binding of 4-23-5 peptide to Flt-1 receptor, 4-23-5 or control peptides were coated at the indicated concentrations, 100 μ l/well, 16 h at 4°C. Wells were washed five times with PBT and the aspecific sites blocked for 3 h at RT with 1 % Bovine Serum Albumin (BSA) in PBS, 200 μ l/well. Wells were washed as above, and recombinant form of extracellular domains of human and mouse Flt-1 receptor fused to human Fc in PBET were added at the indicated concentrations and incubated for 1 h at 37°C followed by 30 min at RT. Wells were washed again and a goat anti-human Fc (Jackson ImmunoResearch) at 1:1000 was added and incubated 1 h at 37°C and 30 min at RT. After the last wash, a donkey anti-goat HRP (Santa Cruz Biotechnology) at 1:1000 was added and incubated 1 h at RT. The HRP substrate and reading of plates was effectuated as reported in paragraph 3.3.

To evaluate the binding of 4-23-5 to VEGFR-2, recombinant human KDR and mouse Flt-1 extracellular domains fused to human Fc (R&D Systems) were used instead of Flt-1 receptors.

5.6 Stability assay

The selected peptide, denoted as 4.23.5 was dissolved in neat DMSO at a 10 mg/mL concentration. The sample was then serially diluted in PBS pH 7.3 containing 10% Fetal Calf Serum (FCS) in order to obtain 100 μ g/ml solutions and incubated at 37 °C for 24 h. 10 μ l aliquots (1.0 μ g total peptide) were removed at 0, 4, 8, 12, 16, 20 and 24 h, were centrifuged for 5 min at 16000 x g and analyzed by RP-HPLC after discarding the pellet. A reference curve was obtained by analyzing, under the same conditions, different amounts of the pure compound dissolved in pure DMSO, where it is fully soluble (>100 mg/ml). The reference curve was used to exclude effects of sample subtraction by non-specific binding to albumin or other serum proteins. The experiment was carried out twice and the data were reported as a plot of peak area (%) versus time.

5.7 Inhibition of Flt-1 phosphorylation assay

HEK-293 over-expressing hFlt-1 cells were grown in Dulbecco's modified Eagle medium (DMEM) supplemented with 10% inactivated fetal bovine serum (Euroclone) and antibiotics until 70% confluence, then they were starved overnight at 37°C in serum free medium. Medium was removed and cells were preincubated with PBS containing Na_3VO_4 at 100 μ M for 5 minutes to inhibit endogenous phosphatase activity. After cells were incubated for 10 min at 37°C with hPIGF alone or with hPIGF and peptide together. Then they were washed two times with pre-chilled PBS/ Na_3VO_4 at 100 μ M and then lysed in a buffer containing 2 mM Tris-HCl at pH 8, 5 mM EDTA, 150 mM NaCl, 1% Triton-X 100, 10% glycerol, 10 mM zinc acetate, 100 μ M Na_3VO_4 and a mixture of protease inhibitors 1x for 1 hr at 4°C in agitation. Then the samples were centrifugated for 10 min at 12000 x g and supernatants were recovered and stored at -80°C. The protein concentration was determined with Bradford method (Bio-Rad assay). To immunoprecipitate Flt-1, 5 μ g/ml of a goat polyclonal antibody against human Flt-1 (Santa Cruz Biotechnology) was incubated with 30 μ l of Protein G-Sepharose resin (Amersham Biosciences) overnight at 4°C. Then the samples were centrifugated at 2000 rpm for 5 min and resins were incubated with 1 mg of proteic extract overnight at 4°C. After the removal of supernatants, resins were washed twice with lysis buffer, twice with lysis buffer without detergent and finally with Tris-buffered saline. The pellets of resin were treated with 20 μ l of Lemly buffer 1x in reducing condition, boiled at 100°C for 5 min and supernatants were loaded on a reducing 8.5% SDS-PAGE. Proteins were detected by western blotting as described above.

To detect the phosphorylation level of Flt-1, the filter was incubated primary with mouse monoclonal antibody against phospho-tyrosine (Sigma) diluted 1:1,000 in BSA 3%/ Tris-

buffered saline (blocking buffer), 1 hr at room temperature and after with an anti-mouse HRP-conjugated antibody (Pierce) diluted 1:10,000 in blocking buffer, as the secondary antibody. The same filter was stripped with β -mercaptoethanol 100 mM, TRIS-Cl 62.5 mM pH 6.7 and SDS 2% for 30 min at 50°C. Then the filter was incubated with mouse monoclonal antibody against VEGFR-1 (Sigma) diluted 1:500 in no fat milk 5% in Tris-buffered saline, 1hr at room temperature followed by incubation with the secondary antibody (Pierce) diluted 1:10,000.

Densitometry analysis to evaluate the degree of Flt-1 phosphorylation was performed using ImageQuant 5.2 software (Amersham Biosciences).

5.8 Capillary-like tube formation assays

A 48 well plate was coated with Matrigel™ (BD Biosciences) diluted 1:1 in endothelial basal medium (EBM)-2 medium (Cambrex) (110 μ l/well) and incubated at 37°C for 30 min. HUVECs (Cambrex) (75000 cells) were seeded in 500 μ l of EBM-2 medium in the presence of both PlGF-1 or VEGF (100 ng/ml) and peptides at a concentration ranging from 4 to 0.16 μ M. Endothelial growth medium (EGM)-2 (Cambrex) and EBM-2 medium were used respectively as positive and negative control. After 6 hours of incubation, capillary-like tube formation was examined under an inverted phase microscope. Cells were fixed with PBS containing 0.2% glutaraldehyde, 1% paraformaldehyde and photographed. To confirm the specificity of selected peptides, an unrelated tetrameric peptide was used at a concentration of 4 μ M. The assays were performed in triplicate. The same protocol was made to test the organic molecules, with the difference that they were added in a concentration range from 2 to 20 μ M.

5.9 Chicken embryo chorioallantoic membrane (CAM) assay

Alginate beads (5 μ l) containing vehicle or 150 ng/embryo of VEGF₁₆₅ with or without peptides (0.25 and 0.025 nmoles/embryo) were prepared as described [87] and placed on top of the CAM of fertilized White Leghorn chicken eggs at day 11 of incubation (6-8 eggs per experimental group). After 72 hours, new blood vessels converging towards the implant were counted by two observers in a double-blind fashion under a stereomicroscope (STEMI-SR, x2/0.12; Zeiss).

5.10 Cornea neo-vascularization

Single injections of 0.4, 4 or 20 nmol of peptide 4-23-5 in DMSO were carried out (33 gauge needle) in the corneas of Balb/c mice (n=3 each group). Eyes were harvested 7 days after injection, corneas were gently isolated and immunohistochemical staining for vascular endothelial cells was performed. Corneas were fixed in 100% acetone for 20 minutes, washed with PBS – 0.05% Tween 20 for 10 minutes four consecutive times, and blocked with 3% BSA in PBS for 48 hours. The corneas were then incubated with FITC-coupled monoclonal anti-mouse CD31 antibody (Pharmingen) at 3:1000 and rabbit anti-mouse LYVE-1 antibody (Abcam) at 3:1000 in 3% BSA PBS solution at 4 °C for 48 h. The corneas were washed as previously described and incubated in Cy3 conjugated donkey anti-rabbit at 3:1000 in 3% BSA PBS solution for 2 h after which they were washed and mounted with an antifading agent (Vectashield). The corneal flat mounts were visualized with a fluorescent microscope (Nikon Eclipse TE2000-E). Blood vessels were defined as CD31 positive and LYVE-1 negative.

VI. References

1. Zhang, J. and S. Hughes, *Role of the ephrin and Eph receptor tyrosine kinase families in angiogenesis and development of the cardiovascular system*. J Pathol, 2006. **208**(4): p. 453-61.
2. Wang, H.U., Z.F. Chen, and D.J. Anderson, *Molecular distinction and angiogenic interaction between embryonic arteries and veins revealed by ephrin-B2 and its receptor Eph-B4*. Cell, 1998. **93**(5): p. 741-53.
3. Gerety, S.S. and D.J. Anderson, *Cardiovascular ephrinB2 function is essential for embryonic angiogenesis*. Development, 2002. **129**(6): p. 1397-410.
4. Pugh, C.W. and P.J. Ratcliffe, *Regulation of angiogenesis by hypoxia: role of the HIF system*. Nat Med, 2003. **9**(6): p. 677-84.
5. Carmeliet, P., *Angiogenesis in health and disease*. Nat Med, 2003. **9**(6): p. 653-60.
6. Ribatti, D., et al., *The history of the angiogenic switch concept*. Leukemia, 2007. **21**(1): p. 44-52.
7. Otrock, Z.K., J.A. Makarem, and A.I. Shamseddine, *Vascular endothelial growth factor family of ligands and receptors: review*. Blood Cells Mol Dis, 2007. **38**(3): p. 258-68.
8. Tischer, E., et al., *The human gene for vascular endothelial growth factor. Multiple protein forms are encoded through alternative exon splicing*. J Biol Chem, 1991. **266**(18): p. 11947-54.
9. Neufeld, G., et al., *Vascular endothelial growth factor (VEGF) and its receptors*. Faseb J, 1999. **13**(1): p. 9-22.
10. Dvorak, H.F., *Vascular permeability factor/vascular endothelial growth factor: a critical cytokine in tumor angiogenesis and a potential target for diagnosis and therapy*. J Clin Oncol, 2002. **20**(21): p. 4368-80.
11. Jakeman, L.B., et al., *Developmental expression of binding sites and messenger ribonucleic acid for vascular endothelial growth factor suggests a role for this protein in vasculogenesis and angiogenesis*. Endocrinology, 1993. **133**(2): p. 848-59.
12. Carmeliet, P., et al., *Abnormal blood vessel development and lethality in embryos lacking a single VEGF allele*. Nature, 1996. **380**(6573): p. 435-9.
13. Xia, Y.P., et al., *Transgenic delivery of VEGF to mouse skin leads to an inflammatory condition resembling human psoriasis*. Blood, 2003. **102**(1): p. 161-8.
14. Larcher, F., et al., *VEGF/VPF overexpression in skin of transgenic mice induces angiogenesis, vascular hyperpermeability and accelerated tumor development*. Oncogene, 1998. **17**(3): p. 303-11.
15. Rossiter, H., et al., *Loss of vascular endothelial growth factor activity in murine epidermal keratinocytes delays wound healing and inhibits tumor formation*. Cancer Res, 2004. **64**(10): p. 3508-16.
16. Ferrara, N., H.P. Gerber, and J. LeCouter, *The biology of VEGF and its receptors*. Nat Med, 2003. **9**(6): p. 669-76.
17. Benjamin, L.E. and E. Keshet, *Conditional switching of vascular endothelial growth factor (VEGF) expression in tumors: induction of endothelial cell shedding and regression of hemangioblastoma-like vessels by VEGF withdrawal*. Proc Natl Acad Sci U S A, 1997. **94**(16): p. 8761-6.
18. Liu, Y., et al., *Hypoxia regulates vascular endothelial growth factor gene expression in endothelial cells. Identification of a 5' enhancer*. Circ Res, 1995. **77**(3): p. 638-43.
19. Levy, N.S., et al., *Hypoxic stabilization of vascular endothelial growth factor mRNA by the RNA-binding protein HuR*. J Biol Chem, 1998. **273**(11): p. 6417-23.
20. Stein, I., et al., *Translation of vascular endothelial growth factor mRNA by internal ribosome entry: implications for translation under hypoxia*. Mol Cell Biol, 1998. **18**(6): p. 3112-9.

21. Gerber, H.P., et al., *Differential transcriptional regulation of the two vascular endothelial growth factor receptor genes. Flt-1, but not Flk-1/KDR, is up-regulated by hypoxia.* J Biol Chem, 1997. **272**(38): p. 23659-67.
22. Barleon, B., et al., *Vascular endothelial growth factor up-regulates its receptor fms-like tyrosine kinase 1 (FLT-1) and a soluble variant of FLT-1 in human vascular endothelial cells.* Cancer Res, 1997. **57**(23): p. 5421-5.
23. Waltenberger, J., et al., *Functional upregulation of the vascular endothelial growth factor receptor KDR by hypoxia.* Circulation, 1996. **94**(7): p. 1647-54.
24. Hood, J.D., et al., *VEGF upregulates eNOS message, protein, and NO production in human endothelial cells.* Am J Physiol, 1998. **274**(3 Pt 2): p. H1054-8.
25. Ferrara, N., *Vascular endothelial growth factor: basic science and clinical progress.* Endocr Rev, 2004. **25**(4): p. 581-611.
26. Maglione, D., et al., *Isolation of a human placenta cDNA coding for a protein related to the vascular permeability factor.* Proc Natl Acad Sci U S A, 1991. **88**(20): p. 9267-71.
27. Persico, M.G., V. Vincenti, and T. DiPalma, *Structure, expression and receptor-binding properties of placenta growth factor (PlGF).* Curr Top Microbiol Immunol, 1999. **237**: p. 31-40.
28. Nagy, J.A., A.M. Dvorak, and H.F. Dvorak, *VEGF-A(164/165) and PlGF: roles in angiogenesis and arteriogenesis.* Trends Cardiovasc Med, 2003. **13**(5): p. 169-75.
29. Autiero, M., et al., *Role of PlGF in the intra- and intermolecular cross talk between the VEGF receptors Flt1 and Flk1.* Nat Med, 2003. **9**(7): p. 936-43.
30. DiSalvo, J., et al., *Purification and characterization of a naturally occurring vascular endothelial growth factor.placenta growth factor heterodimer.* J Biol Chem, 1995. **270**(13): p. 7717-23.
31. Carmeliet, P., et al., *Synergism between vascular endothelial growth factor and placental growth factor contributes to angiogenesis and plasma extravasation in pathological conditions.* Nat Med, 2001. **7**(5): p. 575-83.
32. Odoriso, T., et al., *Mice overexpressing placenta growth factor exhibit increased vascularization and vessel permeability.* J Cell Sci, 2002. **115**(Pt 12): p. 2559-67.
33. Oura, H., et al., *A critical role of placental growth factor in the induction of inflammation and edema formation.* Blood, 2003. **101**(2): p. 560-7.
34. Silins, G., et al., *Analysis of the promoter region of the human VEGF-related factor gene.* Biochem Biophys Res Commun, 1997. **230**(2): p. 413-8.
35. Ristimaki, A., et al., *Proinflammatory cytokines regulate expression of the lymphatic endothelial mitogen vascular endothelial growth factor-C.* J Biol Chem, 1998. **273**(14): p. 8413-8.
36. Nash, A.D., et al., *The biology of vascular endothelial growth factor-B (VEGF-B).* Pulm Pharmacol Ther, 2006. **19**(1): p. 61-9.
37. Enholm, B., et al., *Comparison of VEGF, VEGF-B, VEGF-C and Ang-1 mRNA regulation by serum, growth factors, oncoproteins and hypoxia.* Oncogene, 1997. **14**(20): p. 2475-83.
38. Bellomo, D., et al., *Mice lacking the vascular endothelial growth factor-B gene (Vegfb) have smaller hearts, dysfunctional coronary vasculature, and impaired recovery from cardiac ischemia.* Circ Res, 2000. **86**(2): p. E29-35.
39. Mould, A.W., et al., *Vegfb gene knockout mice display reduced pathology and synovial angiogenesis in both antigen-induced and collagen-induced models of arthritis.* Arthritis Rheum, 2003. **48**(9): p. 2660-9.
40. Joukov, V., et al., *Proteolytic processing regulates receptor specificity and activity of VEGF-C.* Embo J, 1997. **16**(13): p. 3898-911.

41. Karkkainen, M.J., et al., *Vascular endothelial growth factor C is required for sprouting of the first lymphatic vessels from embryonic veins*. Nat Immunol, 2004. **5**(1): p. 74-80.
42. Skobe, M., et al., *Concurrent induction of lymphangiogenesis, angiogenesis, and macrophage recruitment by vascular endothelial growth factor-C in melanoma*. Am J Pathol, 2001. **159**(3): p. 893-903.
43. Fujimoto, J., et al., *Clinical implication of expression of vascular endothelial growth factor-C in metastatic lymph nodes of uterine cervical cancers*. Br J Cancer, 2004. **91**(3): p. 466-9.
44. He, Y., T. Karpanen, and K. Alitalo, *Role of lymphangiogenic factors in tumor metastasis*. Biochim Biophys Acta, 2004. **1654**(1): p. 3-12.
45. Farnebo, F., F. Piehl, and J. Lagercrantz, *Restricted expression pattern of vegf-d in the adult and fetal mouse: high expression in the embryonic lung*. Biochem Biophys Res Commun, 1999. **257**(3): p. 891-4.
46. Saharinen, P., et al., *Lymphatic vasculature: development, molecular regulation and role in tumor metastasis and inflammation*. Trends Immunol, 2004. **25**(7): p. 387-95.
47. Stacker, S.A., et al., *VEGF-D promotes the metastatic spread of tumor cells via the lymphatics*. Nat Med, 2001. **7**(2): p. 186-91.
48. Lyttle, D.J., et al., *Homologs of vascular endothelial growth factor are encoded by the poxvirus orf virus*. J Virol, 1994. **68**(1): p. 84-92.
49. Ogawa, S., et al., *A novel type of vascular endothelial growth factor, VEGF-E (NZ-7 VEGF), preferentially utilizes KDR/Flk-1 receptor and carries a potent mitotic activity without heparin-binding domain*. J Biol Chem, 1998. **273**(47): p. 31273-82.
50. Meyer, M., et al., *A novel vascular endothelial growth factor encoded by Orf virus, VEGF-E, mediates angiogenesis via signalling through VEGFR-2 (KDR) but not VEGFR-1 (Flt-1) receptor tyrosine kinases*. Embo J, 1999. **18**(2): p. 363-74.
51. Wise, L.M., et al., *Vascular endothelial growth factor (VEGF)-like protein from orf virus NZ2 binds to VEGFR2 and neuropilin-1*. Proc Natl Acad Sci U S A, 1999. **96**(6): p. 3071-6.
52. Suto, K., et al., *Crystal structures of novel vascular endothelial growth factors (VEGF) from snake venoms: insight into selective VEGF binding to kinase insert domain-containing receptor but not to fms-like tyrosine kinase-1*. J Biol Chem, 2005. **280**(3): p. 2126-31.
53. Tokunaga, Y., Y. Yamazaki, and T. Morita, *Identification and localization of heparin-binding region of snake venom VEGF and its blocking of VEGF-A165*. Pathophysiol Haemost Thromb, 2005. **34**(4-5): p. 194-6.
54. Shibuya, M., et al., *Nucleotide sequence and expression of a novel human receptor-type tyrosine kinase gene (flt) closely related to the fms family*. Oncogene, 1990. **5**(4): p. 519-24.
55. Peters, K.G., C. De Vries, and L.T. Williams, *Vascular endothelial growth factor receptor expression during embryogenesis and tissue repair suggests a role in endothelial differentiation and blood vessel growth*. Proc Natl Acad Sci U S A, 1993. **90**(19): p. 8915-9.
56. Fong, G.H., et al., *Role of the Flt-1 receptor tyrosine kinase in regulating the assembly of vascular endothelium*. Nature, 1995. **376**(6535): p. 66-70.
57. Sawano, A., et al., *Flt-1, vascular endothelial growth factor receptor 1, is a novel cell surface marker for the lineage of monocyte-macrophages in humans*. Blood, 2001. **97**(3): p. 785-91.
58. Zachary, I. and G. Glikli, *Signaling transduction mechanisms mediating biological actions of the vascular endothelial growth factor family*. Cardiovasc Res, 2001. **49**(3): p. 568-81.

59. Wang, H. and J.A. Keiser, *Vascular endothelial growth factor upregulates the expression of matrix metalloproteinases in vascular smooth muscle cells: role of flt-1*. *Circ Res*, 1998. **83**(8): p. 832-40.
60. Hattori, K., et al., *Placental growth factor reconstitutes hematopoiesis by recruiting VEGFR1(+) stem cells from bone-marrow microenvironment*. *Nat Med*, 2002. **8**(8): p. 841-9.
61. Luttun, A., et al., *Revascularization of ischemic tissues by PIGF treatment, and inhibition of tumor angiogenesis, arthritis and atherosclerosis by anti-Flt1*. *Nat Med*, 2002. **8**(8): p. 831-40.
62. Kaplan, R.N., et al., *VEGFR1-positive haematopoietic bone marrow progenitors initiate the pre-metastatic niche*. *Nature*, 2005. **438**(7069): p. 820-7.
63. Lamszus, K., et al., *Levels of soluble vascular endothelial growth factor (VEGF) receptor 1 in astrocytic tumors and its relation to malignancy, vascularity, and VEGF-A*. *Clin Cancer Res*, 2003. **9**(4): p. 1399-405.
64. Ambati, B.K., et al., *Corneal avascularity is due to soluble VEGF receptor-1*. *Nature*, 2006. **443**(7114): p. 993-7.
65. Matsumoto, T. and L. Claesson-Welsh, *VEGF receptor signal transduction*. *Sci STKE*, 2001. **2001**(112): p. RE21.
66. Shalaby F., R.J., Yamaguchi T. P., Gertsenstein M., Wu X. F., Breitman M. L. and Schuh A. C., *Failure of blood-island formation and vasculogenesis in Flk-1-deficient mice*. *Nature*, 1995. **376**: p. 62-66.
67. Kabrun, N., et al., *Flk-1 expression defines a population of early embryonic hematopoietic precursors*. *Development*, 1997. **124**(10): p. 2039-48.
68. Stinchcombe, T.E. and M.A. Socinski, *Bevacizumab in the treatment of non-small-cell lung cancer*. *Oncogene*, 2007. **26**(25): p. 3691-8.
69. Pajusola, K., et al., *Signalling properties of FLT4, a proteolytically processed receptor tyrosine kinase related to two VEGF receptors*. *Oncogene*, 1994. **9**(12): p. 3545-55.
70. Paavonen, K., et al., *Vascular endothelial growth factor receptor-3 in lymphangiogenesis in wound healing*. *Am J Pathol*, 2000. **156**(5): p. 1499-504.
71. Partanen, T.A., K. Alitalo, and M. Miettinen, *Lack of lymphatic vascular specificity of vascular endothelial growth factor receptor 3 in 185 vascular tumors*. *Cancer*, 1999. **86**(11): p. 2406-12.
72. Jennbacken, K., et al., *Expression of vascular endothelial growth factor C (VEGF-C) and VEGF receptor-3 in human prostate cancer is associated with regional lymph node metastasis*. *Prostate*, 2005. **65**(2): p. 110-6.
73. Valtola, R., et al., *VEGFR-3 and its ligand VEGF-C are associated with angiogenesis in breast cancer*. *Am J Pathol*, 1999. **154**(5): p. 1381-90.
74. Miao, H.Q. and M. Klagsbrun, *Neuropilin is a mediator of angiogenesis*. *Cancer Metastasis Rev*, 2000. **19**(1-2): p. 29-37.
75. Fuh, G., K.C. Garcia, and A.M. de Vos, *The interaction of neuropilin-1 with vascular endothelial growth factor and its receptor flt-1*. *J Biol Chem*, 2000. **275**(35): p. 26690-5.
76. Kitsukawa, T., et al., *Overexpression of a membrane protein, neuropilin, in chimeric mice causes anomalies in the cardiovascular system, nervous system and limbs*. *Development*, 1995. **121**(12): p. 4309-18.
77. Soker, S., et al., *Neuropilin-1 is expressed by endothelial and tumor cells as an isoform-specific receptor for vascular endothelial growth factor*. *Cell*, 1998. **92**(6): p. 735-45.
78. Tordjman, R., et al., *Neuropilin-1 is expressed on bone marrow stromal cells: a novel interaction with hematopoietic cells?* *Blood*, 1999. **94**(7): p. 2301-9.

79. Yuan, L., et al., *Abnormal lymphatic vessel development in neuropilin 2 mutant mice*. Development, 2002. **129**(20): p. 4797-806.
80. Kawasaki, T., et al., *A requirement for neuropilin-1 in embryonic vessel formation*. Development, 1999. **126**(21): p. 4895-902.
81. Glade-Bender, J., J.J. Kandel, and D.J. Yamashiro, *VEGF blocking therapy in the treatment of cancer*. Expert Opin Biol Ther, 2003. **3**(2): p. 263-76.
82. Bando, H., *Vascular endothelial growth factor and bevacitumab in breast cancer*. Breast Cancer, 2007. **14**(2): p. 163-73.
83. Morabito, A., et al., *Tyrosine kinase inhibitors of vascular endothelial growth factor receptors in clinical trials: current status and future directions*. Oncologist, 2006. **11**(7): p. 753-64.
84. Bernatchez, P.N., S. Soker, and M.G. Sirois, *Vascular endothelial growth factor effect on endothelial cell proliferation, migration, and platelet-activating factor synthesis is Flk-1-dependent*. J Biol Chem, 1999. **274**(43): p. 31047-54.
85. Isner, J.M., et al., *Assessment of risks associated with cardiovascular gene therapy in human subjects*. Circ Res, 2001. **89**(5): p. 389-400.
86. Thurston, G., et al., *Angiopoietin-1 protects the adult vasculature against plasma leakage*. Nat Med, 2000. **6**(4): p. 460-3.
87. Luttun, A., M. Tjwa, and P. Carmeliet, *Placental growth factor (PlGF) and its receptor Flt-1 (VEGFR-1): novel therapeutic targets for angiogenic disorders*. Ann N Y Acad Sci, 2002. **979**: p. 80-93.
88. Houghten R. A., W.D.B., Pinilla C., *Drug discovery and vaccine development using mixture based synthetic combinatorial Libraries*. Drug Discovery Today, 2000. **5**(7): p. 276.
89. Merrieffeld, R.B., *Peptide synthesis. I. The synthesis of a tetrapeptide*. Journal of American Chemical Society, 1963. **85**: p. 2149.
90. Shin D.S., K.D.H., Chung W.J., Lee Y.S., *Combinatorial Solid Phase Peptide Synthesis and Bioassays*. Journal of Biochemistry and Molecular Biology, 2005. **38**(5): p. 517.
91. Lam, K.S., et al., *A new type of synthetic peptide library for identifying ligand-binding activity*. Nature, 1991. **354**(6348): p. 82-4.
92. Iyer, S., et al., *The crystal structure of human placenta growth factor-1 (PlGF-1), an angiogenic protein, at 2.0 Å resolution*. J Biol Chem, 2001. **276**(15): p. 12153-61.
93. Errico, M., et al., *Identification of placenta growth factor determinants for binding and activation of Flt-1 receptor*. J Biol Chem, 2004. **279**(42): p. 43929-39.
94. Mitola, S., et al., *Cutting edge: extracellular high mobility group box-1 protein is a proangiogenic cytokine*. J Immunol, 2006. **176**(1): p. 12-5.
95. Fischer C., et al., *Anti-PlGF inhibits growth of VEGF(R)-Inhibitor-Resistant Tumors without Affecting Healthy Vessels*. Cell, 2007. **131**(2): p. 463-75.
96. Bae, D.G., et al., *Anti-flt1 peptide, a vascular endothelial growth factor receptor 1-specific hexapeptide, inhibits tumor growth and metastasis*. Clin Cancer Res, 2005. **11**(7): p. 2651-61.
97. El-Mousawi, M., et al., *A vascular endothelial growth factor high affinity receptor 1-specific peptide with antiangiogenic activity identified using a phage display peptide library*. J Biol Chem, 2003. **278**(47): p. 46681-91.
98. Taylor, A.P. and D.M. Goldenberg, *Role of placenta growth factor in malignancy and evidence that an antagonistic PlGF/Flt-1 peptide inhibits the growth and metastasis of human breast cancer xenografts*. Mol Cancer Ther, 2007. **6**(2): p. 524-31.

VII. Abstracts and Courses

1. **S. Ponticelli**, D. Marasco, M. Ruvo, S. De Falco “New peptide inhibitor of Flt-1 (VEGFR-1) receptor”, Workshop SIICA-SIC “Angiogenesi: basi molecolari e implicazioni terapeutiche”, Certosa di Pontignano (Si), 05-07 giugno 2006.
2. D. Marasco, **S. Ponticelli**, A. Saporito, V. Tarallo, E. Benedetti, C. Pedone, J.M. Stassen, S. De Falco and M. Ruvo “Identification of inhibitors of PlGF/ Flt-1 interaction by the screening of peptide compounds libraries”, 9th Naples Workshop on Bioactive Peptides, Napoli 11-14 giugno 2006.
3. E. Lonardo, **S. Ponticelli**, D. Marasco, A. Saporito, M. Ruvo, S. De Falco, G. Minchiotti “Identification of Cripto inhibitors to direct cell fate specification in ES cells”, Summer school “Stem cell and regenerative medicine “, Hydra 15-21 settembre 2006.
4. E. Lonardo, **S. Ponticelli**, D. Marasco, A. Saporito, M. Ruvo, S. De Falco, G. Minchiotti “A combinatorial approach to direct neuronal fate specification from embryonic stem cells”, VIII National Congress FISV 2006, Riva del Garda 28 settembre- 01 ottobre 2006.
5. **S. Ponticelli**, D. Marasco, V. Tarallo, A. Saporito, M. Ruvo, S. De Falco “New peptide inhibitor of Flt-1 (VEGFR-1) receptor”, VIII National Congress FISV 2006, Riva del Garda 28 settembre- 01 ottobre 2006.
6. De Falco S, Tarallo V., Vesci L., **Ponticelli S.**, Riccioni T., Di Laschi A., Orlandi A, Pisano C. and Persico M.G. “Placental Growth Factor Variants for inhibition of VEGF-dependent tumor growth”, XLVIII Congresso Nazionale della Società Italiana di Cancerologia, Bari 4-8 ottobre 2006.
7. **S. Ponticelli**, D. Marasco, F. Del Piazz, J.M. Stassen, N. De Tommasi, M. Ruvo and S. De Falco “Identification of small molecules able to inhibit Flt-1 activation”, EMBO-IGB Workshop “Cell migration, tissue invasion and disease”, Capri 14-17 ottobre 2006.

Angiogenesi: basi molecolari ed implicazioni terapeutiche



Workshop SIICA-SIC
CERTOSA DI PONTIGNANO (Siena)
5-7 Giugno 2006

New peptides inhibitor of Flt-1(VEGFR-1) receptor

S. Ponticelli¹, D. Marasco², M. Ruvo², S. De Falco¹

¹*Istituto di Genetica e Biofisica "Adriano Buzzati Traverso", CNR, via Pietro Castellino 111, 80131, Naples, Italy,* ²*Istituto di Bioimmagini e Biostrutture, CNR, via Mezzocannone 16, 80134, Naples, Italy*

In the last decade the concept of angiogenic therapy has been developed with the aim to treat both the pathology characterized by a reduced angiogenesis, such as in ischemic injury, and those showing an excessive angiogenesis, such as tumor growth and diabetic retinopathy.

VEGF-A (Vascular Endothelial Growth Factor), the main member of related growth factor family, exerts its action through the binding to two receptors: its specific receptor, VEGFR-2 (KDR), and a second receptor recognized also by other members of the family, like PlGF (Placental Growth Factor) and VEGF-B, named VEGFR-1 (Flt-1). Many efforts have been done to identify inhibitor of VEGF-A /KDR interaction, but recently many data indicates that Flt-1 signaling is involved in the neo-angiogenesis process associated to pathological status, like tumor growth.

In order to identify new molecules able to inhibit the interaction between the tirosine-kinase receptor Flt-1 and the soluble factors PlGF and/or VEGF-A, we have analyzed some combinatorial peptide libraries. The libraries have been screened by an immunological assay based on ELISA methodology with Flt-1 receptor coated on microtiter plate.

The screening of a tetrameric tripeptidic library (complexity: $3^{30} = 27000$ molecules), made with unnatural aminoacids, has allowed the identification of two sequences named 4-23-5 e 4-23-23, that are able to inhibit PlGF /Flt-1 and VEGF-A/Flt-1 interactions with an about $10 \mu\text{M}$ IC_{50} . The observed activity depends both on sequences and on the tetrameric structure as demonstrated in ELISA assays performed respectively with *Ala-scanning* peptides and with structural related peptides. The selected peptides bind exclusively Flt-1 receptor rather than KDR. Moreover the molecules inhibit the formation of a capillary-like network induced by both PlGF and VEGF-A on primary human endothelial cells (HUVEC), at a concentration of about $4 \mu\text{M}$.

Identification of inhibitors of PIGF/ Flt-1 interaction by the screening of peptide compounds libraries.

D. Marasco^{1‡}, S. Ponticelli^{2‡}, A. Saporito¹, V. Tarallo, E Benedetti¹, C. Pedone, J.M. Stassen³, S. De Falco² and M. Ruvo¹.

¹Istituto di Biostrutture e Bioimmagini, Sezione Biostrutture, Napoli-Italy; ²Istituto di Genetica e Biofisica "Adriano B. Traverso" del CNR, Napoli-Italy, ³Thromb-X N.V., Leuven, Belgium.

‡ These authors contributed equally to this work.

Blood vessel formation largely contributes to the pathogenesis of numerous diseases, including ischemia and cancer [1-2]. In this regard therapeutic strategies aim to stimulate vascular growth in ischemic tissues and suppress their formation in pathologies like in tumour and diabetic retinopathy. Placental growth factor (PIGF), an homolog of vascular endothelial growth factor (VEGF), (42% amino acid sequence identity), stimulates angiogenesis and collateral growth in ischemic heart and limb. Whereas VEGF exerts its biological function through the binding to both VEGF receptor-1 (VEGFR-1 or Flt1) and VEGFR-2 (or KDR) PIGF binds specifically to Flt1. The complex PIGF/Flt1 constitutes a potential candidate for therapeutic modulation of angiogenesis and inflammation [3].

The binding between PIGF and Flt-1 has multipunctual features [4] and potential antagonist must have a sufficient molecular surface to spatially distant contact points. We have used an ELISA-like screening assay to select antagonists of PIGF/Flt-1 complex from a large random library of tetrameric unnatural peptides (complexity: $3^{30}=27.000$ molecules) identifying two active molecules with an about 10^{-6} M IC₅₀. The relative stability of identified peptides were assessed in human serum and their inhibitory properties were tested in a capillary-like tube formation assay performed with Human Umbilical Vein Endothelial Cells (HUVEC).

References

1. Bussolino et al. *TIBS*, 1997, 22, 251-256.
2. Iyer, S., et al., *J. Biol. Chem.* 2001, 276(15), 12153-12161
3. Carmeliet P, et al. *Nat Med* 2001, 7(5):575-83
4. Davis-Smyth T. et al *J. Biol. Chem.* 1998, 273(6), 3216-3222

Identification of Cripto inhibitors to direct cell fate specification in ES cells

E. Lonardo, S. Ponticelli, D. Marasco*, A. Saporito*, M. Ruvo*, S. De Falco, G. Minchiotti

Institute of Genetics and Biophysics "A. Buzzati-Traverso", CNR, Via P. Castellino 111, 80131, Naples, Italy. * Institute of Biostructure and Bioimaging, CNR, Via Mezzocannone 16, 80134, Naples, Italy.

Cripto is a cystein-rich protein anchored to the cell membrane through a glycosyl-phosphatidylinositol (GPI)-linkage, and it is the founding member of the EGF-CFC family. *Cripto* is expressed both in the Embryonic Stem (ES) cells and during the early phases of embryo development while, in the adult, it is reactivated in a wide range of epithelial cancers. Recent studies, revealed that *cripto* is a key molecule required for both induction of cardiomyocyte differentiation and repression of neural differentiation in ES cells. Recently, we have show that *in vitro* differentiation of *Cripto*^{-/-} (ES) cells results in increased dopaminergic differentiation and that, upon transplantation into Parkinsonian rats, they result in behavioural and anatomical recovery with no tumor formation (Parish et al, 2005). Indeed, these results strengthen the importance of identifying Cripto inhibitor molecules as a powerful tool to decode the molecular mechanisms of Cripto function both in stem cell differentiation and tumorigenesis. We are thus exploiting a novel experimental approach based on the use of combinatorial chemistry combined to ES cell differentiation, to identify new molecules able to inhibit Cripto signaling by interfering with Cripto binding to the receptor as new tools to direct neuronal fate specification from mouse ES cells. By using an *in vitro* ELISA-based technology, we have screened a tetrameric tripeptide library and identified peptides that are able to inhibit Cripto/Alk4 receptor interaction; selected peptides showing the highest inhibitory effects in the ELISA assay are currently tested in the ES cell differentiation assay. The availability of molecule(s) which antagonize Cripto activity, may represent a powerful tool to dissect the functional role of Cripto in ES cells differentiation.

Parish CL, Parisi S, Lago CT, Persico MG, Arenas E, Minchiotti G. Cripto as a target for improving embryonic stem cell-based therapy in Parkinson's disease. *Stem Cells*. 2005; 23:471-476.

ATTI



FISV
Federazione Italiana
Scienze della Vita

ABCD: Associazione di Biologia Cellulare e del Differenziamento
AGI: Associazione Genetica Italiana
SIBBM: Società Italiana di Biofisica e Biologia Molecolare
SICA: Società Italiana di Chimica Agraria
SIGA: Società Italiana di Genetica Agraria
SIFV: Società Italiana di Fisiologia Vegetale
SIMA: Società Italiana di Mutagenesi Ambientale
SINS: Società Italiana di Neuroscienze
SIMGBM: Società Italiana di Microbiologia Generale e Biotecnologie Microbiche
SIP: Società Italiana di Patologia
SIPaV: Società Italiana di Patologia Vegetale

28 settembre - 1 ottobre 2006 - Riva del Garda TN

8. CONVEGNO

Parallel Minisymposium 4

Stem cells, development and differentiation

PMS.04 · P.37

Role of YAP (Yes-Associated Protein) in epithelial cell differentiation

I. D'Addario, C. Abbruzzese, P. Paterna, O. Golisano
 Lab. Tissue Engineering and Cutaneous Physiopathology, IDI - IRCCS
 Pomezia (Rome)
 » idaddario@libero.it «

It is well known that Δ Np63 α is expressed in keratinocytes with high proliferative potential and that it has an important role in the transcription modulation of 14-3-3 σ , a key protein in the differentiation process. Since Δ Np63 α seems to be necessary but not sufficient for the maintaining of keratinocytes in the staminal compartment, we investigated the role of a common molecular partner of Δ Np63 α and 14-3-3 σ , YES-Associated Protein (YAP), in epithelial cell differentiation. Results indicated that YAP is localized both in nucleus and cytoplasm where it interacts with Δ Np63 α and 14-3-3 σ respectively. Although the total amount of YAP seems not altered during the life-span, we observed that in young cultures YAP is more abundant in the nucleus, whereas in differentiated cells it is preferentially localized in the cytoplasm. This suggests that YAP could be a regulator of keratinocyte differentiation through its different localization during the life-span and therefore through different interactions with molecular partners as 14-3-3 σ and Δ Np63 α . To further investigate the role of YAP, we are currently over-expressing YAP alone and with Δ Np63 α in human normal keratinocytes.

PMS.04 · P.38

Wnt signalling controls hepatic differentiation

M. Colletti¹, C. Cicchini¹, A. Conigliaro¹, R. Manfredini²,
 R. Zini², M. Tripodi¹, L. Amicone¹
¹Dept Cellular Biotechnology, Univ. Rome "La Sapienza" (Rome);
²Dip. Scienze Biomediche, Sez. Chimica Biologica,
 Univ. Modena e Reggio Emilia (Modena)
 » colletti.marta@bce.uniroma1.it «

We previously established and characterized several Met Murine Hepatocyte (MMH) lines derived from transgenic mice expressing constitutively active human Met. MMHs harbour two cell types: fully differentiated hepatocytes (MMH-epithelial) and bipotential precursor cells (MMH-palmate cells), able to differentiate into hepatocytes as well as into cholangiocytes. MicroArray analysis of MMH-palmate cells versus their counterparts fully differentiated into hepatocytes, showed that multiple components of the Wnt signalling, including Wnt members, their receptors, downstream transcriptional factors and other components belonging to this pathway, were differentially expressed. To characterize the role of Wnt signalling in hepatocyte differentiation we i) analysed the pathway activation in different stages of hepatocyte differentiation and ii) examined the effects of the ligand Wnt3a and the Wnt inhibitor FRP3, on hepatic differentiation of MMH-palmate cells. Preliminary results suggest that MMH-palmate cells respond to exogenous Wnt3a increasing nuclear β -catenin. Moreover Wnt signalling activation induces the expression of HNF4 α targets (i.e. Albumin, TTR, PEPCK, Eph and Cyp11A1).

PMS.04 · P.39

p63 regulates cell adhesion and proliferation in mammary epithelial cells

C. Ballarò¹, B. Marinari², A. Costanzo², S. Alemà¹
¹Ist. Biologia Cellulare, CNR (Monterotondo);
²Dip. Dermatologia, Univ. Roma "Tor Vergata" (Roma)
 » cballaro@ibc.cnr.it «

The p63 gene belongs to the p53 gene family and encodes for sequence-specific transcription factors. p63 has been characterized primarily in the context of epidermis where it is implicated in the establishment of keratinocyte cell fate and in maintenance of epithelial self-renewal. p63-null mice completely lack mammary glands, highlighting a critical role for p63 in this tissue. Here, we report on the effect of loss of p63 function in MCF-10A cells, a normal human breast epithelial cell line, which forms growth-arrested acinar structures when cultured in three-dimensional basement membrane gels. Silencing of p63 expression by RNAi induces morphological changes including cell scatter and detachment, and a decrease of EGF-dependent proliferation. Consistent with these data, MCF-10A cells silenced for p63 exhibit a marked reduction in the levels of expression of E-cadherin and EGFR. Moreover, the down-regulation of p63 inhibits the formation of acini. Several traits of this phenotype can be reverted by re-expression of E-cadherin. Thus, our results evidence a role for p63 as a regulator of epithelial cell adhesion and proliferation during the morphogenesis of the mammary gland.

PMS.04 · P.40

A combinatorial approach to direct neuronal fate specification from embryonic stem cells

E. Lonardo¹, S. Ponticelli¹, D. Marasco², A. Saporito², M. Ruvo²,
 S. de Falco¹, G. Minchiotti¹
¹Inst. Genetic and Biophysics "A. Buzzati Traverso", CNR (Naples);
²Inst. Biostructure and Bioimaging, CNR (Naples)
 » lonardo@igb.cnr.it «

Recent breakthroughs in stem cell research underscore the importance of controlling stem cell differentiation for the success of cell-based therapies. In this perspective, recent findings from our laboratory indicate that the EGF-CFC protein Cripto is a key player in the signaling pathways that control neural induction in ES cells. Indeed, disruption of *cripto* in ES cells results in an enhanced ability to generate neurons in the absence of any specific inducing factors. We are exploiting a novel experimental approach based on the use of combinatorial chemistry combined to ES cell differentiation, to identify antagonists of Cripto/receptor interaction as new tools to direct neuronal fate specification from mouse ES cells. By using an *in vitro* ELISA-based technology, we have screened a tetrameric tripeptide library and identified peptides that are able to inhibit Cripto/receptor interaction and are currently tested on ES cell differentiation assays. These molecules will be extremely useful to direct ES cell fate specification without the need to manipulate the cells genetically and may thus permit a direct extension of this strategy to human cells.

Parallel Minisymposium 12

Cell cycle, oncogenes and tumor suppressors

PMS.12 · P.09

New peptides inhibitor of Flt-1(VEGFR-1) receptorS. Ponticelli¹, D. Marasco², V. Tarallo¹, A. Saporito²,
M. Ruvo², S. de Falco¹¹Inst. Genetic and Biophysics "A. Buzzati traverso", CNR (Naples);²Ist. Bioimmagini e Biostrutture, CNR (Naples)

» ponticelli@igb.cnr.it «

Recently many data indicate that Flt-1 signaling is involved in the neo-angiogenesis process associated to pathological status, like tumor growth. Flt-1 is recognized by three members of VEGF(Vascular Endothelial Growth Factor) family, VEGF-A, -B and PlGF(Placental Growth Factor). In order to identify new molecules able to inhibit the interaction between Flt-1 and its ligands PlGF and VEGF-A, we have screened combinatorial peptide libraries in an assay based on ELISA methodology. The screening of a tetrameric tripeptidic library (complexity: 30³ molecules), has allowed the identification of two sequences named 4-23-5 and 4-23-23, that are able to inhibit PlGF/Flt-1 and VEGF-A/Flt-1 interactions at about 10 µM IC₅₀. The observed activity depends both on sequences and on the tetrameric structure as demonstrated in assays performed respectively with *Ala-scanning* peptides and with structural related peptides. The selected peptides bind exclusively to Flt-1 receptor and inhibit the formation of a capillary-like network induced by both PlGF and VEGF-A on primary human endothelial cells at about 4 µM.

PMS.12 · P.11

Proteome analysis of prostate cancer using RNA interfering: discovering new molecular targets of LMW-PTPD. Cirelli, M. Biagini, F. Magherini, R. Marzocchini,
A. Modesti, G. Raugel

Dept Biochemical Sciences, Univ. Florence (Prato)

» domenico.cirelli@email.it «

Diagnosis and treatment of urological malignancies remains quite uncertain and proteomic approach could be very useful. We focused our attention on a prostatic cancer cell line (PC3), in which we found high expression of Low Molecular Weight Tyrosine Phosphatase (LMW-PTP). Several data strongly suggest that LMW-PTP contribute to cancer progression: increase of mRNA and protein level is observed in neoplastic tissue (from colon, kidney, bladder and breast) and correlation with worst prognostic parameters has been assessed. LMW-PTP may be considered a new oncogene overexpressed in many different tumors. With the use of the powerful tool of RNA interfering we obtained a strong decrease of LMW-PTP protein expression in PC3 cell line. Differential proteome analysis (2D gel electrophoresis followed by WB analysis with anti-phosphotyrosine Ab) after specific silencing has been performed in order to investigate changes in LMW-PTP-dependent protein tyrosine phosphorylation. In this way not only new LMW-PTP substrates should be identified but also signaling pathways involved in neoplastic transformation and prostate cancer progression dependent on LMW-PTP may be characterized.

PMS.12 · P.10

LMW-PTP tyrosine phosphatase overexpression correlates with colon carcinoma onset and progressionG. Raugel¹, G. Caderni², M. Biagini¹, F. Malentacchi³, R. Marzocchini¹¹Dept Biochemical Science (Florence); ²Dept Preclinic and ClinicPharmacology (Florence); ³Dept Clinic Physiopathology (Florence)

» raugel@scbio.unifi.it «

Low Molecular Weight Tyrosine Phosphatase (LMW-PTP) plays a key role in cell proliferation control by dephosphorylating/inactivating both tyrosine kinase receptors (such as PDGF, insulin and ephrin receptors) and docking proteins (β-catenin), all involved in cell adhesion and cellular survival. Several data strongly suggest that LMW-PTP contribute to cancer progression: significant increase of mRNA and protein level is observed in neoplastic tissue (from colon, kidney, bladder and breast) and correlation with worst prognostic parameters has been assessed. LMW-PTP may be considered an oncogene overexpressed in many different tumors. Its mode action is not yet precisely understood but enhanced dephosphorylation of Ephrine receptors may play a key role. Proteomic studies are currently in progress for better addressing this point. Induced rat colon carcinoma is a very commonly used model system. Analysis of samples from rat colon tumors induced with DMH revealed a significant increase of LMW-PTP expression, predominantly in tumors from the right colon tract. This study confirm the involvement of LMW-PTP in carcinoma onset and progression.

PMS.12 · P.12

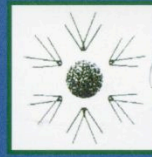
The COOH-terminal of procollagen I induces pro-metastatic changes and angiogenesis in breast carcinoma cells xenograftsD. Palmieri¹, S. Astigiano³, O. Barbieri^{2,3}, G. Casartelli³, P. Damonte³,
S. Zanotti¹, P. Manduca¹¹Dip. Biologia, Univ. Genova (Genova); ²D.O.BI.G, Univ. Genova(Genova); ³Ist. Nazionale per la Ricerca sul Cancro (Genova)

» danielapalmieri@yahoo.com «

We previously showed the the C-terminal of pro-collagen type I (C3) induces in vitro migration, Metalloproteinase-2 and -9, Metalloproteinase Tissue Inhibitor-2 and Vascular endothelial growth factor-A expression in breast carcinoma cells and migration in endothelial cells. C3 upmodulates in vitro the level of mRNA of angiogenesis and migration-associated genes (VEGF-A, VEGF-B, MMP-14 and the VEGF-A receptor Neuropilin). The data might prefigure for C3 a role in the promotion of the angiogenesis and in the progression of carcinomas in vivo. We here report that in xenograft tumors, obtained by subcutaneous implantation of MDA MB231 cells in nude mice, in presence of C3 the expression of MMP-14 and VEGF-A transcripts is enhanced and the angiogenesis is more pronounced showing larger and blood containing vessels. C3 does not affects the apoptotic rate of the cells and does not enhances cell proliferation, or tumor size significantly. These observations confirm that C3 can be considered a stromal factor involved in tumor promotion. C3 might act early in tumor progression by promoting specifically up-modulation of pro-metastatic genes, endothelial cells invasion and vessel morphogenesis.



SOCIETÀ ITALIANA DI CANCEROLOGIA



ISTITUTO TUMORI
"GIOVANNI PAOLO II" - Bari

48°

CONGRESSO NAZIONALE SOCIETÀ ITALIANA DI CANCEROLOGIA

Bari, 1 - 4 ottobre 2006

Villa Romanazzi - Carducci

48th ANNUAL MEETING OF THE ITALIAN CANCER SOCIETY



VOLUME ABSTRACT

**Mercoledì 4 Ottobre /
Wednesday October 4th**

ORAL COMMUNICATIONS

**HOMEOSTASIS AND TUMOR
PROGRESSION**

**AKT AND HYPOXIA-INDUCIBLE FACTOR
1 α PATHWAYS AS TARGETS OF N-(4-
HYDROXYPHENYL)RETINAMIDE**

**Venè R, Tosetti F, Lorusso G, Arena G,
Noonan D, Albini A**

*Laboratorio di Oncologia Sperimentale, Istituto
Nazionale per la Ricerca sul Cancro, Genova,
Italy*

We found that chemopreventive retinoid N-(4-hydroxyphenyl)retinamide (4HPR) exerts a strong anti-angiogenic effect in several ectopic models of tumor growth in nude mice and in angiogenesis assays in vivo. To investigate the mechanisms underlying the anti-angiogenic properties of 4HPR at the molecular level, we considered the signaling pathways regulated by the pro-angiogenic Insulin-like growth factor 1 (IGF-1). Our results show that 4HPR increases intracellular reactive oxygen species (ROS) levels and induces cell death in our cellular models. 4HPR down-regulates ERK-2 and AKT phosphorylation, while increases the stabilization at the protein level of the transcription factor hypoxia-inducible factor 1 α (HIF-1 α). HIF-1 is a key stimulator of tumor angiogenesis under hypoxic conditions that can also be modulated by changes in the redox state of the cell and by ROS production. Accordingly, the effect on HIF-1 α stabilization by 4HPR was partially inhibited by treatment with the antioxidants N-acetyl cysteine and pyrrolidine dithiocarbamate (PDTC), suggesting that 4HPR-mediated ROS increase could be involved in this effect.

AKT down-regulation and the induction of HIF-1 α expression were associated with loss of ATP, GSH and mitochondrial membrane potential in 4HPR-treated cells. We postulate the hypothesis that these events are associated with 4HPR-induced cell death.

**PLACENTAL GROWTH FACTOR VARIANTS
FOR INHIBITION OF VEGF-DEPENDENT
TUMOR GROWTH**

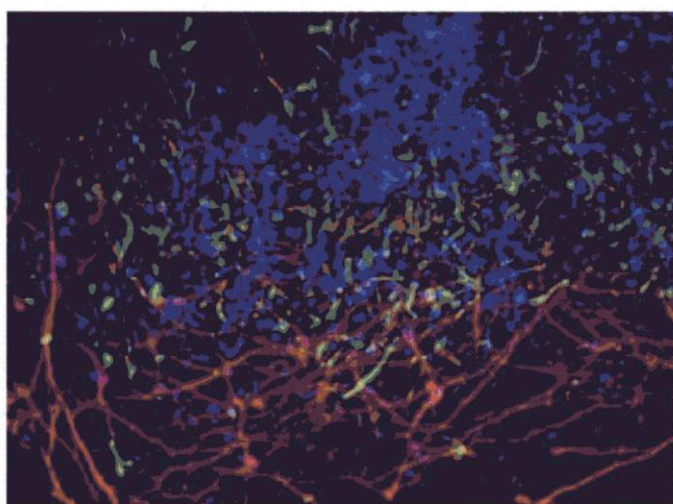
**De Falco S¹, Tarallo V¹, Vesce L², Ponticelli S¹,
Riccioni T², Di Lascio A³, Orlandi A³, Pisano
C² Persico MG¹**

*¹Institute of Genetics and Biophysics 'Adriano
Buzzati-Traverso', CNR, Napoli, Italy; ²Research
and Development, Sigma-Tau S.p.A. Industrie
Farmaceutiche Riunite, Pomezia, Rome, Italy;
³Anatomic Pathology Institute, Tor Vergata
University, Roma, Italy*

Placental Growth Factor (PIGF), a member of Vascular Endothelial Growth Factor (VEGF) family and its specific receptor fms-like tyrosine kinase receptor-1 (Flt-1 also known as VEGFR-1) play a key regulatory role in pathological angiogenesis. We have generated a PIGF variant mutated in the two negatively charged residues, Asp72 and Glu73 (PIGF-DE), that lost the property to bind and activate Flt-1 receptor but retained the property to form heterodimer if co-expressed with VEGF. The over-expression of PIGF in VEGF-expressing cells determines the formation of PIGF/VEGF heterodimer with consequent depletion of VEGF homodimer. Since the heterodimer VEGF/PIGF-DE cannot bind both VEGF receptors, we have hypothesized that the PIGF-DE variant could act as 'inhibitor' of VEGF when over-expressed in VEGF-expressing tumor cells. We have stably transfected two human carcinoma cell lines largely used for tumor xenograft experiments: NCI-H460 (small cell lung carcinoma) and A2780 (ovarian carcinoma). These cell lines have been transfected with PIGF, PIGF-DE or the empty vector. The selected stable clones and, as control, the not transfected cells, have been injected subcutaneously in CD-1 nude mice (n = 10 per group). With both cell lines, PIGF-DE transfected cells showed an irregular and delayed growth and the resulting tumors are significantly reduced with respect to the controls. Immunohistochemical analyses showed in PIGF-DE tumors a dramatic reduction in terms of vessels number and a corresponding increase of necrotic area. Interestingly, cells over-expressing PIGF did not generate larger tumors than the controls, but tumors present more big vessels as well as the smaller necrotic area.



Cell Migration, Tissue Invasion and Disease



Hotel La Palma, Capri, Italy
14 – 17 October, 2006

 IGB Press

Identification of small molecules able to inhibit Flt-1 activation

S. Ponticelli¹, D. Marasco², F. Del Piazz³, J.M. Stassen⁴, N. De Tommasi³,
M. Ruvo² and **Sandro DE FALCO**¹

¹Istituto di Genetica e Biofisica "Adriano B. Traverso" del CNR, Napoli-Italy, ²Istituto di Biostrutture e Bioimmagini, Sezione Biostrutture, Napoli-Italy; ³Dpto di Scienze Farmaceutiche, Univ. degli Studi di Salerno, Fisciano (SA), Italy and ⁴Thromb-X N.V., Leuven, Belgium

Efforts to stimulate or inhibit vessel growth have been primarily focused on VEGF-A and one of its two receptors, VEGFR-2 (KDR in human, Flk-1 in mouse). In the last ten years increasing attention has been devoted to the other receptor of VEGF, named VEGFR-1 (Flt-1) and to another member of VEGF family, placental growth factor (PlGF) that specifically recognizes Flt-1 and seems to act specifically in pathological conditions.

It has been reported that the pathway PlGF/Flt-1 is crucial for recruitment and migration of stem cells from bone marrow microenvironment for hematopoiesis, that Flt-1 positive hematopoietic progenitors are necessary for the formation of pre-metastatic niche as well as that the activation of Flt-1 by both VEGF-A and PlGF are essential for endothelial precursors recruitment for neovascularization in pathological condition. Consequently the search of small molecules able to interfere in Flt-1 activation represents a new opportunity in therapeutic perspective.

In order to identify small molecule inhibitors of PlGF and/or VEGF interaction with Flt-1 receptor, we have used two sources of small molecules: combinatorial peptide libraries and natural compounds extracted from medicinal plants. The screening of chemical collections have been performed using a competitive ELISA assay in which soluble PlGF binds to coated Flt-1 receptor and compounds have been tested for their inhibitory properties. Experiments have been conducted with PlGF since it shows highest affinity for Flt-1 than VEGF.

We have screened five peptide libraries and from a library based on tripeptide tetrameric structure, we have identified two molecules that are able to inhibit the interaction of both PlGF and VEGF to Flt-1 receptor, with an IC_{50} around 8-10 μ M. These peptides interact specifically with Flt-1 and are able to inhibit capillary-like tube formation induced by both PlGF and VEGF on human primary endothelial cells.

Regarding the natural compounds, we have screened many kinds of extracts obtained from different plants. One of this extracts showed an interesting inhibition activity, it has been fractionated and tested again, and at the end of procedure a single active compound has been identified. It interacts with both PlGF and VEGF as determined by Biacore assays, and inhibits the interaction with Flt-1 receptor with an IC_{50} around 7-8 μ M. This molecule is able to inhibit capillary-like tube formation of human primary endothelial cells.

The identified inhibitors will be assayed in vivo in the models of tumor growth and corneal neo-vascularization.

May 2006: Participation as Pratical Teacher to “ Stem Cell Differentiation Training course” organized by ‘Stem cell fate lab’ at ‘Istituto di Genetica e Biofisica A. Buzzati-Traverso’ CNR, Naples Italy.



Stem Cell Fate Lab
in collaboration with
CELBIO



“Stem Cell Differentiation Training Course”

May 29 - June 1 2006

This course has been designed to provide a detailed practical training in the basic techniques to work with mouse ES cell lines. We intend to offer on-site hands-on training in experimental procedures for culturing and differentiating ES cells to cardiomyocytes and neurons. All facilities required to this purpose are available at the IGB. The course will consist of a combination of theoretical and laboratory education. A series of lectures will familiarise the participants with the underlying theory and concepts of current work with ES cells.

The course will be in Italian
The number of participants is 25
ECM have been requested to the Ministero della Sanità

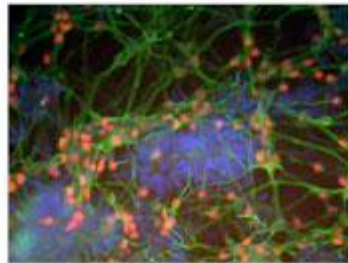
The cost of the course is Euro 400,00

The course will be held at:
Stem Cell Fate Lab
IGB Istituto di Genetica e Biofisica
“Adriano Buzzati-Traverso”, CNR
via Pietro Castellino 111 - 80131 Napoli

Information and application instructions:
<http://www.igb.cnr.it/>

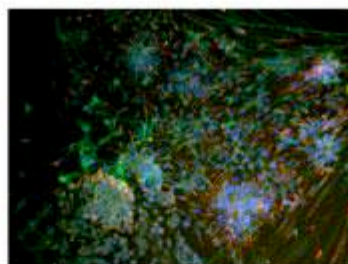
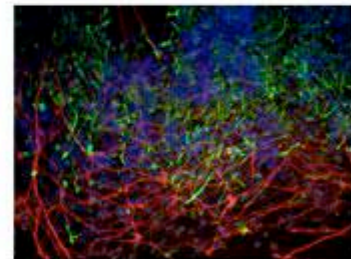
IGB Scientific Secretariat
Laura Casalino: igb_edu@igb.cnr.it

Organizing Secretariat
CELBIO S.p.A.
Luisella Martini: registration@celbio.it



Invited Speakers
Luciano Conti
Giulio Cossu

Scientific Organizers
Dario De Cesare
Sandro De Falco
Stefania Filosa
Gabriella Minchiotti



Senior Teachers
Annalisa Fico
Enza Lonardo
Francesca Paglialunga

Junior Teachers
Giuseppina Lambazzi
Dario Magnani
Genesia Manganelli
Salvatore Ponticelli



VI. Publications and Patents

D. Marasco, A. Saporito, **S. Ponticelli**, A. Chambery, S. De Falco, C. Pedone, G. Minchiotti and M. Ruvo: "The chemical synthesis of mouse Cripto CFC variants", *Proteins*. 2006 Aug 15;64(3):779-88.

E. Pizzo, P. Buonanno, A. Di Maro, **S. Ponticelli**, S. De Falco, N. Quarto, M.V. Cubellis and G. D'Alessio: "Ribonucleases and angiogenesis from fish", *J. Biol. Chem.* 2006, Sep 15; 281(37):27454-27460.

Salvatore Ponticelli, Daniela Marasco, Atsunobu Takeda, Stefania Mitola, Jean-Marie Stassen, Marco Presta, Jayakrishna Ambati, Menotti Ruvo, and Sandro De Falco: "Modulation of angiogenesis by a tetrameric tripeptide that antagonizes vascular endothelial growth factor receptor 1", manuscript submitted.

Inventors: Sandro De Falco, Napoli, Italy; Ruvo Menotti, Treviso, Italy; Jayakrishna Ambati, Lexington, Kentucky; **Salvatore Ponticelli**, Napoli, Italy Daniela Marasco, Napoli, Italy; Jean-Marie Stassen, Lubbeek, Belgium.

Applicant: Thrombogenics

Title of patent: Angiogenesis modulating peptides and compounds

Date of filing:

August 7, 2007

Patent Application number: US 60/963,679

Chemical Synthesis of Mouse Cripto CFC Variants

Daniela Marasco,¹ Angela Saporito,¹ Salvatore Ponticelli,² Angela Chambery,³ Sandro De Falco,² Carlo Pedone,¹ Gabriella Minchiotti,^{2*} and Menotti Ruvo^{1*}

¹Istituto di Biostrutture e Bioimmagini del CNR, Sezione Biostrutture, Napoli, Italy

²Istituto di Genetica e Biofisica "Adriano B. Traverso" del CNR, Napoli, Italy

³Facoltà di Scienze MMFFNN, Seconda Università di Napoli, Caserta, Italy

ABSTRACT We report for the first time the chemical synthesis of refolded CFC domain of mouse Cripto (mCFC) and of two variants bearing mutations on residues W107 and H104 involved in Alk4 binding. The domains undergo spontaneous and quantitative refolding in about 4 h, yet with very different kinetics. Disulfide linkages have been assessed by enzyme digestion and mass spectrometry analysis of resulting fragments, and the first experimental studies on structural organization have been conducted by circular dichroism spectroscopy under different pH conditions. Upon refolding, the domains considerably change their conformations, although they do not assume canonical structures, and become highly resistant to enzyme degradation. A comparative study of receptor binding shows that the CFC domain can bind Alk4 and confirms the importance of W107 and H104 for receptor recognition. *Proteins* 2006;64:779–788. © 2006 Wiley-Liss, Inc.

Key words: peptide synthesis; CD spectroscopy; domain refolding; enzyme digestion; receptor binding

INTRODUCTION

hCripto is the founding member of a family of soluble and cell-bound growth factors known as EGF-CFC [reviewed in Refs. 1–5] distinguished by the presence of an N-terminal signal peptide, two distinct CRDs, and a C-terminal hydrophobic region involved in cell-surface attachment by a posttranslational GPI modification.⁶ The characteristic CRDs, known as EGF-like and CFC domains (from the first members Cripto, FRL1 and Cryptic), both span about 40 residues with three disulfide bridges each, which, presumably, besides a possible functional modularity, also confer them a structural independence.

EGF-CFC proteins range from 171 to 223 amino acids in length and share an overall sequence similarity estimated between 22–32%. In converse, isolated CRD domains are considerably more conserved among all variants, showing a 60–70% (EGF) and 35–48% sequence homology (CFC), a feature suggestive of highly conserved functionalities. The sequence of mouse and human Cripto CFC are nearly identical, sharing about 80% of sequence identity (Fig. 1). Previous investigations conducted by using synthetic polypeptides and supported by molecular modeling have suggested that EGF-like domains display the same disulfide arrangement as canonical EGFs, namely, C1–C3,

C2–C4, and C5–C6,⁷ so they reasonably exhibit a more compact tertiary structure compared with classical EGF motifs, because of a shorter B loop and the lack of the A loop. According to these peculiar features, the EGF-CFC proteins are unable to directly interact with any EGF receptor.⁸ CFC domains, however, have been so far uniquely found in EGF-CFC proteins: they do not carry any posttranslational modification, and experimental data regarding 3D structural organization have so far not been reported. The disulfide bridges arrangement, initially thought to be equivalent to that of the EGF, has been recently elucidated by mass spectrometry analysis of peptide fragments derived by proteolytic degradation and it has actually resulted in a C1–C4, C2–C6, C3–C5 pattern.⁹ In the same report, a study by disulfide pattern search and comparative modeling has also suggested that the CFC domain of human Cripto could be structurally homologous to the von Willebrand factor type C-like domain, VWFC (the region encompassing the first six cysteines) and that a 3D structural model can be derived by using as a template the NMR structure of PMP-C, a serine protease inhibitor having the same pattern of disulfide connections.⁹ By using both the 3D structural model derived for the CFC and a model derived by the NMR structure of the murine EGF, a 3D representation of the whole protein has been proposed that is consistent with data obtained from functional studies.^{9–12} Previous studies, performed by homology modeling¹⁰ proposed a

Abbreviations: hCripto, human Cripto; EGF, epidermal growth factor; CRD, cysteine-rich domain; 3D, three-dimensional; NMR, nuclear magnetic resonance; TGF, transforming growth factor; CHT, chymotrypsin; PDA, photo diode array; CD, circular dichroism; ECD, extracellular domain; RT, room temperature; HBTU, 1-H-benzotriazolium, 1-[bis(dimethylamino)methylene]-hexafluorophosphate(1-),3-oxide; HOBt, N-hydroxybenzotriazole; DIEA, diisopropylethylamine; Fmoc, fluorenylmethoxycarbonyl; TFA, trifluoroacetic acid; TIS, triisopropylsilane; TPCK, 1-chloro-3-tosylamido-4-phenyl-2-butanone; TLCK, 1-chloro-3-tosylamido-7-amino-2-heptanone; GPI, glycosylphosphatidylinositol; RP-HPLC, reversed phase-high performance liquid chromatography.

Daniela Marasco and Angela Saporito contributed equally to this work.

*Correspondence to: Menotti Ruvo, Istituto di Biostrutture e Bioimmagini del CNR, Sezione Biostrutture, via Mezzocannone 16, 80134, Napoli. E-mail: ruvo@chemistry.unina.it or Gabriella Minchiotti, Istituto di Genetica e Biofisica "Adriano B. Traverso" del CNR, via P. Castellino, 111, I-80126, Napoli. E-mail: minchiotti@igb.cnr.it

Received 22 December 2005; Accepted 27 March 2006

Published online 2 June 2006 in Wiley InterScience (www.interscience.wiley.com). DOI: 10.1002/prot.21043

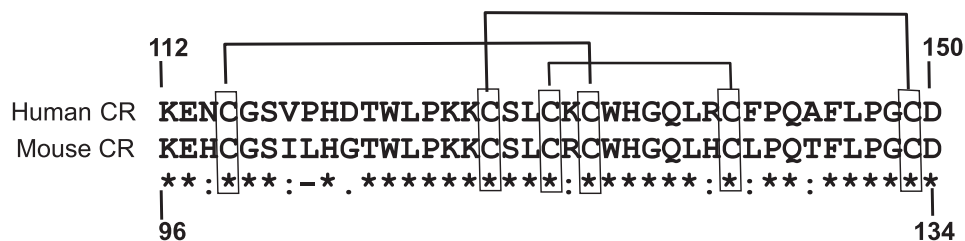


Fig. 1. Alignment of primary sequences of mouse and human Cripto CFC domains. The two domains have been prepared as N-terminal acetylated and C-terminal amidated derivatives. Disulfide bridges are indicated. The asterisk indicates the conserved residues, whereas a colon indicates amino acids with similar properties.

model of Cripto having a β -trefoil structure similar to that of FGF. This model, built assuming for the CFC an EGF-like disulfide structure, although supporting most of the observations derived by site mutagenesis, seems to be incorrect. Nevertheless, the true structure of the whole Cripto protein, as well as of the single domains, are still far to be elucidated, possibly because of the difficulty in obtaining sufficient amounts of refolded Cripto protein.

Different roles of Cripto have created considerable interests; indeed, Cripto is a key regulator of early embryo development,^{13,14} of embryonic stem cell differentiation,¹⁵ and, in adults, of mammary gland development.¹⁶ Moreover, Cripto is now recognized as an important modulator of angiogenesis, as very recently demonstrated by Bianco and coworkers.¹⁷ The increasing interest in the EGF-CFC proteins and in particular in human Cripto is, however, mainly elicited by their strong implication in the growth and maintenance of a large variety of tumors.^{2,8,18,19} Indeed, Cripto is overexpressed in a wide range of epithelial cancers, including breast, colon, and stomach carcinomas, whereas its expression is reduced or even absent in normal tissues.^{8,18,19} Furthermore, either exposure of mammary cells to Cripto protein or its hyperproduction *in vivo* in transgenic mice^{16,20–23} has provided direct evidence of cell transformation and mammary gland carcinoma development capacities. Recent reports^{18,24,25} have demonstrated the successful use of anti-Cripto monoclonal antibodies as effective anticancer agents in several xenograft models, thus further classifying Cripto both as an established player of deregulated cell growth and as an important point of therapeutic intervention for treating several widespread cancers.^{18,24} Cripto enters several distinct pathways that lead to enhanced cell proliferation, survival, and motility^{2,18,26,27} and it is conceivable that all can validly concur to promote tumor formation and progression.⁴ Among the others, regulation of a serin/threonin kinase activin receptor complex (ActRIB/ActRIIB),²⁸ the activation of MAPK/akt proliferative,²⁹ and the p38/JNK antiapoptotic¹⁸ pathways have been convincingly demonstrated. Regulation of activin receptors seems to occur through binding to both receptors and ligands, notably Nodal^{30,31} and Activin^{24,25}; however, the relative contribution of the interactions, mediated by single Cripto CRD, to downstream activation is still largely debated. It has been shown that Cripto binds to nodal through the EGF-like domain, where the fucose modification has an important role,^{12,31} while it anchors to ActRIB (Alk4), as well as to

activin B, via the CFC.^{9,11,18,24} In this respect, an intriguing model has been proposed in which the CFC-mediated binding of Cripto to Alk4 and/or to activin B^{2,24,25,27} might eventually induce the oncosuppressive activity of activin^{32–36} and, possibly, of other TGF β proteins.³⁷ These studies have suggested a prominent role for the single CRDs in Cripto-mediated carcinogenesis and now prompt the expenditure of major efforts for the comprehension of their 3D features, as well as for the identification of effective antagonists. Most studies performed on the CFC domain have been focused on the loop comprised between Cys115 and Cys128 (mouse numbering, Fig. 1) and involved His104, Trp107, and Leu122, whose substitution with alanine or glycine^{10,11,13,24} produces inactive variants.

In the present work, we have focused our attention on the CFC domain of mouse Cripto. The domain has been produced by stepwise solid phase synthesis, along with variants bearing mutation on H104 and W107 (H120 and W123 according to the human numbering) that have been described as crucial residues for Alk4 receptor recognition. Both variants have been purified and refolded, achieving the correct disulfide bridges, and comparatively analyzed by CD spectroscopy under different pH conditions, thus obtaining, for the first time to our knowledge, experimental insights on the structural arrangements of this new class of protein domains. Furthermore, the binding properties of both wild type and mutated CFC domains to Alk4 receptor have been determined by using an ELISA-based assay. Our results demonstrate that the CFC domain alone can directly bind Alk4 in the absence of additional ligands and, furthermore, confirm a role of H104/W107 in Cripto/Alk4 interaction.

EXPERIMENTAL PROCEDURES

Materials and Instrumentations

Protected N $^{\alpha}$ -Fmoc-amino acid derivatives, coupling reagents, and Rink amide MBHA resin were purchased from Calbiochem-Novabiochem (Laufelfingen, Switzerland). DIEA was from Applied Biosystem (Foster City, CA). All other chemicals were commercially available from Sigma-Aldrich, Fluka (Bucks, Switzerland), or LabScan (Stillorgan, Dublin, Ireland) and used as received unless otherwise stated. Sequencing-grade trypsin and α CHT were from Sigma-Aldrich (Milano, Italy). Other reagents and chemicals suppliers are indicated in the Methods section.

Solid-phase peptide synthesis was performed on a fully automated peptide synthesizer, Applied Biosystems model 433A. Analytical RP-HPLC was performed on a Shimadzu 10A-LC using a Phenomenex C18 column (Torrance, CA), 4.6 × 250 mm 5 μm. Preparative RP-HPLC was performed on a Shimadzu LC-8A, equipped with an SPD-M10 AV detector on a Phenomenex COMBI C18 column (5 × 2.2 cm ID; 10 μm). LC-MS analysis was performed on an LCQ DECA XP Ion Trap mass spectrometer (ThermoElectron, Milan, Italy) equipped with an OPTON ESI source, operating at 4.2-kV needle voltage and 320°C, and with a complete Surveyor HPLC system, comprising an MS pump, an autosampler, and a PDA. Narrow bore 50 × 2 mm C18 BioBasic LC-MS columns from ThermoElectron were used for these analyses. CD spectra were obtained at room temperature on a Jasco J-715 dichrograph, calibrated at 290 nm with an aqueous solution of D(+)-10-camphor sulphonic acid,³⁸ using 0.1-mm quartz cuvettes. UV-Vis spectra were performed by using a UV-Vis Jasco (Easton, MD) model 440 spectrophotometer with a path length of 1 cm. The ECD of Alk4 fused to Fc (Alk4-Fc) was from R&D Systems; reagents for ELISA assays were all from Sigma-Aldrich (Milano, Italy).

METHODS

Synthesis of CFC Domains

The mouse CFC domain 96-134 (mCFC) and the mutated variants CFC 96-134 H104A and CFC 96-134 W107A (mCFC-H104A and mCFC-W107A), all as acetylated and amidated derivatives, were obtained by stepwise solid phase synthesis following standard Fmoc/HBTU methodologies³⁹ on a 100 μmol scale (RINK amide resin, 1.1 mmol/g). A 10-fold excess of amino acids, preactivated with HBTU/HOBt/DIEA (1:1:2), was used throughout the synthesis. Coupling and deprotection times were kept at 25 and 15 min, respectively. Standard side-chain protection groups for Fmoc chemistry were used for all residues; the six cysteines, introduced as trityl (Trt) derivatives, produced after cleavage as many free thiol groups.

After resin assembling, polypeptides were removed from the solid support by treatment with a TFA/H₂O/TIS (94:3:3 v/v/v) mixture (RT, 4 h, 1.0 mL mixture/100 mg resin), precipitated in cold ethyl ether (Et₂O) and lyophilized. Crude products were analyzed by RP-HPLC using a gradient from 20 to 45% B over 50 min at 1.0 mL/min flow rate, using a Jupiter 250 × 4.6 mm ID C18 column (solvent A was H₂O, 0.08% TFA; solvent B was CH₃CN, 0.05% TFA). Crude polypeptides were fully reduced in 100 mM DTT/100 mM TRIS, pH 7.0 at 37°C for 2 h and purified by reversed-phase HPLC using a Phenomenex COMBI C18 column 5 × 2.1 cm ID and applying a gradient of B from 20 to 45% over 30 min (flow rate was 20 mL/min). Purified polypeptides were then characterized by analytical RP-HPLC and ESI-MS mass spectrometry and lyophilized. For refolding, the polypeptides were again reduced in 100 mM DTT for 30 min at RT, then the reducing agent was removed by rapid reverse-phase adsorption/desorption, using 95% CH₃CN, 0.05% TFA to elute the peptides. After CH₃CN rapid evaporation under reduced pressure, the

residual solutions were diluted up to a 0.2 mg/mL final concentration (about 44 μM) using either 100 mM carbonate buffer, pH 8.5 or 100 mM TRIS, 0.5 mM EDTA, 20% DMSO, pH 8.5 (refolding buffer⁴⁰). This process was required to trigger the refolding on purified, completely reduced materials. The refolding solutions were left at RT for 16 h and the refolding progression was monitored by using LC-MS analysis, following retention time shifts and MW changes. A gradient from 20 to 35% B over 50 min at 0.2 mL/min flow rate was applied to elute the polypeptides. The spectrometer source was kept at 4.2 kV and 320°C; sheath and auxiliary gas were fixed at 70 and 15 unit, respectively. Other ESI source parameters were optimized by automatic tuning using diluted solutions of the analytes. Refolded molecules were purified by preparative RP-HPLC, using a gradient from 20 to 45% B over 12 min with a flow rate of 20 mL/min. The purest fractions were collected, lyophilized, and extensively characterized by using RP-HPLC and ESI-MS mass spectrometry for exact mass determination. MS analysis was performed by infusing diluted solutions (10 μg/mL) of the purified molecules at 5 μL/min, and keeping the source at 180°C. Other parameters were left unchanged.

Analysis of Refolding Progression

One hundred-microgram aliquots of mCFC, mCFC-H104A, and mCFC-W107A in 500 μL refolding solutions, were placed in the LC-MS autosampler, thermostated at 20°C. A BioBasic 50 × 2 mm ID RP18 column was equilibrated at 0.2 mL/min (column temperature was kept at 25°C) with 20% CH₃CN, 0.05% TFA (solvent B) and 5-μL aliquots (1 μg) were automatically injected and analyzed using a gradient from 20 to 35% B over 50 min after 0, 90, 180, 270, 360, 450, 540, and 630 min, respectively. PDA data were collected between 200–320 nm (1-nm bandwidth), whereas mass spectra were continuously acquired between 400–2,000 amu (normal mode) and 1,200–3,200 amu (high mode). The source was kept at 320°C, the needle voltage at 4.2 kV, and the sheath and auxiliary gas at 70 and 15 unit, respectively.

Estimation of Free Thiols

In a second experiment, 20 μg of reduced mCFC, mCFC-H104A, and mCFC-W107A were dissolved in 0.1 mL of refolding buffer. From each solution, 20-μL aliquots were taken out after 0, 30, 60, 240, and 600 min and treated with 1 μL of a 200 mM 4-vinylpyridine⁴¹ solution in DMSO for 30 min at 45°C, then 1% TFA was added (10 μL) to quench the reaction. Five-microliter aliquots (1 μg) were analyzed by using LC-MS as described for the refolding experiment.

Assessment of Disulfide Bridges

Disulfides linkages were assessed on mCFC and mCFC-W107A by treatment of polypeptides with TPCK-treated trypsin followed by TLCK-treated αCHT and mass analysis of resulting fragments. To this aim, 100-μg polypeptide aliquots were treated overnight (ca. 16 h) with trypsin at 1:100 enzyme/substrate ratio (w/w), in 100 μL of buffer, 50

mM TRIS, 20 mM CaCl₂, pH 8.5, at 37°C. Sample aliquots were removed, treated with 50 mM DTT and analyzed by using MALDI-TOF MS (1 μL treated with C18 ZIP-TIP, Waters). After the MALDI-TOF MS analysis, 1:100 αCht (w/w) was added to the remaining samples and the reaction incubated for 3 h at 25°C and for further 2 h at 37°C. A 2-μL aliquot (2 μg) was removed, diluted with 18 μL of 2% solvent B in solvent A (v/v), and analyzed (10 μL, 1 μg) by using LC-MS on the BioBasic column, applying a gradient from 2 to 55% CH₃CN, 0.05% TFA over 160 min. Detection was achieved, as described, by PDA and mass analysis. In this last case, data dependent analysis was also conducted, carrying a fragmentation of all precursor ions with a fixed 40% energy value.

CD Analysis

CD spectra of refolded polypeptides were recorded on solutions with C_{pep} = 1.0 × 10⁻³ M, calculated by UV measurements using a molar extinction coefficient at 280 nm of 5,500 M⁻¹cm⁻¹ for mCFC-W107A and 11,000 M⁻¹cm⁻¹ for wild type mCFC and mCFC-H104A. Three separate 1.0 × 10⁻³ M solutions for each domain were prepared at pH 7.0 (10 mM phosphate buffer), pH 5.0 (10 mM acetate buffer), and pH 3.0 (10 mM citrate buffer). Spectra were recorded using a 0.1-mm path length quartz cuvette. Data were collected at 0.2-nm intervals with a 20-nm min⁻¹ scan speed, a 2-nm bandwidth, and a 16-s response, from 260 to 190 nm. Three spectra for each sample were recorded, averaged, and transformed in molar ellipticity/residue [θ].

Binding Assays With Alk4

To determine the binding activity of the CFC domains to the Alk4 receptor, the ECD of Alk4-Fc recombinant protein was adsorbed to 96-well microtiter plates (20 ng/well) and incubated overnight at RT. After blocking the plates in 2% milk, the CFC peptides (wild type, W107A, or H104A) were added at concentrations ranging from 50 to 2,000 ng/mL (11–454 nM, assuming an average MW of 4,400 amu for all domains) and incubated for 1 h at 37°C followed by 1 h at RT. Anti-mouse Cripto rabbit polyclonal antibodies,¹⁰ immunopurified on a Sepharose-CFC peptide column, were then added to the plates at a concentration of 6 μg/mL and incubated for 1 h at 37°C followed by 1 h at RT. Dilutions (1:10,000) of anti-rabbit immunoglobulin G conjugated to horseradish peroxidase (Santa Cruz Biotechnology, Santa Cruz, CA) were added to the plates and further incubated for 1 h at RT. Finally, the plates were developed with *o*-phenylenediamine peroxidase substrate (Sigma-Aldrich) and the absorbance was read at 490 nm on a microplate reader (Biorad BenchMark). OD values were reported versus peptide concentration. Data represent the means of three independent experiments.

RESULTS AND DISCUSSION

The sequence of mouse Cripto CFC domain was chosen on the basis of the reported literature (Fig. 1). In a first attempt, synthesis and refolding of segment 99-133¹⁰ was unsuccessful, as no refolded product was obtained (data

not shown). The sequence was therefore extended on the N-terminal side, up to residue K96, whereas the D134 residue was added on the C-terminus. Polypeptides were assembled by stepwise solid phase synthesis on RINK AMIDE resin and removed from the solid support by treatment with a TFA-scavengers solution. After lyophilization and extensive reduction with DTT, the crude products were analyzed by using RP-HPLC observing an average 70% purity for all products (not shown). Reduction greatly improved the chromatographic profile of crude polypeptides, pointing out that highly reactive cysteine thiols were present even at very acidic pH. DTT-reduced products were purified by preparative RP-HPLC and again characterized by analytical RP-HPLC and ESI-MS mass spectrometry. Products were highly homogeneous (not shown) and MWs were in very good agreement with calculated values; mCFC_{Exp/Calcd}: 4,475.61 ± 0.05/4,475.30 amu; mCFC-W107A_{Exp/Calcd}: 4,360.16 ± 0.11/4,360.30 amu; mCFC-H104A_{Exp/Calcd}: 4,409.16 ± 0.15/4,409.28 amu (average MW). Aliquots were refolded in diluted solutions using DMSO as slightly oxidizing agent and monitoring the reaction by LC-MS. The polypeptides underwent spontaneous and quantitative conversion [Fig. 2(A–C)], showing, on RP-HPLC analysis, single, sharp peaks with considerable shorter retention times compared with the starting material (under the reported analysis conditions, about 8 min for the wild type domain, about 7 min for the mCFC-H104A, and about 5 min for the mCFC-W107A). Furthermore, a mass loss of 6 amu, suggestive of three disulfide bridge formation, was measured by using ESI-MS analysis on all refolded domains. As shown in Figure 2(A–C), the mCFC-W107A polypeptide exhibited the highest reactivity compared with the wild type CFC and the H104A variant, as, once dissolved in the DMSO-containing buffer (actually, after about 5 min, considering the time that the autosampler needs to perform the first injection), new small peaks with shorter and longer retention times were detected [Fig. 2(B), chromatogram *t* = 0]. Conversely, the H104A mutant appeared rather unreactive, being highly refractory to transformation until about 180 min. Small amounts of refolded H104A mutant [Fig. 2(C), arrow, Rt: 33.4 min] were detectable only after 270 min, then a rapid conversion occurred in the following 90 min, producing more than 50% of refolded product, as estimated by area integration. In the following 90 min (from 360 to 450 min), almost 90% of the final product was formed. In the same time interval, both wild type mCFC and mCFC-W107A were completely refolded, yet with very different kinetics. After the apparent initial inertness, the wild type domain rapidly evolved in the first 90 min, converting for about 30% to the refolded form. After 180 min, about 70% was refolded, whereas the remaining 30% was nearly present as a single intermediate species (Rt = 31.4 min), with two disulfide bridges [Fig. 2(A), arrow; MW: 4,471.51 amu]. At the same time, the W107A mutant was formed for about 60%, but the remaining 40% was spread on a very large number of intermediates containing one or two disulfide bridges. After 270 min, both wild type and W107A domains were almost fully refolded, compared

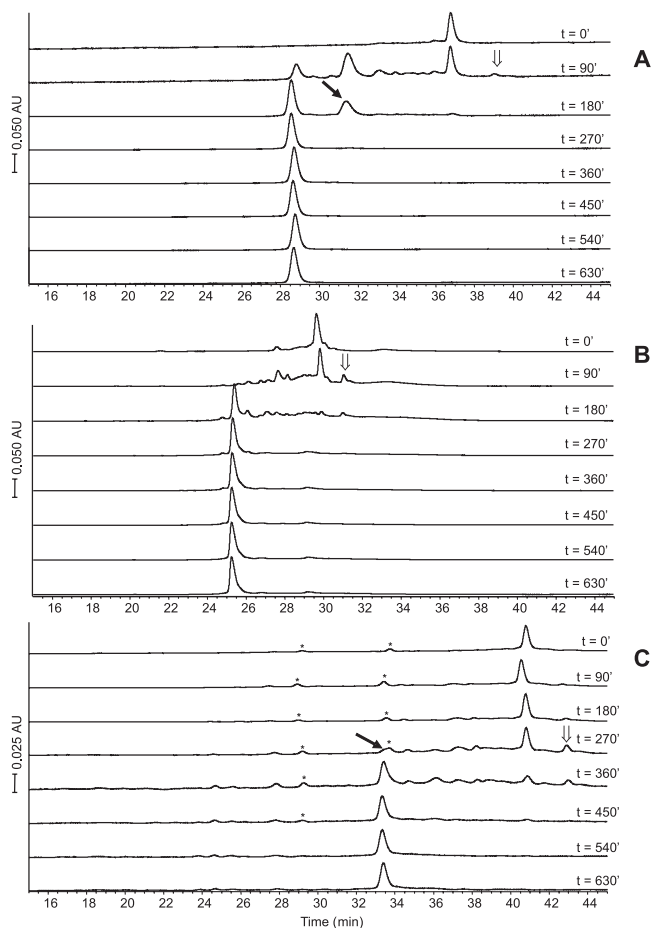


Fig. 2. Time-course analysis by LC-MS of refolding progression of mCFC (A), mCFC-W107A (B), and mCFC-H104A (C). The analysis has been performed by injecting 1 μ g (wt and W107A) or 0.5 μ g (H104A) of total peptide after the indicated time intervals. Reported chromatograms refer to traces at 215 nm and have been extracted from total PDA analysis between 200 and 320 nm. Contextual MS analysis has been performed obtaining molecular masses of all eluted species. Asterisks in C indicate impurities.

with the H104A mutant that required some 450 min to completely convert to the final product. Interestingly, the rate of transformation for all variants rapidly increased after the appearance of a small, slightly hydrophobic peak, indicated by a downward arrow (\Downarrow) in Figure 2(A–C), at 39.0 min for the wild type mCFC, at 31.0 min for the mCFC-W107A, and at 42.8 min for the mCFC-H104A, respectively. These peaks, corresponding to cyclic polypeptides with a single disulfide bridge (as determined by on-line mass analysis), are likely highly reactive precursors that promote the subsequent fast transformation into refolded products.

All refolded polypeptides showed sharp, very clean peaks, with the expected MW and UV spectra in the region 240–320 nm (determined by on-line PDA analysis, not shown). The apparent higher hydrophilicity of refolded domains, as compared with the starting material, was considered as a first indication of correct domain assembling, because, as expected for globular proteins, most hydrophobic residues remain buried inside the protein

body upon refolding (assuming they are in a pseudo-native state under the HPLC analysis conditions). Furthermore, the molecular surface of a globular domain available for interaction with the column stationary phase is greatly reduced compared with large, randomly organized polypeptides. After reverse-phase purification, the polypeptides were again characterized by using RP-HPLC analysis [observing >95% RP-HPLC purities, Fig. 3(A–C)] and MW determination by ESI-Ion Trap MS. MWs were $4,353.90 \pm 0.14$ (mutant W107A), $4,403.20 \pm 0.15$ (mutant H104A), and $4,469.22 \pm 0.22$ amu (wild type), respectively, in very good agreement with the theoretical values of 4,354.16, 4,403.24, and 4,469.30 amu [see Fig. 3(D–F)]. By these analyses, we can conclude that refolding is kinetically and thermodynamically strongly influenced by the point mutations. In particular, substitution of W107 with an alanine does not greatly affect the kinetics, but has a strong effect on relative stability of refolding intermediates that probably rapidly interchange with each other. However, exchange of H104 with an alanine not only involves a reduction of intermediates stability, but also has a profound influence on refolding kinetics, producing a marked decrease in conversion rate.

Estimation of Free Thiols

To rule out the presence of partially refolded products or the occurrence of reshuffling reactions, an estimation of residual free thiols was performed on the refolded domains. To this aim, reduced polypeptides were refolded as described and small aliquots were removed after 0, 30, 60, 240, and 600 min and subjected to extensive thiol alkylation using 4-vinylpyridine.⁴¹ Analysis by LC-MS, under the same conditions reported for the refolding monitoring, showed that the fully reduced products took up six 4-VP (MW increase of $105.2 \times 6 = 630.8$ amu), whereas the refolded polypeptides were unaffected by the alkylating reagent. Refolding intermediates carrying only one or two disulfide bridges were also easily identified in the reaction mixtures, up to 240 min reaction time, as tetra- and di-VP adducts having MW increases of 420.6 and 210.3 amu, respectively. In Figure 4 is reported the LC-MS analysis of samples taken after 0, 60, and 240 min referred to the W107A mutant. The absence of vinyl-pyridine adducts indicated that no residual free thiols were present in the refolded domains and that they did not undergo thiol exchange reactions, further suggesting a high structural stability.

Disulfide Bridges Assessment

To assess the correctness of disulfide bridges, two of the three domains, mCFC and mCFC-W107A, were subjected to proteolysis with a combination of trypsin and α CHT. Single enzyme treatments had provided single, disulfide-linked molecules, devoid of linkages information. Long incubation times were required to obtain diagnostic fragments, as both domains exhibited a marked resistance to enzyme proteolysis. After the first enzyme addition (1:100 enzyme/substrate ratio), reactions were incubated for 16 h at 37°C. Mass analysis of the DTT-reduced mixture evi-

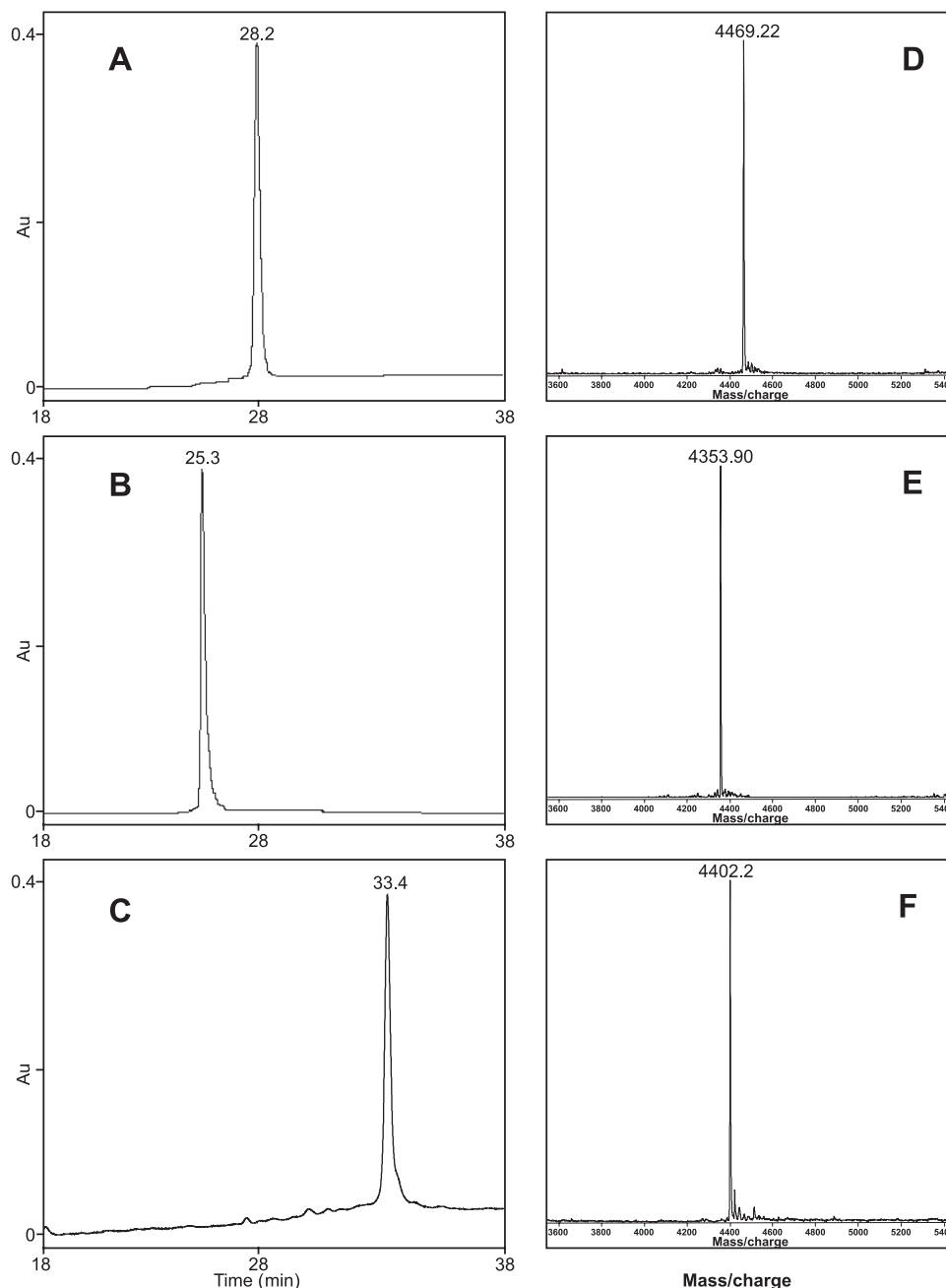


Fig. 3. RP-HPLC analysis of purified refolded domains mCFC (A), mCFC-W107A (B), and mCFC-H104A (C) on a BioBasic 50 \times 2 mm ID column applying a 20–35% solvent B (CH_3CN , 0.05% TFA) over 50 min (flow rate 0.2 mL/min). D–F: ESI-MS spectra of purified domains obtained by infusion analysis at 5 $\mu\text{L}/\text{min}$ of a 10 $\mu\text{g}/\text{mL}$ solution in 0.1% HCOOH in water. Molecular masses are in very good agreement with expected theoretical values. Molecular masses were obtained by deconvolution of multicharge spectra using the Biomass software implemented in the Bioworks 3.1 software package provided by ThermoElectron.

denced the presence of the expected fragments 97–110, 112–116, and 117–134, along with a number of other higher MW peaks corresponding to partially cleaved fragments. Digestion with αCHT on both domains provided, among other peaks because of partial cleavages, the three expected disulfide-linked peptides [EHCGSIL]-[CW], MW 1,062.3 amu (disulfide bridge Cys99–Cys117, 1–4), [CSL]-[LPGCD], MW 822.2 amu (disulfide bridge

Cys112–Cys133, 2–6), and [CR]-[HCLPQTF], MW 1,119.4 amu (disulfide bridge Cys115–Cys124, 3–5). In Figure 5(A–D), the base peak chromatograms (A, C) and the corresponding extracted ion chromatograms (B, D) of masses relative to the diagnostic peaks (see legends) are reported. Given the similar behavior of the H104A mutant upon refolding, we assumed that this molecule was also fully refolded.

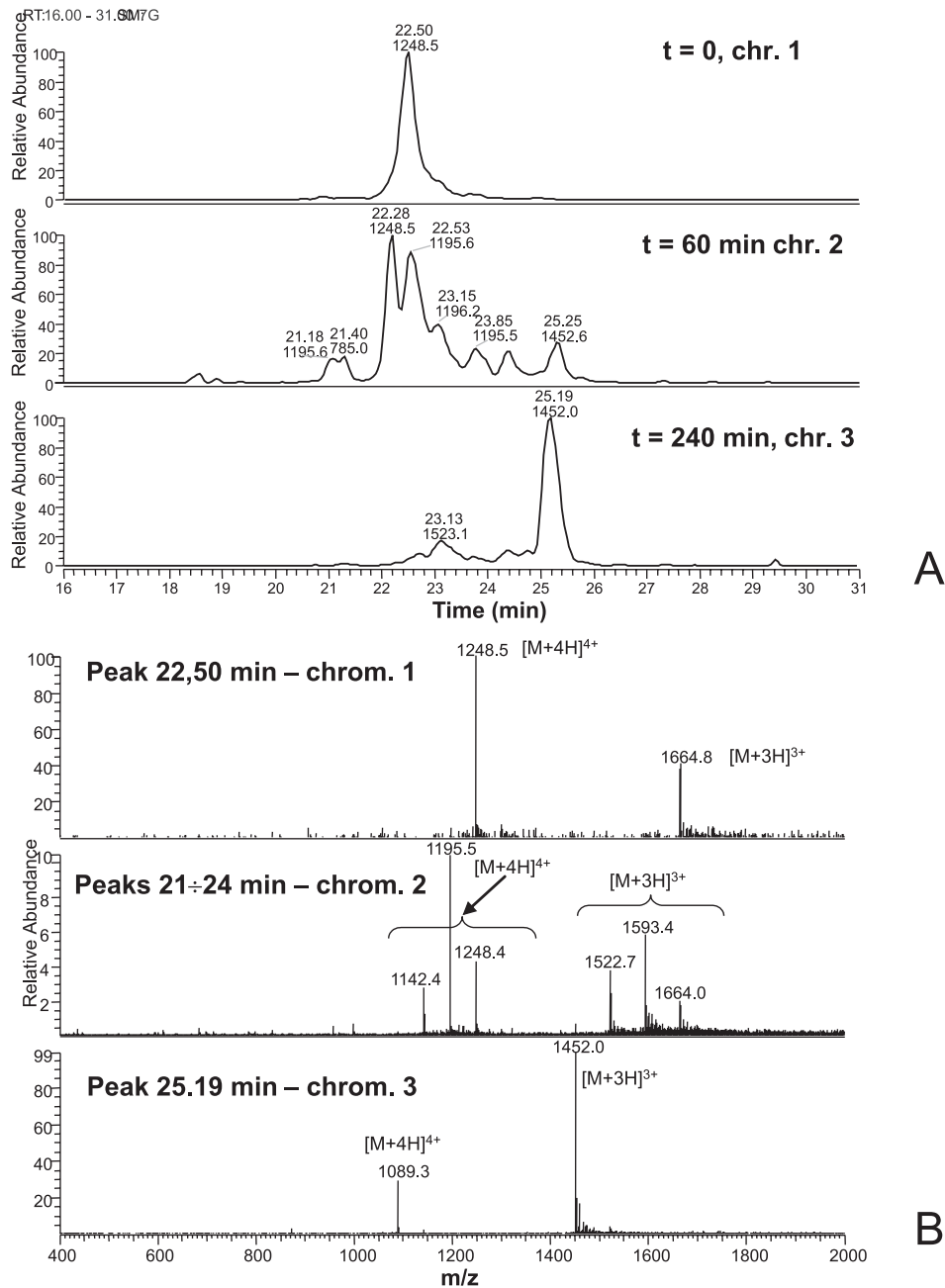


Fig. 4. **A:** LC-MS analysis of 4-vinylpyridine-treated refolding intermediates of mCFC-W107A at 0, 60, and 240 min. The base peak chromatogram are reported. At $t = 0$ min, a single peak corresponding to the hexa-alkylated polypeptide is observed (chromatogram $t = 0$, MW increase of $105.2 \times 6 = 630.8$ amu); at 60 min (chromatogram 2) all possible intermediates are present carrying 0, 2, 4, or 6 vinylpyridines. After 240 min exposure to refolding conditions (chromatogram 3), a major product, not alkylated by vinylpyridine is eluted at about 25.2 min, corresponding to the fully refolded domain. In **(B)**, mass spectra taken at the indicated times are reported.

CD Analysis

Cripto domains were studied in solution by using CD to obtain the first structural insights and to determine their overall tridimensional organization. CD spectra of the three domains at neutral (7.0) and slightly acidic pH [Fig. 6(A–C)] were all dominated by broad negative bands centered at about 200–205 nm. At neutral pH, a second

band centered at about 220 nm for the mCFC and mCFC-H104A and at 230 nm for the mCFCW107A variant was clearly visible. None of them showed canonical spectral characteristics, although the curves were indicative of well-organized structures with α and β structure contributions. When analyzed in more acidic environments at pH 3.0, CD spectra did not change considerably from those at

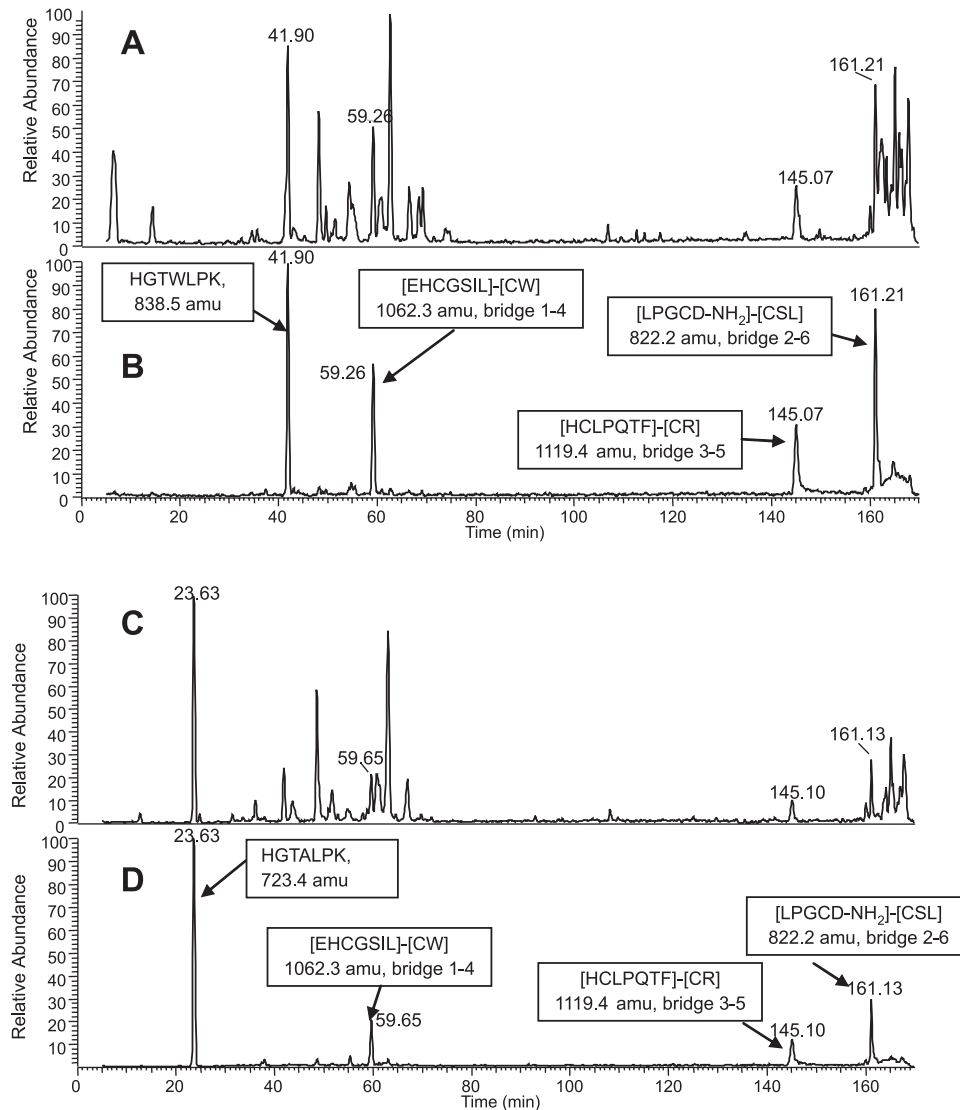


Fig. 5. LC-MS analysis of wild type mCFC as obtained after extensive trypsin (16 h, 1:100, w/w) and α CHT (5 h, 1:100, w/w) digestion (base peak chromatogram) (A). In (B), the extracted ion chromatogram relative to ions $837 \div 840$ amu, $1,061 \div 1,064$ amu, $1,118 \div 1,131$ amu, and $821 \div 824$ amu is reported. The other peaks account for bigger fragments derived by partial cleavage. The same analysis performed on digested mCFC-W107A (C, D). The peak at Rt 23.63 min accounts for the peptide 104–110 that bears the W107A mutation. Disulfide-linked peptides disappeared upon analysis executed after DTT reduction.

pH 5.0, confirming partial loss of the original structure (not shown). CD analysis also evidenced that polypeptide chains drastically change their conformations upon refolding (not shown) and that, despite the single amino acid substitution, remarkable structural differences exist under the diverse conditions explored. Moreover, domain structures were almost unaffected by TFE addition (not shown), showing an outstanding conformational stability.

Binding Assays

ELISA-based binding assays to the Alk4 receptor were performed by using immobilized Fc-fused receptor and adding increasing amounts of soluble domains. Detection was performed by using anti-CFC rabbit polyclonal antibod-

ies (pAb) immuno-purified from whole anti-Cripto pAb¹⁰ on Sepharose-immobilized synthetic CFC. wtCFC bound to immobilized Alk4 in a dose-dependent manner and the binding was saturable for concentrations higher than 450 nM, about 2 μ g/mL (Fig. 7). In sharp contrast, the binding of the corresponding W107A and H104A variants was instead strongly reduced as compared with the wild type. In particular, the H104A showed a residual activity of about 40% at the highest concentration, whereas the W107A was almost inactive.

Several experimental approaches indicate that Cripto CFC domain is required for Cripto/Alk4 interaction and has a pivotal role in intracellular signaling for both tumor maintenance and progression^{4,5,24} and for cardiomyocyte

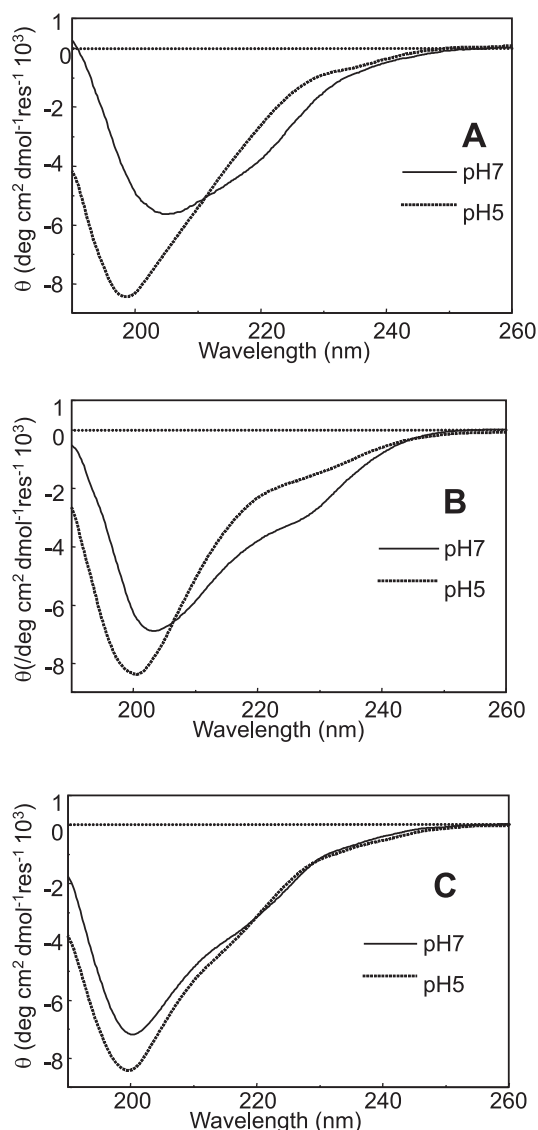


Fig. 6. CD spectra of refolded mCFC domain at pH 5.0 and 7.0 (A). The same spectra recorded for the W107A mutant (B) and for the H104A mutant (C). Spectra have been acquired on 1×10^{-3} M solutions using a 0.1-mm path length quartz cuvette. The domains show a progressive loss of structure with reducing pH, reaching at pH 3.0 (not shown) complete random conformations.

differentiation of stem cells. Molecular mechanisms underlying receptor binding and activation have been partially elucidated by site-directed mutagenesis and involve residues located within the largest loop comprised between the first and the second cysteine residue (Fig. 1). Further studies of structure–activity relationship have been so far hampered by the lack of adequate amounts of homogeneously refolded proteins and consequently by the lack of structural insights about the tridimensional organization and active conformations. To start a study on conformational properties of the CFC domain as well as to assess the influence of single mutations on overall domain organization and receptor binding, we needed to overcome difficulties associated with preparation of sufficient amounts

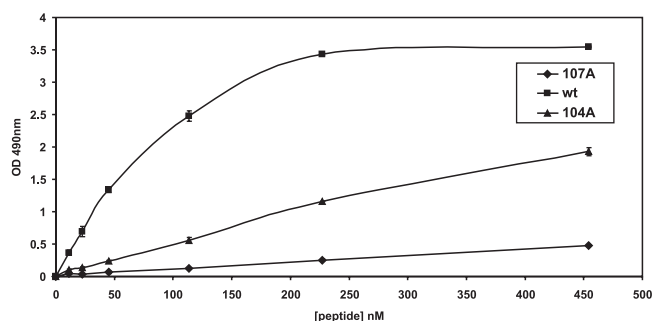


Fig. 7. Binding assays of the two synthetic domains to the recombinant Alk4 (as Fc fusion protein). The assay has been performed as described in the Methods section. Detection has been performed with CFC affinity purified anti-Cripto polyclonal antibodies. The strong binding capacities of wild type CFC domain are completely lost by W107 replacement with alanine, whereas a residual binding is displayed by the H104A mutant.

of structurally homogeneous molecules. To this end, we have undertaken the chemical synthesis of mouse CFC domain, both wild type and mutated variants. The size of the CFC domain is far below the actual limits of stepwise chemical synthesis: accordingly, both yields and purity levels of crude products were relatively high, as evaluated by RP-HPLC. Correct disulfide bridges reconstitution was achieved by spontaneous formation and no chemical strategies of selective protection/oxidation were necessary, a fact indicative of a strong tendency of polypeptides to adopt the correct conformation. Both wild type and mutated CFC domains are indeed able to refold into native structures by exposure to slightly oxidative conditions, such as alkaline buffers and DMSO. This important property, along with the capacity to bind the receptor, suggests that CFC domains possess a structural independence and, furthermore, indicates that refolding is probably not influenced by the close vicinity of a second, highly structured domain (i.e., the EGF-like). Binding data strongly indicate that not only the imidazolic and indolic moieties of histidine 104 and of tryptophan 107 make relevant contacts with the receptor, but they also considerably contribute to domain structural stability, as conformations are remarkably affected by substitution with alanine.

CONCLUSIONS

Herein we show, for the first time to our knowledge, that the CFC domain of mouse Cripto, which is stabilized by three disulfide bridges, can be conveniently prepared by chemical synthesis, refolded by spontaneous oxidation in diluted solutions, and purified to homogeneity by simple RP-HPLC chromatography. The protein and its domains are gaining a growing interest for their proven implication in tumorigenesis and stem cell differentiation; in this respect, the proposed chemical synthesis provides a valuable alternative to recombinant methods for the production of refolded, fully active CFC domains. CFC variants, bearing mutations on W107 and H104, can also be obtained in the same way. We also show that the three domains exhibit different kinetics of refolding and different secondary structure, despite the single amino acid

substitutions. These results represent the first step for further studies aimed at determining, at atomic level, the tridimensional structure of this prototypic member of a new class of protein domains that has a potential application as soluble receptor antagonist to block molecular events leading to tumor progression. Finally, we have shown that binding of CFC domain to Alk4 receptor can occur in the absence of additional ligands and confirmed that receptor recognition and binding by CFC involves residues H104 and W107, as the corresponding Ala-substituted mutants exhibit strongly reduced binding affinities.

ACKNOWLEDGMENTS

The authors acknowledge the Ministero dell'Istruzione, dell'Università e della Ricerca (M.I.U.R.), the National Research Council (C.N.R.) of Italy, and Associazione Italiana Ricerca sul Cancro (AIRC). The technical support of Dr. Giuseppe Perretta is also gratefully acknowledged.

REFERENCES

- Dono R, Scalera L, Pacifico F, Acampora D, Persico MG, Simeone A. The murine cripto gene: expression during mesoderm induction and early heart morphogenesis. *Development* 1993;118:1157–1168.
- Adamson ED, Minchiotti G, Salomon DS. Cripto: a tumor growth factor and more. *J Cell Biol* 2002;190:267–278.
- Bianco C, Normanno N, Salomon DS, Ciardiello F. Role of the cripto (EGF-CFC) family in embryogenesis and cancer. *Growth Factors* 2004;22:133–139.
- Minchiotti G. Nodal-dependent Cripto signaling in ES cells: from stem cells to tumor biology. *Oncogene* 2005;24:5668–5675.
- Wechselberger C, Strizzi L, Kenney N, et al. Human Cripto-1 overexpression in the mouse mammary gland results in the development of hyperplasia and adenocarcinoma. *Oncogene* 2005;24:4094–4105.
- Minchiotti G, Parisi S, Liguori G, et al. Membrane-anchorage of Cripto protein by glycosylphosphatidylinositol and its distribution during early mouse development. *Mech Dev* 2000;90:133–142.
- Lohmeyer M, Harrison PM, Kannan S, et al. Chemical synthesis, structural modeling, and biological activity of the epidermal growth factor-like domain of human cripto. *Biochemistry* 1997;36:3837–3845.
- Salomon DS, Bianco C, Ebert AD, et al. The EGF-CFC family: novel epidermal growth factor-related proteins in development and cancer. *Endocr Relat Cancer* 2000;7:199–226.
- Foley SF, van Vlijmen HW, Boynton RE, et al. The CRIPTO/FRL-1/CRYPTIC (CFC) domain of human Cripto. Functional and structural insights through disulfide structure analysis. *Eur J Biochem* 2003;270:3610–3618.
- Minchiotti G, Manco G, Parisi S, Lago CT, Rosa F, Persico MG. Structure-function analysis of the EGF-CFC family member Cripto identifies residues essential for nodal signalling. *Development* 2001;128:4501–4510.
- Yeo CY, Whitman M. Nodal signals to Smads through Cripto-dependent and Cripto-independent mechanisms. *Mol Cell* 2001;7:949–957.
- Yan Y, Liu J, Luo YEC, Haltiwanger RS, Abate-Shen C, Shen MM. Dual roles of Cripto as a ligand and coreceptor in the nodal signaling pathway. *Mol Cell Biol* 2002;22:4439–4449.
- Shen MM, Schier AF. The EGF-CFC gene family in vertebrate development. *Trends Genet* 2000;16:303–309.
- Whitman M. Nodal signaling in early vertebrate embryos. Themes and variations. *Dev Cell* 2001;1:605–617.
- Parisi S, D'Andrea D, Lago CT, Adamson ED, Persico MG, Minchiotti G. Nodal-dependent Cripto signaling promotes cardiomyogenesis and redirects the neural fate of embryonic stem cells. *J Cell Biol* 2003;163:303–314.
- Salomon DS, Bianco C, De Santis M. Cripto: a novel epidermal growth factor (EGF)-related peptide in mammary gland development and neoplasia. *Bioessays* 1999;21:61–70.
- Bianco C, Strizzi L, Ebert A, et al. Role of human cripto-1 in tumor angiogenesis. *J Natl Cancer Inst* 2005;97:132–141.
- Xing PX, Hu XF, Pietersz GA, Hosick HL, McKenzie IFC. Cripto: a novel target for antibody-based cancer immunotherapy. *Cancer Res* 2004;64:4018–4023.
- Ciardiello F, Kim N, Saeki T, et al. Differential expression of epidermal growth factor-related proteins in human colorectal tumors. *Proc Natl Acad Sci USA* 1991;88:7792–7796.
- Herrington EE, Ram TG, Salomon DS. Expression of epidermal growth factor-related proteins in the aged adult mouse mammary gland and their relationship to tumorigenesis. *J Cell Physiol* 1997;170:47–56.
- De Luca A, Casamassimi A, Selvam MP, et al. EGF-related peptides are involved in the proliferation and survival of MDA-MB-468 human breast carcinoma cells. *Int J Cancer* 1999;80:589–594.
- Kenney NJ, Smith GH, Maroulakou IG, et al. Detection of amphiregulin and Cripto-1 in mammary tumors from transgenic mice. *Mol Carcinog* 1996;15:44–56.
- Wechselberger C, Strizzi L, Kenney N, et al. Human Cripto-1 overexpression in the mouse mammary gland results in the development of hyperplasia and adenocarcinoma. *Oncogene* 2005;24:4094–4105.
- Adkins HB, Bianco C, Schiffer SG, et al. Antibody blockade of the Cripto CFC domain suppresses tumor cell growth in vivo. *J Clin Invest* 2003;112:575–587.
- Gray PC, Harrison CA, Vale W. Cripto forms a complex with activin and type II activin receptors and can block activin signaling. *Proc Natl Acad Sci USA* 2003;100:5193–5198.
- Persico MG, Liguori GL, Parisi S, D'Andrea D, Salomon DS, Minchiotti G. Cripto in tumors and embryo development. *Biochim Biophys Acta* 2001;1552:87–93.
- Bianco C, Normanno N, Salomon DS, Ciardiello F. Role of the cripto (EGF-CFC) family in embryogenesis and cancer. *Growth Factors* 2004;22:133–139.
- Song J, Oh SP, Schrewe H, et al. The type II activin receptors are essential for egg cylinder growth, gastrulation, and rostral head development in mice. *Dev Biol* 1999;213:157–169.
- Bianco C, Adkins HB, Wechselberger C, et al. Cripto-1 activates nodal- and ALK4-dependent and independent signaling pathways in mammary epithelial cells. *Mol Cell Biol* 2002;22:2586–2597.
- Schier AF, Shen MM. Nodal signalling in vertebrate development. *Nature* 2000;403:385–389.
- Schiffer SG, Foley S, Kaffashan A, et al. Fucosylation of Cripto is required for its ability to facilitate nodal signaling. *J Biol Chem* 2001;276:37769–37778.
- Barcellos-Hoff MH, Ewan KB. Transforming growth factor-beta and breast cancer: mammary gland development. *Breast Cancer Res* 2000;2:92–99.
- Derynck R, Akhurst RJ, Balmain A. TGF-beta signaling in tumor suppression and cancer progression. *Nat Genet* 2001;29:117–129.
- Risbridger GP, Schmitt JF, Robertson DM. Activins and inhibitors in endocrine and other tumors. *Endocr Rev* 2001;22:836–858.
- Wakefield LM, Roberts AB. TGF-beta signaling: positive and negative effects on tumorigenesis. *Curr Opin Genet Dev* 2002;12:22–29.
- Harrison CA, Gray PC, Vale WW, Robertson DM. Antagonists of activin signaling: mechanisms and potential biological applications. *Trends Endocrinol Metab* 2005;16:73–78.
- Cheng SK, Olale F, Bennett JT, Brivanlou AH, Schier AF. EGF-CFC proteins are essential coreceptors for the TGF-beta signals Vg1 and GDF1. *Gene Dev* 2003;17:31–36.
- Johnson WC Jr. Protein secondary structure and circular dichroism: a practical guide. *Proteins* 1990;7:205–214.
- Fields GB, Noble RL. Solid phase peptide synthesis utilizing 9-fluorenylmethoxy-carbonyl amino acids. *Int J Pept Protein Res* 1990;35:161–214.
- Tam JP, Wu CR, Liu W, Zhang JW. Disulfide bond formation in peptides by dimethyl sulfoxide. Scope and applications. *J Am Chem Soc* 1991;113:6657–6662.
- Moroney JV, Fullmer CS, McCarty RE. Characterization of the cysteinyl-containing peptides of the gamma subunit of coupling factor 1. *J Biol Chem* 1984;259:7281–7285.

Ribonucleases and Angiogenins from Fish*

Received for publication, June 8, 2006, and in revised form, July 20, 2006. Published, JBC Papers in Press, July 21, 2006, DOI 10.1074/jbc.M605505200

Elio Pizzo[‡], Pasquale Buonanno[‡], Antimo Di Maro[§], Salvatore Ponticelli[¶], Sandro De Falco[¶], Natalina Quarto[‡], Maria Vittoria Cubellis[‡], and Giuseppe D'Alessio[‡]1

From the [‡]Department of Structural and Functional Biology, University of Naples Federico II, Complesso M. S. Angelo, Via Cintia, 80126 Napoli, Italy, [§]Department of Life Sciences, Second University of Naples, Via Vivaldi, 81100 Caserta, Italy, and [¶]Institute of Genetics and Biophysics "A. Buzzati Traverso," Consiglio Nazionale delle Ricerche, Via Pietro Castellino 111, 80131 Napoli, Italy

For the first time fish RNases have been isolated and characterized. Their functional and structural properties indicate that they belong to the RNase A superfamily (or tetrapod RNase superfamily), now more appropriately described as the vertebrate RNase superfamily. Our findings suggest why previously repeated efforts to isolate RNases from fish tissues have met with no success; fish RNases have a very low ribonucleolytic activity, and their genes have a low sequence identity with those of mammalian RNases. The investigated RNases are from the bony fish *Danio rerio* (or zebrafish). Their cDNAs have been cloned and expressed, and the three recombinant proteins have been purified to homogeneity. Their characterization has revealed that they have indeed a very low RNA-degrading activity, when compared with that of RNase A, the superfamily prototype, but comparable with that of mammalian angiogenins; that two of them have angiogenic activity that is inhibited by the cytosolic RNase inhibitor. These data and a phylogenetic analysis indicate that angiogenic fish RNases are the earliest diverging members of the vertebrate superfamily, suggesting that ribonucleases with angiogenic activity were the ancestors of all ribonucleases in the superfamily. They later evolved into both mammalian angiogenins and, through a successful phylogenesis, RNases endowed with digestive features or with diverse bioactivities.

One of the largest and most studied superfamilies of proteins is that of extracellular, pyrimidine-specific, animal RNases. It has been labeled with different names on different bases: the "RNase A superfamily," a mostly historical name, recognizes bovine pancreatic RNase A, one of the most successfully investigated proteins, as the superfamily prototype; the "pancreatic-type RNase superfamily," which includes not only the large family of RNases isolated from the pancreas of many animals but also all other RNases phylogenetically related to them; or "the tetrapod RNase superfamily," as to date the investigated members of this superfamily comprise RNases from mammals, birds, reptiles, and amphibians but not from fish (1).

Some of the tetrapod RNases have diverse bioactivities, distinct from the ribonucleolytic activity, but strictly dependent

on it, including immunosuppressive, cytotoxic, microbicidal, and angiogenic activity (2). The RNases with angiogenic activity, the angiogenins, form a distinct family within the superfamily and are identified by their ability to stimulate the growth of blood vessels (3, 4). Angiogenins with confirmed angiogenic activity, investigated so far only in mammals, are RNases characterized by a very low catalytic activity, albeit essential to their angiogenic activity, and the presence in their structure of only three disulfides, compared with the four disulfide bridges of most mammalian RNases (3–5).

Studies carried out mostly with human angiogenin (hANG)² have indicated that hANG is recognized by a putative 170-kDa receptor on endothelial cells (6) and is translocated to the cell nucleus (7) where it stimulates rRNA processing (8). It should be added that hANG and mouse angiogenins 1 and 4 also have been found to possess microbicidal activity (9). Angiogenins are fully inhibited (10) by the cytosolic RNase inhibitor (cRI), a Leu-rich repeat protein ubiquitous in mammals (11, 12). In fact, hANG binds cRI with the highest affinity so far measured for an RNase (K_i is lower than 1 fM), and the structure of the human cRI·hANG complex has been studied at 2 Å resolution by x-ray crystallography (13).

For an investigation of fish RNases we selected zebrafish (*Danio rerio*), a tropical bony fish, and one of the most favored model organism for the study of vertebrate development including angiogenesis (14). Zebrafish has been also proposed as an animal system for assaying angiogenesis (15, 16). Furthermore, two sequences apparently related to RNase superfamily members are present in a zebrafish DNA data base (Washington University Zebrafish EST Project 1998).

As fish RNases have not been investigated to date, we cloned and expressed in *Escherichia coli* the cDNAs encoding three RNase sequences from the genome of zebrafish. All three recombinant proteins, purified to homogeneity, were active as ribonucleases. Two of them also were found to possess angiogenic activity. These findings, and an analysis of the phylogenetic relationships of the zebrafish RNases/angiogenins with the other RNases of the superfamily, have led to the proposal that fish angiogenins were the ancestral members of the vertebrate RNase superfamily.

* This work was supported by a PRIN (Progetti di Rilevante Interesse Nazionale) grant from the Ministry of Education and University, Italy. The costs of publication of this article were defrayed in part by the payment of page charges. This article must therefore be hereby marked "advertisement" in accordance with 18 U.S.C. Section 1734 solely to indicate this fact.

¹ To whom correspondence should be addressed. Tel.: 39-081-679157; Fax: 39-081-679159; E-mail: dalessio@unina.it.

² The abbreviations used are: hANG, human angiogenin; ZF-RNase, a ribonuclease from zebrafish; cRI, cytosolic RNase inhibitor; EST, expressed sequence tag; MES, 4-morpholineethanesulfonic acid.

EXPERIMENTAL PROCEDURES

Isolation and Cloning of Zebrafish RNase cDNAs—Identification of three genes encoding zebrafish RNases, and cloning of their cDNAs were carried out as follows. The sequence subsequently labeled *zf-rnase-1* was first identified in the Washington University Zebrafish EST Project 1998 data base, with accession number wz5727.1. It contained the EST sequence fb58b02.y1 clearly encoding a member of the pancreatic-type superfamily, termed in the data base an “angiogenin-related protein precursor.” A large fragment, obtained from the Resource Center and Primary Database (RZPD GmbH, Berlin, Germany), cloned in pSPORT1 vector, was found to contain the sequence. The N terminus of the encoded protein was identified using the SignalP 3.0 Server program. However, an inspection of the sequence in the Zebrafish genome data base, under completion in the Sanger Institute (Cambridge, UK) revealed that the sequence was incomplete, as it lacked the 15-nucleotide stretch upstream of the cDNA stop codon that encodes the last five amino acid residues at the C terminus of the expected protein. Thus, two PCR steps were performed.

By a first PCR, the fragment starting with the 5′-end of the cDNA encoding the expected RNase, devoid of the signal peptide, was amplified. The oligonucleotides (synthesized by MWG Biotech, Firenze, Italy) employed were: 5′-GGAATCCATATGCATGTAAAGGAGCGT-3′ (forward) and 5′-CCCAAGCTTATCCGACGTTGACTTCGTCTTCATGATAATGCA-3′ (reverse). The reaction was performed with the Taq polymerase High Fidelity Kit (Roche Applied Science) following the manufacturer’s instructions. The PCR procedure included 5 min at 95 °C and 35 cycles consisting of 45 s at 95 °C, 30 s at 60 °C, 1 min at 72 °C, and 7 min at 72 °C. The amplified fragment was isolated by low melting, 1% agarose gel electrophoresis and purified using the Product Purification Kit (Roche Applied Science).

The second PCR was carried out for the addition of the missing sequence encoding the five C-terminal amino acid residues. The forward oligonucleotide sequence was the same as for the previous PCR, and the reverse was: 5′-CGACGTTGACTTCGTCTTCATGATAATGCACA-GGCCA-TCCCTCC-3′. The PCR procedure and the isolation and purification of the amplified product were as described above for the first PCR. The amplified cDNA fragment, previously treated with restrictases NcoI and EcoRI (Novagen, Madison, WI), was cloned into the pET22b(+) expression vector.

The gene sequence labeled *zf-rnase-2* was also found in the Washington University Zebrafish EST Project 1998 data base, with accession number fd55b09.y1, and was recognized in the data base as encoding a “mouse-angiogenin-related protein.” A DNA fragment from the RZPD data base was found to contain the sequence and was acquired from RZPD as cloned in plasmid pSPORT1. The N- and C-terminal ends of the encoded protein were identified as described above for *zf-rnase-1*. The cDNA of interest (devoid of the signal peptide) was obtained by PCR using the following oligonucleotides: forward, 5′-GTAAAGC-CATGGATAATGAGTCCCCTTATG-3′; reverse, 5′-GAGA-AAGAATTCTTAGCCTGAGCTGTTTACA-3′. The PCR

procedure and the isolation and purification of the cDNA were as described above for *zf-rnase-1*. The obtained cDNA was then treated with NdeI and HindIII restrictases and inserted into the pET22b(+) expression vector.

The third RNase-type sequence (*zf-rnase-3*) from zebrafish genome was identified on the basis of its relatedness to RNase-encoding genes in the zebrafish genome data base (accession number ENSDARG36171) under completion in the Sanger Institute (Cambridge, UK). Reverse transcription-PCR was performed with mRNA from adult (6-month) zebrafish specimens. The oligonucleotides were: forward, 5′-TGGCCTGTGCAT-TATCAT-3′; reverse, 5′-TTAGG-GGC-GGTTTATTTTC-3′. The PCR was carried out under the following conditions: one cycle at 94 °C for 4 min followed by 35 cycles at 94 °C for 1 min, 50.7 °C for 2 min, 72 °C for 3 min, and finally one cycle at 72 °C for 15 min. The amplified fragment was isolated by electrophoresis on a low melting, 1% agarose gel and purified as described above. The excised band of interest was cloned in a pGEM T-easy plasmid. The sequence encoding the signal peptide, identified as described above for the other cDNAs, was excised from the plasmid through a PCR with the following oligonucleotides: 5′-GGAATCCATATGGAAAT-AAGGCGCCGT-3′ (forward); 5′-CCCAAGCTTAAAT-AACACCTTTTTCATAGT-3′ (reverse). The resulting cDNA, treated with NdeI and HindIII, was cloned into the pET22b(+) expression vector.

All cloned, purified DNAs were certified through sequencing (MWG Biotech) before processing. It should be noted that the sequence of *zf-rnase-3* in the zebrafish genome data base contained at position 91 a guanine and at position 214 a thymine, whereas in the sequence isolated from adult zebrafish and used for expression of the recombinant protein, we found a cytosine at both positions. This did not produce any change in the amino acid encoded by the triplet 214–216 (leucine), but it altered the amino acid encoded by the triplet 91–93 (from glycine to arginine). Likely, the observed changes are due to single nucleotide polymorphism, nonsynonymous in the latter case.

Expression and Purification of Zebrafish RNases—The three expression plasmids, each containing a cDNA encoding a presumed zebrafish RNase, were used to transform competent *E. coli* strain BL21(DE3) (provided by Invitrogen). Cells were grown at 37 °C to an $A_{600} = 1$ and then induced with 0.1 M isopropyl-1-thio-D-galactopyranoside and grown overnight. Pelleted cells were sonicated at 20 kHz in an Ultrasonic sonicator (Heat System Ultrasonic, Farmingdale, NY) with 30-s impulses, each followed by a 30-s rest, for a 15-min total time.

The sonicated cells were centrifuged for 1 h at 12,000 rpm to separate inclusion bodies. As the three proteins were found to be expressed exclusively in inclusion bodies, these were solubilized with 7 M guanidine-HCl in 100 mM Tris acetate, pH 8.4, containing 1 mM glutathione. After flushing nitrogen for 10 min, each preparation was left for 2 h at room temperature. Renaturation was obtained through an initial dilution 1:20, drop by drop, in 100 mM Tris acetate, pH 8.4, containing 0.5 M L-arginine and 1 mM oxidized glutathione.

After 24 h at room temperature, the three preparations were dialyzed against 50 mM Tris-HCl, pH 7.4, and loaded on SP-Sepharose columns (Amersham Biosciences) equilibrated in

Ribonucleases and Angiogenins from Fish

the same buffer and run on an Akta purifier (Amersham Biosciences). Elution was carried out with a gradient from 0 to 1 M NaCl in the same buffer. In the range 0.3 of 0.4 M NaCl a protein peak was eluted, which for each preparation was found by SDS-PAGE (17) to contain essentially a single protein with the approximate molecular size of an RNase; a low level of RNase activity was revealed through zymograms (see Fig. 1). These proteins were thus labeled ZF-RNase-1, -2, and -3. The fractions containing ZF-RNase-1 and -3 from the chromatographic runs on SP-Sepharose were loaded on a reverse-phase C-4 column (Amersham Biosciences) equilibrated in 100% solution A (composed of 5% acetonitrile (v/v) and 0.1% (v/v) trifluoroacetic acid). The column was eluted with a gradient in which the concentration of solution B (composed of 90% acetonitrile containing 0.1% trifluoroacetic acid) was raised to 100% in 1 h. For each preparation a single, major protein component was eluted, which by SDS-PAGE was found to contain a single protein (see Fig. 1). As for the ZF-RNase-2 protein eluted from the SP-Sepharose column, the corresponding fractions were loaded on a Resource-S column (Amersham Biosciences) equilibrated in 50 mM Tris-HCl, pH 7.4, eluted first with a gradient from 0 to 0.3 M NaCl in the same buffer, and then with an isocratic run at 0.3 M NaCl. The major component eluted with 0.3 M NaCl was finally purified on a reverse-phase C-4 column, run as described above for the final purification of ZF-RNase-1 and -3.

Assays of RNase Activity—Zymogram assays of RNase activity were carried out as described previously (18) on 15% SDS-polyacrylamide gels (17). Quantitative assays of RNase activity were carried out with the fluorogenic substrate 6-carboxy-fluorescein-dArUdAdA-6-carboxy-tetramethylrhodamine (Integrated DNA Technologies, Coralville, IA) (19). The assay mixture contained 0.1 M MES, pH 6.0, 0.1 M NaCl, 20–60 nM substrate depending on the enzyme activity, and suitable enzyme aliquots. Inhibition by cRI (Fermentas International, Burlington, Ontario, Canada) of the RNase activity of the zebrafish enzymes was measured by repeating the assays in the presence of stoichiometric amounts of cRI.

Assays of Angiogenic Activity—The assay was based on previously described assays (20, 21) with the following modifications. A 48-well plate was coated with Matrigel (150 μ l/well, purchased from BD Biosciences) for 30 min at 37 °C. human umbilical endothelial vein cells (3.5×10^4 cells/well, obtained from Cambrex, Milan, Italy) were seeded in 250 μ l of EBM-2 medium (Cambrex) in the presence of hANG (a kind gift of Dr. Guo-fu Hu, Harvard Medical School) or one of the three zebrafish RNases at 200 ng/ml. Complete EGM-2 medium (Cambrex) and unsupplemented EBM-2 basal medium were used as positive and negative controls, respectively.

After 6 h of incubation, capillary-like tube formation was examined under an inverted phase microscope. Cells were fixed with phosphate-buffered saline containing 0.2% glutaraldehyde, 1% paraformaldehyde and photographed.

The effects of the human cytosolic RNase inhibitor on the angiogenic activity of zebrafish RNases were analyzed by adding to the medium a 5-fold molar excess of inhibitor. All assays were performed in duplicate, and repeated three times.

Bioinformatic Tools—DNA and protein sequences were analyzed using the programs BLAST and FUGUE (22). FUGUE utilizes environment-specific substitution tables and structure-dependent gap penalties, so that scores for amino acid matching and insertions/deletions are evaluated depending on the local environment of each amino acid residue in a known structure. It thus produces the best possible alignment to sequences of proteins with known three-dimensional structures, which can be used as input for modeling. The template chosen was the structure of human angiogenin (Protein Data Bank code 1a4y), and the program was MODELLER (23).

Cladistic analyses were performed by ClustalW alignments and with the previously described program, MEGA 3.0 (Molecular Evolutionary Genetics Analysis (24)). For this procedure the neighbor-joining option was used with Poisson-corrected distances to generate an unrooted phylogenetic tree. Phylogeny was tested by 2000 bootstrap replications.

RESULTS

Isolation, Cloning, and Expression of Zebrafish RNases—Two putative zebrafish RNase-type sequences were available; one of them was incomplete in the published data bases, in which they were identified as proteins phylogenetically related to RNases or angiogenins. The cDNAs encoding these putative RNases, isolated from purchased DNA fragments, were trimmed, reconstructed, and cloned in expression vectors. A third RNase-type sequence was identified in the zebrafish genome, under completion in the Sanger Institute (Cambridge, UK). The latter was isolated through reverse transcription-PCR with mRNA from adult zebrafish specimens. Details on the cloning are under “Experimental Procedures.” An inspection of the genes encoding the zebrafish RNases indicated (data not shown) that, as for all RNase genes investigated thus far, they are comprised in a single exon and have signal peptides for extracellular expression.

Each cDNA was cloned in the expression vector pET22b(+) and used to transform competent *E. coli* strain BL21(DE3). The proteins, expressed exclusively in inclusion bodies, were subjected to denaturation/renaturation steps and purified to homogeneity by cation exchange chromatography followed by reverse-phase high pressure liquid chromatography as described under “Experimental Procedures.”

Fig. 1 shows an SDS-PAGE analysis and a zymogram of the purified proteins carried out with yeast RNA as a substrate. The three purified proteins had ribonucleolytic activity when relatively high protein aliquots (10 μ g) were used. Their molecular sizes, determined by mass spectrometry, were those expected from their amino acid sequences (reported in parentheses following). They were: 14,323.91 \pm 0.48 Da (14,330.44); 14,455.49 \pm 0.27 Da (14,461.42); and 14,464.78 \pm 0.49 Da (14,471.41) for ZF-RNase-1, -2 and -3, respectively. These findings also indicated that the six Cys residues in each sequence form three disulfide bridges, as there is a difference of 6 Da between the observed and the theoretical mass values. Furthermore, amino acid sequencing carried out for the N-terminal 25 residues indicated that the three proteins had the expected N-terminal sequences.

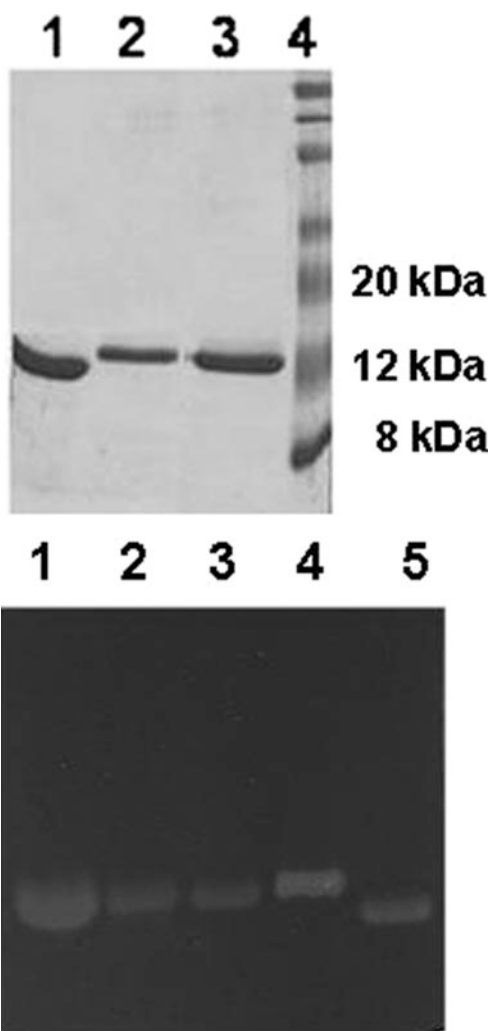


FIGURE 1. SDS-PAGE and zymogram of recombinant zebrafish RNases. Upper and lower panels: lane 1, ZF-RNase-1; lane 2, ZF-RNase-2; lane 3, ZF-RNase-3. Upper panel: lane 4, standard protein markers. Lower panel: lane 4, RNase A; lane 5, human angiogenin.

An examination of these sequences revealed that the catalytically essential residues of RNase A, namely His-12, His-119, and Lys-41, were present at correspondingly close sequence positions in all three proteins (see Fig. 2). Furthermore, all three proteins had the standard "RNase signature," *i.e.* CKXXNTEF, whereas the other RNase signature, namely PVHXD/E, was present in ZF-RNase-2 but was only partially conserved in ZF-RNase-1 and -3, as it occurs in several sequences of non-mammalian RNases.

The overall sequence identity values of the three proteins with respect to RNase A were: 31.3, 33.3, and 30.8%, for ZF-RNase-1, -2, and -3, respectively. Higher identity values could be calculated for the three proteins with respect to human angiogenin, an RNase with angiogenic activity. The latter values were: 35.4, 36.2, and 36.2 for ZF-RNase-1, -2, and -3, respectively. In particular, all three proteins shared with all mammalian angiogenins thus far analyzed a consensus sequence within the first 12 N-terminal residues characterized as "YXX-FLXQH." All three ZF-RNases possess three disulfides (see above) as has been found for non-mammalian RNases and mammalian angiogenins as well.

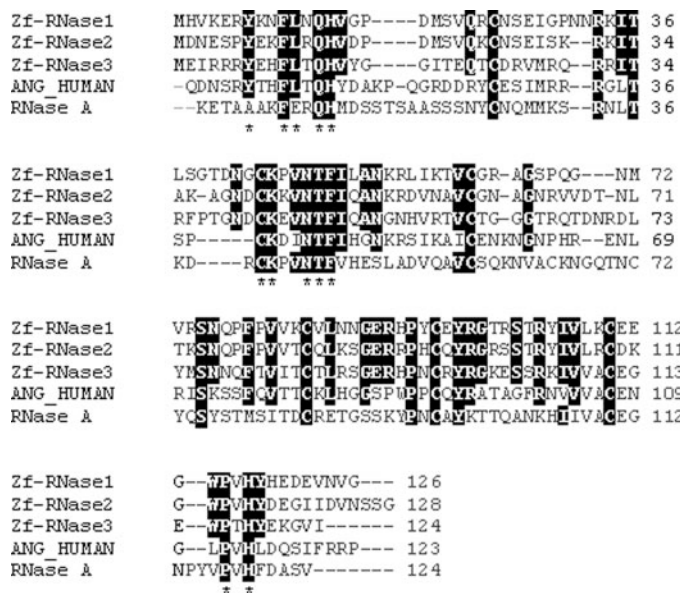


FIGURE 2. Amino acid sequences of zebrafish RNases. To allow comparisons, the sequences of bovine pancreatic RNase A and human angiogenin (ANG_HUMAN) are also shown. In the expressed sequences of zebrafish RNases, the signal sequences of the ribonucleases were replaced by methionine codons. Residues shared by all three zebrafish RNases and residues shared also by either RNase A or hANG or both are shown with a dark background. The putative RNase and angiogenin sequence "signatures" (see "Experimental Procedures") are marked with asterisks. At position 32 of ZF-RNase-3 there is an Arg residue, as encoded by a cgc triplet in the cDNA employed for expression (see "Experimental Procedures"), whereas in the sequence from the zebrafish genome data base under completion in the Sanger Institute (Cambridge, UK), a ggc triplet is present at that position, encoding a Gly residue.

Characterization of Zebrafish RNases—The purified proteins were tested for RNase activity with a sensitive assay (19). This led to the evaluation of the low activity of these enzymes and provided a direct determination of k_{cat}/K_m values. As tabulated in Table 1, the three zebrafish proteins have a very low RNase activity with respect to that of RNase A, but it is comparable with that of human angiogenin.

When we tested the three RNases in the presence of cRI, the human cytosolic RNase inhibitor, we found that under the conditions of the assay stoichiometric amounts of cRI fully inhibited (100%) the RNase activity of ZF-RNase-1 and -2, whereas ZF-RNase-3 was inhibited only by 23%.

The finding of a very low RNase activity of the zebrafish enzymes, typical of angiogenins and the sequence similarities reported above between the zebrafish RNases and mammalian angiogenins motivated us to determine whether the zebrafish enzymes possess angiogenic activity. The assays were based on the formation of capillary-like microtubules when primary endothelial cells were grown on Matrigel in the presence of the effectors (20, 21). Fig. 3 shows that ZF-RNase-1 and -2 were found to possess a marked angiogenic activity, comparable with that of human angiogenin. ZF-RNase-3, instead, was found to have no angiogenic activity. Interestingly, the angiogenic activity of ZF-RNase-1 and -2 was completely inhibited by the cytosolic RNase inhibitor (see Fig. 3).

These findings led us to analyze the structure of the zebrafish RNases through modeling based on the structure of human angiogenin (Protein Data Bank code 1a4y) as a template. The

TABLE 1

Ribonuclease activity of zebrafish RNases compared with the activities of RNase A and hANG

Enzyme	k_{cat}/K_m $M^{-1} s^{-1}$
RNase A	$1.6 \pm 0.12 \times 10^7$
Zf-RNase-1	$2.3 \pm 0.25 \times 10^3$
Zf-RNase-2	$6.3 \pm 0.50 \times 10^2$
Zf-RNase-3	$6.0 \pm 0.74 \times 10^3$
hANG	$7.4 \pm 0.72 \times 10^2$

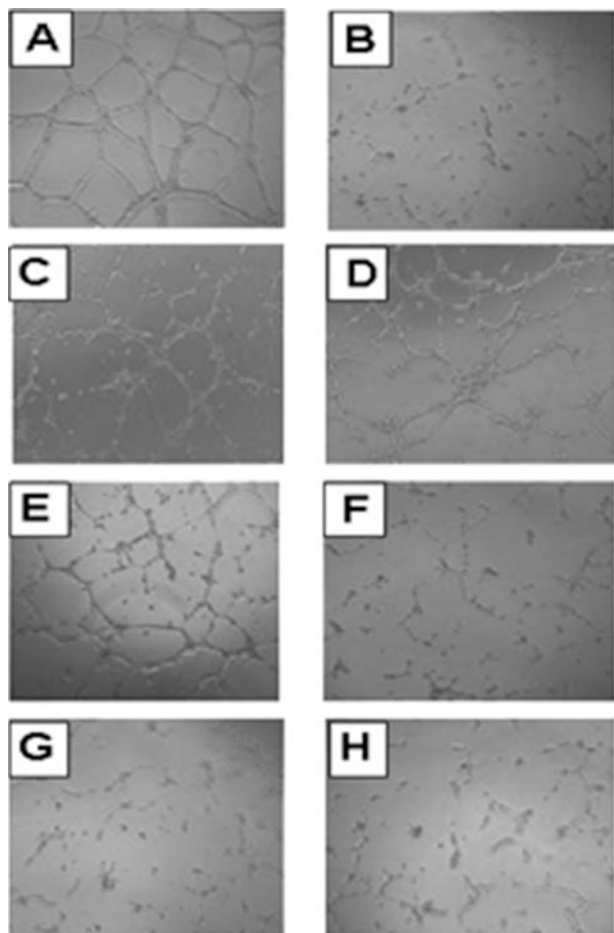


FIGURE 3. Angiogenic activity of ZF-RNase-1 and -2. Assays were carried out with primary human umbilical endothelial vein cells. Positive (A) and negative (B) controls were obtained by using complete EGM-2 medium and non-supplemented EBM-2 medium, respectively. C, assay for human angiogenin. D and E, positive results obtained with ZF-RNase-1 and -2. F, negative result with ZF-RNase-3. G and H, respectively, show the effects of the cytosolic RNase inhibitor on the angiogenic activity of ZF-RNase-1 and -2.

models were validated using ANOLEA (25), and the occurrence of dihedral ϕ and ψ angles outside allowed areas of the Ramachandran plot was assessed with SEGNO (26).

As expected from the sequence-structure alignments of the sequences as produced by FUGUE (see Fig. 2), the models constructed for Zf-RNase1, -2, and -3 (shown in Fig. 4) closely resemble the structure of angiogenin, with two significant differences: the loop between the first and second α -helix is shorter in zebrafish RNases; and the loop that follows the second α -helix in the sequence was found to be longer in the zebrafish proteins (see Figs. 2 and 4).

ZF-RNases in the RNase Vertebrate Superfamily—A preliminary phylogenetic analysis of zebrafish RNases was carried out

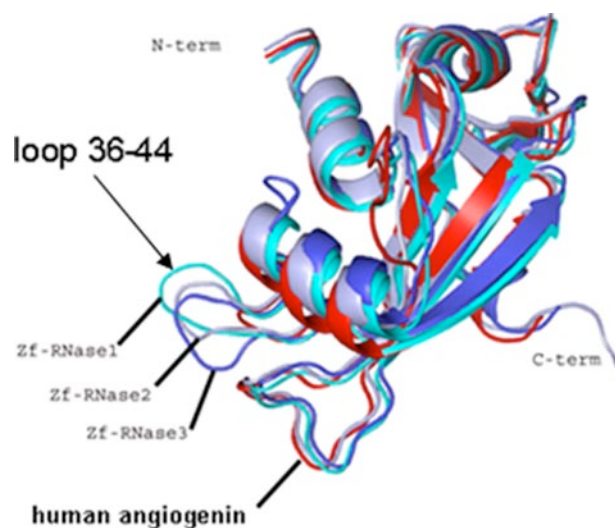


FIGURE 4. Structural models of zebrafish RNases. ZF-RNase-1, ZF-RNase-2, and ZF-RNase-3 are shown in cyan, gray, and blue, respectively. The structure of human angiogenin (Protein Data Bank code 1a4y) is shown in red. The N- and C-terminal ends are marked. The extended loop in region 36–44 (ZF-RNases numbering) is shown.

by comparing their amino acid sequences with those available in the vertebrate RNase superfamily. The rootless tree illustrated in Fig. 5, with radiant branches, includes representative members from the main classes of vertebrate RNases. The bootstrap values are satisfactory, allowing inspection of the relationships among clades with low or no ambiguity. Only for the divergences, bird/mammal and fish/amphibian bootstrap values lower than 50% were found (42 and 46%, respectively).

The monophyletic group of fish RNases, including the three zebrafish RNases and a sequence identified in salmon (NCBI accession number BG936674), appears to be closely related to the family that comprises non-mammalian RNases from amphibians, reptiles, and birds. Mammalian pancreatic RNases (RNases 1) are quite distant from fish and other non-mammalian RNases. The independent clade of mammalian angiogenins (RNases 5) is instead more closely related to the early diverged non-mammalian RNases than to mammalian pancreatic RNases 1. It should be noted that ZF-RNase-3, which has been found devoid of angiogenic activity, appears to be more closely related to salmon RNase than to the other two ZF-RNases endowed with angiogenic activity.

DISCUSSION

We report here the first investigation on RNases from fish. As RNases thus far have been found and studied in all tetrapods, the characterization of three fish proteins as RNA-degrading enzymes leads to a more appropriate definition of the animal, extracellular, pyrimidine-specific RNase superfamily as the vertebrate RNase superfamily.

Based on the inspection of RNase genes, it has been proposed (27) that the earliest members of the RNase superfamily are related to the families of RNases 5 (angiogenins) and/or non-mammalian RNases. The findings reported here on the characterization of three fish RNases provide experimental support to this hypothesis. Moreover, based on the evidence that indeed two fish RNases, namely ZF-RNase-1 and -2 from zebrafish, are

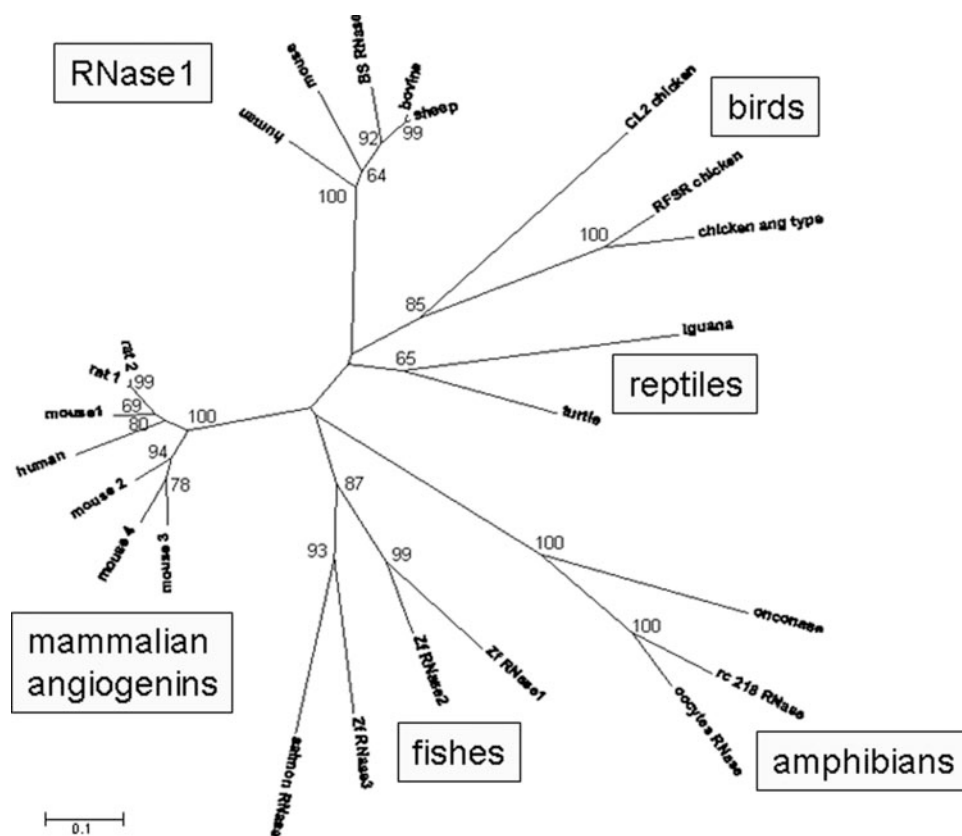


FIGURE 5. Rootless phylogenetic tree of the vertebrate RNase superfamily. The tree shows the close relationship of fish RNases with mammalian angiogenins on one hand and non-mammalian RNases on the other. Mammalian pancreatic (and seminal) RNases 1 appear to be more distant. ZF-RNase-3, devoid of angiogenic activity, is more closely related to salmon RNase than to the other ZF-RNase-1 and -2. The neighbor-joining method was used with Poisson-corrected distances.

endowed with angiogenic activity, we propose that all vertebrate RNases evolved from early diverged angiogenic RNases from fish. Upon evolution, they diversified and experienced selection, thus engendering two distinct evolutionary major clades: (i) that of pancreatic RNases possessing digestive abilities, or diverse noncatalytic bioactions, that were still based on their ability to degrade RNA (2); (ii) that of mammalian angiogenins, with angiogenic activity and a low but essential RNase activity (4).

In fact, as one of the three investigated zebrafish RNases, ZF-RNase-3, does not have angiogenic activity, we can suggest that RNases with or without angiogenic activity diverged at a very early stage in the evolution of fish, before the divergence of the closely related amphibian RNases. However, early diverged fish RNases have all the features of superfamily members: they are encoded in a single exon, possess a signal peptide, are stabilized by disulfides, and are endowed with ribonucleolytic activity determined by the presence of two critically positioned His residues and a Lys residue. Work is in progress on the identification of RNases from hagfish, lampreys, and elasmobranchs (dogfish) to verify whether the RNase/angiogenin scaffold preceded the divergence of bony fishes. It should be noted that RNase superfamily members have not been found in invertebrates (28). It would be interesting to verify whether the fish angiogenins investigated here have any microbicidal activity, as has been found for human and some mouse angiogenins (9).

A comparison of the two zebrafish RNases with angiogenic activity, ZF-RNase-1 and -2, with the best characterized mammalian angiogenins shows that similarities, but also differences, are detectable. As found for mammalian angiogenins (7), the zebrafish angiogenic ZF-RNase-2 contains in its sequence a putative nuclear translocation signal at positions 30–36 (KRKITAK). A string of basic amino acids is also present in ZF-RNase-3 (RRITR at positions 30–34), but ZF-RNase-3 does not display angiogenic activity. The fish angiogenins do not present in their primary structures the two Asn residues (at sequence positions 61 and 109 of human angiogenin) in which deamidation leads to a loss of angiogenic activity (4). It has been presumed that mouse Ang-4 is devoid of angiogenic activity because it presents a replacement of Asn with Lys at position 61 (3); however, ZF-RNase-1 and -2 do not present this critical residue, yet they have angiogenic activity. It should be noted that the angiogenic activity of human and other mammalian angiogenins were assayed with a

chicken experimental system (29), whereas fish angiogenins were assayed with a human system (see “Experimental Procedures”). Tests carried out on mammalian and fish angiogenins with identical assay systems should help to verify the actual significance of sequence signals in the tested angiogenins.

The availability of the angiogenins described here can help to investigate angiogenesis in zebrafish and the role(s) of the newly isolated angiogenins in the angiogenic process, both in the adult animals and in developing zebrafish embryos. In fact angiogenesis has been successfully studied in zebrafish as a very convenient experimental system (14), and developing zebrafish embryos have been proposed as a model for angiogenic/anti-angiogenic drug screening (15).

It is surprising that the human cytosolic RNase inhibitor can exert its inhibitory effects on fish RNases. The presence of cRI has been reported only in mammals (11, 12, 30). Furthermore, cRI has been found to inhibit all tested mammalian RNases, with the exception of seminal RNase, a finding explained by the dimeric structure of this RNase, which is the only RNase of the superfamily with such a structure (31). It does not inhibit an amphibian RNase such as onconase (32), whereas RNase inhibitors from birds and amphibians do not inhibit RNase A, the superfamily prototype (30). Thus, either fishes possess an RNase inhibitor homologous to mammalian cRI that has not yet been detected in evolutionarily related species, or we have a

Ribonucleases and Angiogenins from Fish

case of proteins that just happen to interact apart from any basic biological significance, as in the case of biotin and avidin.

Acknowledgment—We thank Dr. Robert Shapiro for valuable criticism of the manuscript and suggestions.

REFERENCES

1. Beintema, J. J., Breukelman, H. J., Carsana, A., and Furia, A. (1997) in *Ribonucleases: Structures and Functions* (D'Alessio, G., and Riordan, J. F., eds) pp. 245–269, Academic Press, San Diego
2. D'Alessio, G. (1993) *Trends Cell Biol.* **3**, 106–109
3. Strydom, D. J. (1998) *Cell. Mol. Life Sci.* **54**, 811–824
4. Riordan, J. F. (1997) in *Ribonucleases: Structures and Functions* (D'Alessio, G., and Riordan, J. F., eds) pp. 446–466, Academic Press, New York
5. Adams, S. A., and Subramanian, V. (1999) *Angiogenesis* **3**, 189–199
6. Hu, G. F., Riordan, J. F., and Vallee, B. L. (1997) *Proc. Natl. Acad. Sci. U. S. A.* **94**, 2204–2209
7. Moroianu, J., and Riordan, J. F. (1994) *Biochemistry* **33**, 12535–12539
8. Xu, Z. P., Tsuji, T., Riordan, J. F., and Hu, G.-F. (2003) *Biochemistry* **42**, 121–128
9. Hooper, L. V., Stappenbeck, T. S., Hong, C. V., and Gordon, J. I. (2003) *Nat. Immunol.* **4**, 269–273
10. Shapiro, R., and Vallee, B. L. (1987) *Proc. Natl. Acad. Sci. U. S. A.* **86**, 1573–1577
11. Dickson, K. A., Haigis, M. C., and Raines, R. T. (2005) *Prog. Nucleic Acid Res. Mol. Biol.* **80**, 349–374
12. Lee, F. S., and Vallee, B. L. (1993) *Prog. Nucleic Acids Res. Mol. Biol.* **44**, 1–30
13. Papageorgiou, A. C., Shapiro, R., and Acharya, K. R. (1997) *EMBO J.* **16**, 5162–5177
14. Childs, S., Chen, J. N., Garrity, D. M., and Fishman, M. C. (2002) *Development (Camb.)* **129**, 973–982
15. Serbedzija, G. N., Flynn, E., and Willett, C. E. (1999) *Angiogenesis* **3**, 353–359
16. Staton, C. A., Stribbling, S. M., Tazzyman, S., Hughes, R., Brown, N. J., and Lewis, C. E. (2004) *Int. J. Exp. Pathol.* **85**, 233–248
17. Laemmli, U. K., and Favre, M. (1973) *J. Mol. Biol.* **80**, 575–599
18. Blank, A., Sugiyama, R. H., and Dekker, C. A. (1982) *Anal. Biochem.* **120**, 267–275
19. Kelemen, B. R., Klink, T. A., Behlke, M. A., Eubanks, S. R., Leland, P. A., and Raines, R. T. (1999) *Nucleic Acids Res.* **27**, 3696–3701
20. Lawley, T. J., and Kubota, Y. (1989) *J. Invest. Dermatol.* **93**, Suppl. 2, 59S–61S
21. Kanzawa, S., Endo, H., and Shioya, N. (1993) *Ann. Plast. Surg.* **30**, 244–251
22. Shi, J., and Blundell, T., and Mizuguchi (2001) *J. Mol. Biol.* **310**, 243–257
23. Sali, A., and Blundell, T. L. (1993) *J. Mol. Biol.* **234**, 779–815
24. Kumar, S., Tamura, K., Jakobsen, I. B., and Nei, M. (2001) *Bioinformatics (Oxf.)* **17**, 1244–1245
25. Melo, F., Devos, D., Depiereux, E., and Feytmans, E. (1997) *Proc. Int. Conf. Intell. Syst. Mol. Biol.* **5**, 187–190
26. Cubellis, M. V., Cailleux, F., Blundell, T. L., and Lovell, S. C. (2005) *Proteins* **58**, 880–892
27. Cho, S., Beintema, J. J., and Zhang, J. (2005) *Genomics* **85**, 208–220
28. Beintema, J. J., and Kleideidam, R. G. (1998) *Cell. Mol. Life Sci.* **54**, 825–832
29. Knighton, D., Ausprunk, D., Tapper, D., and Folkman, J. (1977) *Br. J. Cancer* **35**, 347–356
30. Hofsteenge, J. (1997) in *Ribonucleases: Structures and Functions* (D'Alessio, G., and Riordan, J. F., eds) pp. 621–658, Academic Press, San Diego
31. D'Alessio, G., Di Donato, A., Mazzarella, L., and Piccoli, R. (1997) in *Ribonucleases: Structures and Functions* (D'Alessio, G., and Riordan, G., eds) pp. 383–423, Academic Press, New York
32. Wu, Y., Saxena, S. K., Ardelt, W., Gadina, M., Mikulski, S. M., De Lorenzo, C., D'Alessio, G., and Youle, R. J. (1995) *J. Biol. Chem.* **270**, 17476–17481